Adam Mickiewicz University in Poznan
Faculty of Biology
Laboratory of Genome Biology
Uniwersytet im. Adama Mickiewicza w Poznaniu
Wydział Biologii
Pracownia Biologii Genomu

PhD thesis

Identification and genetic characterization of SNI1, a gene encoding the subunit of SMC5/6 complex, as a natural modifier of meiotic recombination in *Arabidopsis thaliana*

Rozprawa doktorska

Identyfikacja i charakterystyka genetyczna SNI1, genu kodującego podjednostkę kompleksu SMC5/6, jako naturalnego modyfikatora rekombinacji mejotycznej u *Arabidopsis thaliana*

M.Sc. Longfei Zhu

SUPERVISOR: dr. hab. Piotr Andrzej Ziółkowski, prof. UAM

Poznan, Poland 2022

FUNDING

This work was supported by the following sources:

1. The Polish National Science Centre grant (016/21/B/NZ2/01757)
2. The KNOW RNA Research Centre in Poznan (01/KNOW2/2014)
3. The European Union: Passport to the future - Interdisciplinary doctoral studies at the Faculty of Biology, Adam Mickiewicz University. (POWR.03.02.00-00-I006/17-00)

SCIENTIFIC COLLABORATIONS

Scientific experiments were performed at the Laboratory of Genome Biology, Institute of Molecular Biology and Biotechnology, Faculty of Biology, Adam Mickiewicz University, Poznan in collaborations with Departamento de Genética, Fisiología y Microbiología, Facultad de Ciencias Biológicas, Spain; Department of Plant Sciences, University of Cambridge, UK.

PUBLICATIONS

The results discussed in this thesis are presented in a research article titled:

"**Natural variation identifies SNI1, the SMC5/6 component, as a modifier of meiotic crossover in *Arabidopsis*"-** PNAS August 17, 2021 118 (33).

ACKNOWLEDGEMENTS

Firstly, I would like to express my sincere gratitude to Prof. Piotr Andrzej Ziółkowski for giving me a chance to be a part of Genome Biology Group and to do research under his guidance. His guidance and support throughout the entire of my PhD accompanied by scientific discussions (although sometimes boring) and ideas (although sometimes exaggerated) were instrumental in supporting me during my research. He has been a great mentor and always tells me not to complain. I would like to thank you both for guidance, advice, and supervision of this thesis.

I would like to express my gratitude to all members of Genome Biology Group, both past and present, from whom I learned a lot and could always ask for advice. Particularly, I am thankful to Dr. Tomasz Bieluszewski and Dr. Weronika Sura for training me how to perform a CRISPR knockout experiment. I am thankful to my colleagues Maja Szymańska-Lejman, Julia Dłużewska and Alexandre Pelé for assisting my PhD project and analyzing data. I would also like to thank my colleagues Nadia Kbiri and Wojciech Dzięgielewski for giving me good advice when I am lost and tired. I would like to thank our group technician Hanna Korcz-Szatkowska for her perfect technical assistance.

This work would not be possible without all the collaborations with people from other labs to whom I would like to convey my sincere thanks.

I am sending special thanks to Tarczyński, the Polish brand of sausage, which always provides energy when I am hungry.

Finally, this work would not have been possible without the love and support of my family.

Dedicated to my Country

CONTENTS

Abstract

Meiotic recombination plays a fundamental role in shaping genetic diversity in eukaryotes. The frequency and distribution of meiotic crossovers are tightly controlled; however, crossover frequency is extensively variable within and between species. In my Ph.D. project I used a reporter system *420* based on segregation of genes encoding fluorescent proteins expressed in seeds to efficiently measure crossover frequency in large populations of *Arabidopsis thaliana*. Previously, this method was used to map two major quantitative trait loci (QTL) on the chromosome 1 and 4 derived from a cross between Col-*420* and substitution line LLCLL. As QTL4 was not identified, I focused on mapping this locus using Col-*420* × CCCLC population. Thanks to extensive mapping, I narrowed down the QTL to a 19kb credible interval, which contained 6 genes. Next, I used a combination of genetic techniques including mutant analysis and complementation tests to demonstrate that *SUPPRESSOR OF NPR1-1, INDUCIBLE* (*SNI1*), a gene encoding the component of STRUCTURAL MAINTAINANCE OF CHROMOSOME 5/6 (SMC5/6) complex, is corresponding to the QTL4. I showed that $SNI1^{Col}$ and $SNI1^{Ler}$ alleles differ in their response to high temperature.

Furthermore, I conducted extensive characterization of the *sni1* mutant in meiosis. I showed that *sni1* exhibits a modified pattern of recombination across the genome with crossovers elevated in chromosome distal regions, but reduced in pericentromeres. Mutations in *SNI1* result in reduced crossover interference and can partially restore the fertility of a Class I crossover pathway mutant, which suggests that the protein is involved in non-interfering crossover repair. Genetic analysis of other SMC5/6 mutants confirms the observations of crossover redistribution made for *sni1*. This indicates that the effect observed in plants lacking *SNI1* is due to the role of this protein in the SMC5/6 complex functions. SMC5/6 was shown to be involved in DNA damage repair by affecting activity of DNA helicases and my data indicates that it also plays a role in meiotic crossover formation. Analyses of genetic interactions with key meiotic DNA helicases showed that *SNI1* acts mostly independently on Fanconi Anemia, Complementation Group M (FANCM).

In summary, the data obtained in this thesis reveals for the first time that SNI1 naturally limits *Arabidopsis* crossovers and will extend our current knowledge of the SMC5/6 complex.

Streszczenie

Rekombinacja mejotyczna odgrywa fundamentalną rolę w kształtowaniu różnorodności genetycznej eukariontów. Częstotliwość i rozkład mejotycznych crossing-over są ściśle kontrolowane, jednak częstotość zachodzenia crossing-over jest bardzo zmienna zarówno w obrębie gatunku, jak i między gatunkami. W moim projekcie doktorskim użyłem systemu reporterowego *420* opartego na segregacji genów kodujących białka fluorescencyjne eksprymowane w nasionach, aby skutecznie mierzyć częstotliwość crossing-over w dużych populacjach *Arabidopsis thaliana*. Wcześniej metoda ta była stosowana do mapowania dwóch głównych loci cech ilościowych (QTL) na chromosomach 1 i 4 pochodzących z krzyżówki Col-*420* i linii substytucyjnej LLCLL. Ponieważ QTL4 nie został zidentyfikowany, skupiłem się na mapowaniu tego locus przy użyciu populacji Col-*420*ÍCCCLC. Dzięki zastosowaniu rozbudowanego mapowania zawęziłem QTL4 do wiarygodnego przedziału o wielkości 19 kpz, który zawierał 6 genów. Następnie wykorzystałem kombinację technik genetycznych, w tym analizę mutacji i testy komplementacji, aby wykazać, że *SUPRESSOR OF NPR1-1, INDUCIBLE* (*SNI1*), gen kodujący składnik kompleksu STRUCTURAL MAINTANANCE OF CHROMOSOME 5/6 (SMC5/6) jest odpowiedzialny za QTL4. Pokazałam także, że allele $SNI1^{Col}$ i $SNI1^{Ler}$ różnią się odpowiedzią na wysoką temperaturę.

Ponadto przeprowadziłem obszerną charakterystykę mutanta *sni1* w mejozie. Pokazałem, że *sni1* wykazuje zmodyfikowany wzór rekombinacji w całym genomie z częstotliwością crossing-over podwyższoną w regionach dystalnych chromosomów, ale obniżoną w regionach przycentromerowych. Mutacje w *SNI1* powodują zmniejszoną interferencję crossing-over i mogą częściowo przywrócić płodność mutanta szlaku crossing-over klasy I, co sugeruje, że białko to bierze udział w naprawie poprzez nieinterferujące crossing-over. Analiza genetyczna innych mutantów SMC5/6 potwierdza obserwacje redystrybucji crossing-over dokonane dla *sni1*. Wskazuje to, że efekt obserwowany u roślin pozbawionych SNI1 wynika z roli tego białka w funkcjach kompleksu SMC5/6. Wykazano, że SMC5/6 bierze udział w naprawie uszkodzeń DNA, wpływając na aktywność helikaz DNA, a moje dane wskazują, że odgrywa również rolę w tworzeniu mejotycznych crossing-over. Analizy interakcji genetycznych z kluczowymi dla mejozy helikazami DNA wykazały, że SNI1 działa głównie niezależnie od Fanconi Anemia, Complementation Group M (FANCM).

Podsumowując, dane uzyskane w tej pracy po raz pierwszy pokazują, że SNI1 w naturalny sposób ogranicza powstawanie crossing-over u Arabidopsis i poszerzają naszą obecną wiedzę na temat kompleksu SMC5/6.

List of Abbreviation

ASAP1	**ARABIDOPSIS SNI ASSOCIATED PROTEIN 1**
ATR	**ATAXIA TELANGIECTASIA MUTATED AND RAD3-RELATED**
BRCA2	**BREAST CANCER 2**
CO	**Crossover**
cM	**Centimorgan**
CTL	**Columbia Traffic Line**
Col	**Columbia**
Ct-1	**Catania-1**
CRISPR	**Clustered Regularly Interspaced Short Palindromic Repeats**
DDR	**DNA Damage Response**
DMC1	**DNA MEIOTIC RECOMBINASE 1**
DNA	**Deoxyribonucleic Acid**
DSB	**Double Strand Break**
DHJ	**Double Holliday Junction**
EDS1	**ENHANCED DISEASE SUSCEPTIBILITY 1**
FANCM	**Fanconi anemia, Complementation Group M**
GBS	**Genotyping By Sequencing**
gRNA	**Guide Ribonucleic Acid**
Ler	**Landsberg Erecta**
mRNA	**Messenger Ribonucleic Acid**
MUS81	**MMS AND UV SENSITIVE 81**
MMS21	**METHYL METHANESULFONATE 4**

MRE11	**MEIOTIC RECOMBINATION 11**
NPR1	**NONEXPRESSER OF PR GENES 1**
NCO	**Non-Crossover**
NSE	**Non-SMC-Element**
PR1	**PATHOGEN RESISTANCE GENE 1**
QTL	**Quantitative Trait Locus**
RAD51	**RADIATION SENSITIVE 51**
SPO11	**SPORE11**
SMC	**Structural Maintenance of Chromosomes**
SEI	**Single-End Invasion**
SA	**Salicylic Acid**
SAR	**Systemic Acquired Resistance**
SDSA	**Synthesis Dependent Strand Annealing**
SNI1	**SUPPRESSOR OF NPR1-1, INDUCIBLE**
SGS1	**SLOW GROWTH SUPPRESSOR 1**
SSA	**Single Strand Annealing**
T-DNA	**Transfer DNA**
TOP3A	**DNA TOPOISOMERASE III ALPHA**

1. Introduction

With the development of society and the human population growth, the demand for food has increased significantly. Current progress in crop productivity is, however, not sufficient to fit the demand. A global analysis of crop yields shows that despite the continuous increase in yields, yields either never improve, stagnate or collapse across 24–39% of maize-, rice-, wheat- and soybean-growing areas (Ray, et al. 2012). Plant breeding is an efficient way to settle the food demand problem while it requires the adaptation of new technologies and breeding strategies to increase crop yields (Li, et al. 2018).

The purpose of plant breeding is to create new varieties that perform better than the parents by combining their valuable traits mainly in terms of high yields, good quality, and strong adaptability. Boosting crop production requires reshuffling of the genome to produce new favorable gene combinations in the progeny (Moose and Mumm 2008). The reshuffle of genetic information, which generates genetic diversity, occurs during meiosis.

Meiosis is a special type of cell division in which two rounds of chromosome segregation follow a single round of DNA replication, producing haploid gametes with an intact genome. Meiosis can be divided into two stages: Meiosis I and Meiosis II, which represent reductional and equational divisions, respectively (Figure 1). During Meiosis I, homologous chromosomes undergo genetic information exchange, known as crossover (CO), generating genetic variation by creating new alleles and new combinations of alleles, which is an important evolutionary driving force and is required for proper chromosome segregation (Mercier, et al. 2015). Moreover, COs are required for proper chromosome segregation in meiosis and their absence or reduction causes disturbances in chromosome segregation that may result in aneuploidy(Mercier, et al. 2015).

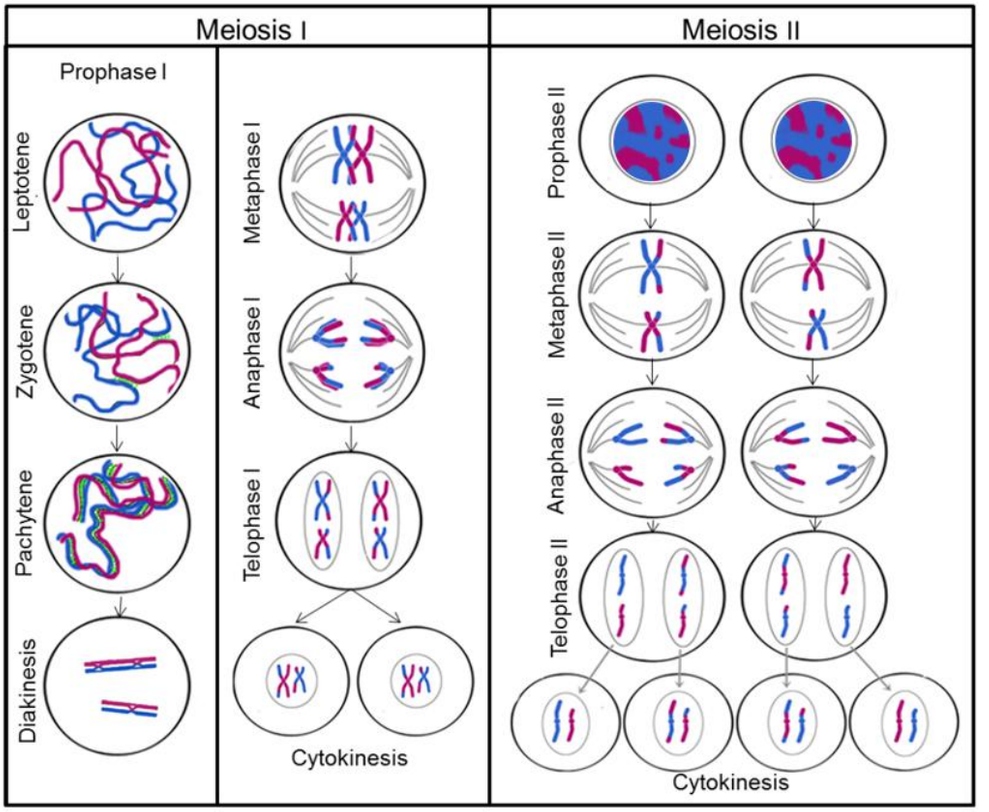

Figure 1. Scheme of meiosis (Lambing et al., 2017).

Normally, crossover rate is kept at a low level in populations, with only one or two crossovers per chromosome per meiosis (Mercier, et al. 2015). However, significant variation in crossover frequency is observed within and between species despite the strict regulation of crossover. The underlying molecular basis for the variation in recombination rate remains unknown, especially in plant species. Furthermore, crossover rate is known to be affected by many factors, including, but not limited to, chromatin structure, DNA sequence, and environmental factors (e.g. temperature)(Mercier, et al. 2015). Research on plants could improve our understanding of the complicated process of meiosis (Mercier, et al. 2015). Although many key molecular factors involved in the meiotic recombination pathway have been elucidated, how these factors shape the crossover landscape remains elusive.

In this thesis, I used natural variation in crossover rate in *Arabidopsis thaliana* to gain further insight into molecular basis of variation in natural populations and identify new proteins that modify crossover frequency. To accomplish this, segregating mapping populations were created to identify modifiers of recombination frequency using a Quantitative Trait Loci (QTL) approach. This led to identification of *SUPPRESSOR OF NPR1-1, INDUCIBLE 1* (*SNI1*) as a casual gene. To provide a context for this work, I will discuss the relevant literature, including the model of meiotic recombination, modification of meiotic recombination, and function of the SMC5/6 complex to which the newly identified protein belongs.

1.1 The model of meiotic recombination

1.1.1 DNA double-strand-break formation

Meiotic recombination leading to CO formation is initiated by programmed double-strand breaks (DSBs), which are catalyzed by SPO11 (Figure 2), a homolog of the TOP6A type II topoisomerase from the archaeon *Sulpholobus shibatae* (Bergerat, et al. 1997; Keeney, et al. 1997). SPO11 is thought to act as a dimmer to catalyze DSBs. There are three SPO11 paralogues in *Arabidopsis*; two of them, namely SPO11-1 and SPO11-2, are required for meiotic DSBs formation; mutation in either *SPO11-1* or *SPO11-2* results in complete sterility due to fail in meiotic recombination initiation, indicating they act together as a heterodimer (Hartung, et al. 2007). The situation is more complicated in rice, where five putative homologs of topoisomerase VIA were described (Jain, et al. 2006).

In *S. cerevisiae*, SPO11 requires nine additional proteins (RAD50, MRE11, XRS2, REC102, REC104, REC114, SKI8, MER2 and MEI4) for meiotic DSB formation. Little is known about the function of these proteins (de Massy 2013). In plants, five new genes required for meiotic DSB formation were isolated (*PRD1*, *PRD2*, *AtPRD3*/*OsPAIR1*, *DFO*, and *CRC1*) (De Muyt, et al. 2009; De Muyt, et al. 2007; Miao, et al. 2013; Nonomura, et al. 2004; Zhang, et al. 2012). A study revealed that topoisomerase MTOPVIB is also involved in DSB formation through interaction with SPO11, but how MTOPVIB affects DSB formation is still poorly understand (Xue, et al. 2016).

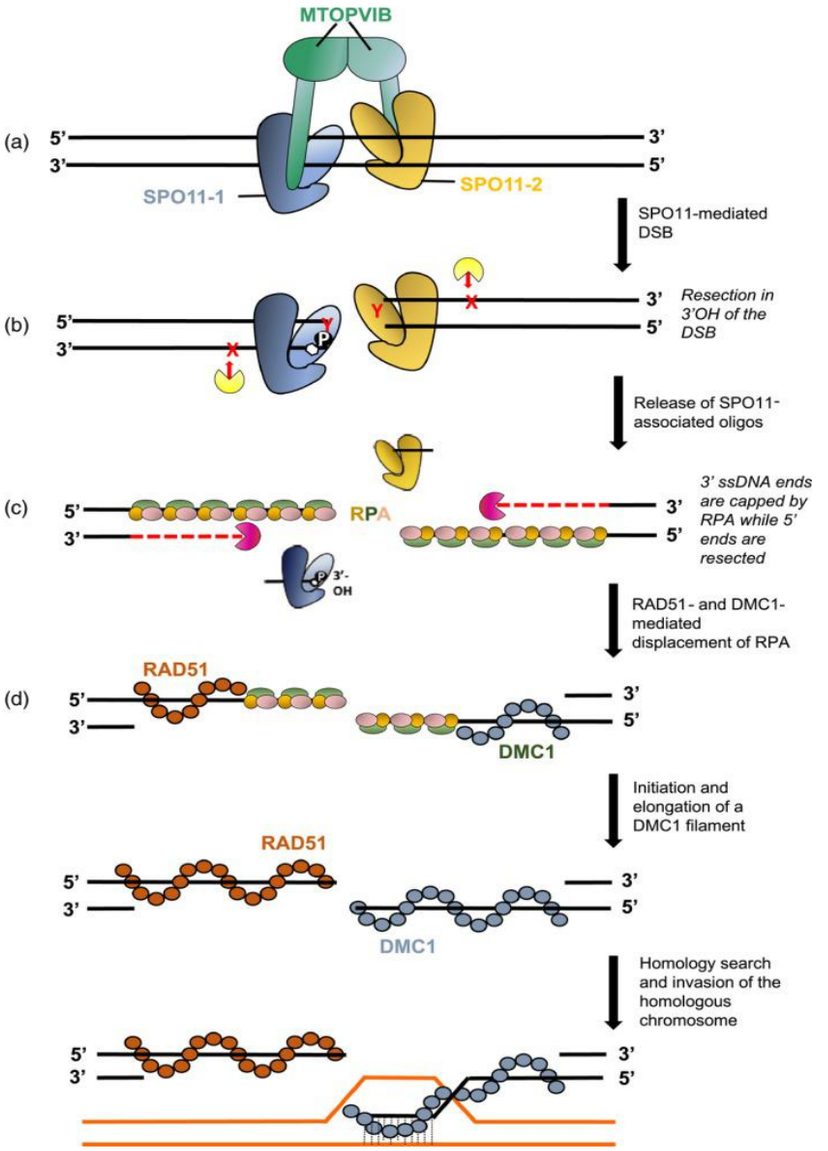

Figure 2. The current model in meiotic recombination initiated by SPO11

(a) SPO11-1 and SPO11-2 act together with M-TOPOVI-B as heterotetramer to induce DSBs. (b) While SPO11 heterodimer is attached to the 5′ end of the break, 3′ OH resection of single-stranded DNA takes place (endonuclease activity is indicated in yellow), thus releasing SPO11-bond oligonucleotides. (c) The 5′ ends are then resected (exonuclease activity is shown in purple) to release 3′ end ssDNA on the complementary strand. (d) The RAD51 and DMC1 recombinases that replace RPAs were recruited and loaded to the strand to form a nucleoprotein filament ready for homology search and heteroduplex formation (Ian Fayos et al., 2019).

1.1.2 DSB processing

SPO11 proteins are covalently attached to 5' end of a DSB after generation of the break and subsequently removed with endonuclease followed by exonuclease activities(Neale, et al. 2005). The removal of SPO11 is mediated by

MRE11-RAD50-XRS2/NBS1 (MRN) complex and COM1/SAE2 (Osman, et al. 2011). Further DSB processing is carried out by Exonuclease 1(Exo1) to produce 3'-overhanging single-stranded DNA (ssDNA) required for meiotic recombination (Gray and Cohen 2016). In *Arabidopsis*, AtMRE11 and AtRAD50 are involved in mitotic and meiotic DNA repair but not in DSB formation (Bundock and Hooykaas 2002; Gallego, et al. 2001), whereas AtNBS1 is non-essential to meiosis (Waterworth, et al. 2007). AtCOM1 has a meiotic function similar to AtMRE11 and AtRAD50 (Uanschou, et al. 2007), which may act together with AtMRE11 and AtRAD50 in DNA end processing (Fayos, et al. 2019).

1.1.3 Strand invasion

Following DSB processing, the 5'ends are further resected to release 3' end ssDNA tails on the complementary strand. This processing is dependent on Exo1 and the Sgs1 helicase in yeast (Fayos, et al. 2019). The 3'ends are first bound by a heterotrimeric RPA (RPA 1, 2, 3) protein complex and then loaded by the RecA homologs RAD51 and DMC1 which replace RPA to form nucleoprotein filament that can promote strand invasion of a paired homologous chromosome, or a sister chromatid (Gray and Cohen 2016; Mercier, et al. 2015), leading to the formation of a displacement loop (D-loop). The formation of a crossover relies on strand invasion and DSB repair guided by the homologous chromosomes rather than by the sister chromatid, which is known as inter-homolog bias (Brown and Bishop 2014).

The RecA family member RAD51 and DMC1 possess overlapping but different functions, as reflected in the divergent meiotic phenotype of r*ad51* and *dmc1* mutants in *Arabidopsis*. The *rad51* plants are completely sterile due to extensive meiotic chromosome fragmentation (Da Ines, et al. 2013). In contrast, the *dmc1* plants are able to repair DSBs using the sister chromatid, thus they do not show chromosome fragmentation; however, as no crossover is formed in *dmc1*, chromosomes segregate randomly during meiosis leading to significant reduction of fertility (Couteau, et al. 1999). These data suggest that DMC1 alone is sufficient to promote interhomolog recombination during meiosis, whereas RAD51 could support DMC1 activity and mediate intersister recombination in the absence of DMC1 (Da Ines, et al. 2013; Kurzbauer, et al. 2012).

1.1.4 DNA synthesis

The 3' end of ssDNA serves as a primer for DNA synthesis following strand invasion and is thought to stabilize the D-Loop and form a strand invasion intermediate (Figure 3). The processing of these intermediates will determine its fate as crossover (CO) or non-crossover (NCO) (Fayos, et al. 2019). Single-strand annealing on the other side of the DSB can be triggered by the extension of the D-loop, a process called second-end capture. Further DNA synthesis and ligation will promote the formation of heteroduplex DNA configurations called double Holliday

junctions (dHJs) that can be resolved as either a crossover or non-crossover, or be dissolved by anti-crossover factors.

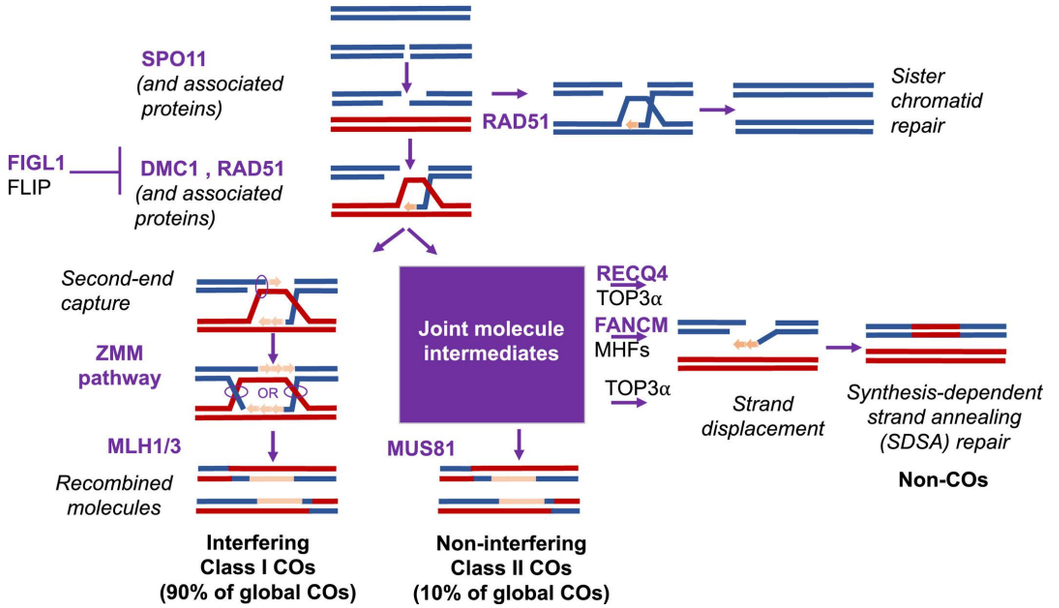

Figure 3. Overview of meiotic recombination pathways (Ian Fayos et al., 2019). The ZMM- and MUS81-dependent pathways generate COs and NCOs at meiosis following the programmed DSBs initiated by the SPO11 complex. Most joint molecules intermediates are resolved by three anti-crossover factors, namely RECQ4 and FANCM and TOP3α, producing NCOs. In contrast to DMC1 and RAD51, The AAA-ATPase FIDGETIN-LIKE 1 (figl1) forms a protein complex with its partner FIDGETIN-LIKE-1 INTERACTING PROTEIN (FLIP), catalyzing the DNA exchange step of homologous recombination.

1.1.5 Class I crossovers

Most joint molecule intermediates can be resolved by dissolution of the D-loop without second-end capture, leading to NCOs (McMahill, et al. 2007). One pathway termed ZMM which is well-conserved across eukaryotes, provides the major activity for COs formation via dHJ intermediates(McMahill, et al. 2007) . These crossovers, so called Class I crossovers, undergo a phenomenon known as interference, meaning that crossovers are spaced more widely than expected by chance (Mercier, et al. 2015). Class I crossovers depend on a group of proteins initially identified in *S. cerevisiae* and termed ZMM proteins (ZIP1, ZIP2, ZIP3, ZIP4, MER3, MSH4, and MSH5) (Borner, et al. 2004). Within plants, the ZMM pathway includes MER3 DNA helicase, ZIP4, HEI10 E3 ligase (ZIP3), SHORTAGE IN CHIASMATA1 (SHOC1/ZIP2), PARTING DANCERS (PTD), and MSH4-MSH5 ($MutS_{\gamma}$) (Mercier, et al. 2015).

The MSH4/5 acts as a heterodimer to bind dHJs and stabilize them (Snowden, et al. 2004). MER3 is a DNA helicase which promotes strand invasion *in vivo* (Mercier, et al. 2005). ZIP4 is required for Class I crossovers in plants (Chelysheva, et al. 2007) and is involved in formation of the synaptonemal complex in yeast (Tsubouchi, et al. 2006). HEI10 is a SUMO/ubiquitin E3 ligase but its activity and substrates in plants remain unknown (Chelysheva, et al. 2012). Recent study reveals that overexpression

of HEI10 is sufficient to boost euchromatic crossovers and that this protein naturally limits *Arabidopsis* crossovers (Ziolkowski, et al. 2017). SHOC1 interacts with PTD to produce an XPF/ERCC1 nuclease-like complex that is able to act on branched DNA molecules *in vitro* (Macaisne, et al. 2008; Wijeratne, et al. 2006). Eventually, dHJs are primarily resolved by the endonuclease MLH1-MLH3 heterodimer, which is however not considered as ZMM protein as it has important and extensive functions also in somatic DNA repair (Dion, et al. 2007; Jackson, et al. 2006).

1.1.6 Class II crossovers

The number of crossovers is reduced to approximately 15% of the wild-type level in both single and combinatorial *zmm* mutants (Chelysheva, et al. 2007; Chelysheva, et al. 2012; Higgins, et al. 2004; Higgins, et al. 2008), indicating that the ZMM pathway is the major crossover pathway that accounts for 85-90% crossovers in plants. Also, in other eukaryotes ZMM pathway is the most prominent crossover pathway (Hunter 2015). A minority of crossovers (10-20%) form via second recombination pathway which is dependent on MUS81 endonuclease (Figure 3). To date, MUS81 is the only characterized protein in this pathway in plants, but it is believable that there are many other factors involved in it. These crossovers are termed Class II crossovers and do not show interference (Berchowitz, et al. 2007). In addition, Class II crossovers are strongly suppressed by anti-crossover factors in wild type (Serra, et al. 2018). Loss of MUS81 function results in a 10% reduction in crossover frequency, while the residual crossovers in a *zmm mus81* double mutant cause a further 30% reduction, suggesting that the formation of crossovers may occur by other unknown mechanisms (Higgins, et al. 2008).

1.1.7 Anti-crossover factors

In *Arabidopsis*，meiotic recombination is initiated by ~150-200 DSBs while only ~10 crossovers are formed by the end of prophase I per meiosis, implying that most DSBs are repaired as non-crossovers, where recombination intermediates are resolved without the exchange of flanking regions. Non-crossovers are thought to form via the synthesis dependent strand annealing (SDSA) pathway, in which the extended D-Loop is disassembled, resulting in a nonexchange event (McMahill, et al. 2007).
Several anti-crossover pathways act to promote non-crossover formation are identified in *Arabidopsis*, including (i) FANCM, MHF1 and MHF2, (ii) FIDGETIN-LIKE-1 (FIGL1) and FIGL1 INTERACTING PROTEIN (FLIP), and (iii) RECQ4A, RECQ4B, RMI1, and TOPOISOMERASE3a (Mercier, et al. 2015). FANCM was initially identified through a mutant screening to search for suppressors of *zip4* mutants. Loss of FANCM function led to a three-fold increase in crossovers compared to wild-type, and similar increases were also observed in *mhf1* and *mhf2* mutants (Crismani, et al. 2012b; Girard, et al. 2014). These additional crossovers were exclusively generated via the Class II crossover pathway, as crossover increases in

fancm are not sensitive to interference (Crismani, et al. 2012a). In addition, mutation of FANCM in rice hybrid could boost genome-wide crossover frequency by 2.3-fold (Mieulet, et al. 2018), whilst reduce crossover frequency in different *Arabidopsis* hybrid contexts. These results suggest that FANCM activity varies across species in terms of the genomic context.

TOP3α and the BLOOM homolog RECQ4 helicases, RECQ4A and RECQ4B were also identified through the suppressor screening of *zmm* mutants (Hartung, et al. 2008; Seguela-Arnaud, et al. 2015). Loss of these proteins limits crossover formation via the Class II pathway, in a similar manner to *fancm*. However, they act independently of FANCM, since the combined mutations cause an additive crossover increase (Seguela-Arnaud, et al. 2015). This result reveals that at least two parallel pathways prevent crossover formation. Recent studies demonstrated a massive increase in crossover frequency in the *recq4a recq4b* double mutant suggesting that TOP3α/RECQ4 helicase is the major anti-recombinational helicase in *Arabidopsis* (Serra, et al. 2018). The meiotic function(s) of TOP3α and RMI1 roles are difficult to distinguish, as they both are involved in crossover regulation and resolving chromosome interlocks (Seguela-Arnaud, et al. 2017).

The third characterized anti-crossover factors are the AAA-ATPase proteins FIGL1 and its partner FLIP. Loss of either gene can significantly boost meiotic crossover frequency. FIGL1 adopts a role in regulating DMC1 and RAD51 localization, with a two-fold increase of the number of RAD51 foci in *figl1* while no increase of the number of DMC1 foci (Fernandes, et al. 2018; Girard, et al. 2015). Moreover, FIGL1 was able to directly interact with RAD51 and DMC1 in a yeast two hybrid assay (Fernandes, et al. 2018). Taken together, FIGL1-FLIP likely limits interaction between homologues chromosomes during the early stages of meiotic recombination (Girard, et al. 2015).

1.2 Modification of meiotic recombination

Although the core meiotic pathway is well conserved across the species, crossover frequency varies greatly between species. For instance, compared to a 0.2 cM Mb^{-1} in the 17 000 Mb wheat genome, a crossover frequency of ~5 cM Mb^{-1} occurs in the 125 Mb *Arabidopsis* genome (Choulet, et al. 2014; Lawrence, et al. 2017; Salome, et al. 2012). Furthermore, crossover rates are not uniformly distributed across the genome and genomes are divided into gene-rich euchromatin and repeat-rich heterochromatin, the latter of which is determined to be associated with suppression of meiotic crossovers (Anderson, et al. 2001; Choulet, et al. 2014). These properties suggest that meiotic recombination is regulated at multiple levels.

Meiotic recombination can be modified by two types of genetic factors, known as *cis*- and *trans*-acting modifiers. *Cis* modification is defined as a change in crossover frequency caused by polymorphisms present at the site of recombination, or on the same chromosome. In contrast, *trans* modification is a result of polymorphic loci encoding diffusible molecules, eg. proteins, which can modulate recombination on the same or other different chromosomes (Lawrence, et al. 2017).

1.2.1 *Cis*-acting modifiers

Inter-homolog sequence polymorphism (i.e. heterozygosity) exerts an effect on crossover formation at a range of scales. Heterozygosity is usually associated with reduced crossovers. For example, an indel polymorphism at the *A3* hotspot in mice is associated with a reduction in crossover frequency, but does not affect DSB formation (Cole, et al. 2010). Pollen typing of the *14a* hotspot in *Arabidopsis thaliana* demonstrates the polymorphism levels and crossover rates in Col × L*er*, Col × Pyl-1, and Col × Ws-4 heterozygotes are negatively correlated (Drouaud, et al. 2013). These results suggest that *cis* polymorphisms could shape the local hotspot recombination rate. Recently, an interesting phenomenon called juxtaposition effect has been reported in *Arabidopsis*, where homozygous and heterozygous regions are juxtaposed on the same chromosome: the authors observed an increase in crossovers in the heterozygous regions with reciprocal decreases in the adjacent homozygous regions (Ziollowski, et al.2015). These results suggest that the pattern of heterozygosity can also affect recombination pattern at the megabase scale, although the mechanism for the heterozygosity juxtaposition effect remains elusive.

DNA rearrangements at the large-scale (kilobase and megabase), for example, insertions, deletions, inversions and translocations, can inhibit crossovers. In *Arabidopsis*, the heterochromatic knob inversion resulted from a transposition event on chromosome 4 is crossover suppressed (Fransz, et al. 2000; Fransz, et al. 2016). Crossover suppression effect caused by chromosomal rearrangements has frequently been connected with adaptation. For example, large inversions have been shown to be associated with ecological adaptations in maize (Fang, et al. 2012). Rearrangements frequently occurred at mating-type loci and on sex chromosomes, where they inhibit the occurrence of recombination between genes that control sexual differentiation (Charlesworth 2002). An intriguing phenomenon, known as the interchromosomal effect, was demonstrated in *D. melanogaster*: when crossovers at some chromosomal regions were inhibited by inversion, crossovers genome (Stalker 1976). A similar but intrachromosomal observation was found in *Arabidopsis*: chromosomes carrying deletions and inversions could inhibit recombination within the modified region, whilst yield compensatory crossover increases were observed elsewhere on the same chromosome (Ederveen, et al. 2015). However, interchromosomal effects were not reported in plants.

There is growing evidence that crossover formation in plants and other species is influenced by chromatin structure and epigenetic modifications. DNA methylation has been shown to affect crossover distributions in *Arabidopsis*. Loss of function of MET1 and DDM1 that predominantly maintain GC context of DNA methylation led to a global crossover redistribution away from the centromere and towards the chromosome arm (Melamed-Bessudo and Levy 2012; Mirouze, et al. 2012; Yelina, et al. 2012). An interesting result was observed in *cmt3* where disruption of non-CG DNA methylation is sufficient to increase both DSB and crossover formation within pericentromeric regions. It was also shown that disruption of the H3K9me2 epigenetic mark could boost pericentromeric DSBs and crossovers (Underwood, et al. 2018).

Hence, DNA methylation and H3K9me2 can act as *cis* modifiers to modulate recombination; although CG and non-CG DNA methylation possess distinct effects.

1.2.2 *Trans*-acting modifiers

Polymorphisms within the coding and promoter regions of *trans* modifier genes may modulate protein activity or interactions and influence gene expression, leading to a within-species variation in crossover frequency or distribution. Most research on *trans* modifiers is primarily conducted in mammals. PRDM9 is a meiosis-specific zinc finger histone H3 methyltransferase that has been shown to control genome-wide distribution but not the number of crossover hotspots in mice and humans (Baudat 2010; Grey, et al. 2009; Parvanov, et al. 2010). Modification of PRDM9 zinc finger sequences could alter the location of H3K4me3 peaks during meiosis, DSB and crossover hotspot activity, resulting in a genome-wide recombination distribution in mice (Grey, et al. 2011).

RNF212 has also been shown to impact crossover rate in humans, cattle and sheep populations (Chowdhury, et al. 2009; Johnston, et al. 2016; Sandor, et al. 2012). RNF212 is an E3 ligase and exerts a dosage effect on crossovers in mice (Reynolds, et al. 2013). HEI10 is another E3 ligase in mammals and antagonizes RNF212. These two proteins together act in a ubiquity–SUMO relay during meiosis and promote crossover resolution (Qiao, et al. 2014; Rao, et al. 2017).

In *Arabidopsis*, two major QTL located in on chromosomes 1 and 4 were identified as polymorphic between the Col-0 and L*er*-0 accessions (Ziolkowski, et al. 2017). The QTL on chromosome 1 corresponds to HEI10, which is a ubiquitin/SUMO E3 ligase that promotes Class I (ZMM-dependent) crossovers, yet the QTL on chromosome 4 have not been identified. Introduction of additional HEI10 copies boosts a global crossover level (Ziolkowski, et al. 2017). The dose-sensitivity exhibited by HEI10 and RNF212 may be the basis of their regulation of crossover frequency in a range of eukaryotic species. Recently, a genetic modifier called TBP-ASSOCIATED FACTOR 4b (TAF4b) was identified between Col-0 and Bur accessions (Lawrence, et al. 2019). TAF4b encodes a subunit of the RNA polymerase II general transcription factor TFIID, mutation of which causes widespread meiosis transcriptional changes, indicating the underlying mechanism of crossover control.

1.2.3 The impact of environmental factors on crossover rate

In addition to genetic factors, many environmental factors including intrinsic (i.e. age) and extrinsic (i.e. temperature) could influence crossover frequency and distribution (Bomblies, et al. 2015). The effect of age on recombination frequency has been well-characterized in humans. However, perceptions of the effect on the crossover rate in humans are controversial. An increase in meiotic recombination with maternal age was discovered within most studies, while several observed the opposite pattern (Bomblies, et al. 2015). It had also been shown that the effect of interference

negatively correlates with increasing maternal age in humans and cattle (Campbell, et al. 2015; Wang, et al. 2016). In contrast, research on *Arabidopsis* showed that recombination frequency did not change with age in most genetic intervals tested, despite a minority display alteration associated with plant age (Li, et al. 2017a).

Temperature is frequently described to influence recombination rate, yet the relationship between them varies across species (Modliszewski and Copenhaver 2015). In *Arabidopsis thaliana*, elevated temperature could increase crossovers and these additional crossovers were derived from the major Type I interference sensitive pathway. Crossover frequency could also increase under certain circumstances where temperature was reduced below ambient levels (Bomblies, et al. 2015; Lloyd, et al. 2018). Like *Arabidopsis*, barley also exhibited an increase in crossover rate at higher temperatures, despite only in male meiosis (Phillips, et al. 2015). The mechanism of how temperature influences crossover rate remains unclear. However, a study in *Arabidopsis* demonstrated that crossover hotspots are associated with H2A.Z, occupancy of which positively correlates with temperature (Kumar and Wigge 2010). In addition, the increase in crossover frequency at low temperature was not observed in the *arp6* mutant where H2A.Z deposition is defective (Choi, et al. 2013). Hence, temperature or other environmental factors, could possibly mediate crossover alteration by interacting with epigenetic *cis* factors.

1.3 Structural maintenance of chromosomes (SMC) protein complexes

Structural maintenance of chromosomes (SMC) complexes plays a key role in regulating chromatin dynamics and maintaining chromosome structure and integrity (Losada and Hirano 2005; Uhlmann 2016). SMC proteins were initially discovered in *Escherichia coli* (Niki, et al. 1992). SMC proteins, which are core subunits of SMC complexes, contain an ATP-binding cassette (ABC) located in the C- and N-terminus globular domains called *walker A* and *walker B*, respectively. Proper folding at the hinge domain and coiling of the arms is the prerequisite for SMC function, which brings the hinge domain in a dimerization state with ATP-dependent DNA binding activity (Kanno, et al. 2015) and a heterodimeric V-shaped structure formed by SMC proteins.

There are three major SMC complexes in eukaryotes, namely, cohesin (SMC1-SMC3), condensin (SMC2-SMC4) and SMC5-SMC6 (SMC5/6). Cohesin is the most characterized SMC complex, which is thought to affect various chromosomal processes by regulating dynamics of sister chromatid cohesin (Jeppsson, et al. 2014). Condensin is the key regulator of chromosome folding and segregation during cell division. The third complex, SMC5/6, was known mostly for its role in DNA replication and maintaining genome stability though its specific function in this process remains enigmatic.

1.3.1 The SMC5/6 complex structure

SMC5/6 complex includes two core proteins, namely, SMC5 and SMC6 proteins. In addition to SMC5 and SMC6, the complex possesses additional NON-SMC ELEMENT (NSE) subunits (Figure 4). NSE1 is an ubiquitin ligase-like protein containing a RING finger domain and is essential for SMC5/6 holocomplex integrity in yeast (McDonald, et al. 2003). NSE/MMS21 is an E3 SUMO ligase-like protein, which is required for DNA damage repair (Potts and Yu 2005). NSE3 could form a subcomplex with NSE1 and NSE4 and spore viability is reduced in yeast *nse3* (Pebernard, et al. 2004). NSE5 and NSE6 are associated with the hinge domain essential for complex stabilization in budding yeast (Verver, et al. 2016).

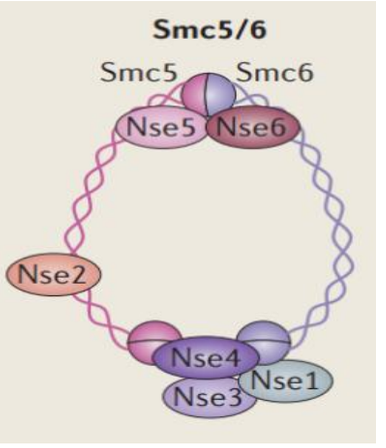

Figure 4. Structure of the yeast SMC5/6 complex (Jeppsson et al., 2014)

1.3.2 Functions of the SMC5/6 complex

SMC5/6 complex was initially identified as a DNA repair complex by genetic screening based on mutant hyper-sensitivity to genotoxic stress (Lehmann, et al. 1995). Based on this finding its major role in DNA repair was proposed. Recent studies, however, demonstrated that SMC5/6 complex is involved in other processes than DNA damage repair, such as DNA replication, homologous recombination and meiosis (Verver, et al. 2016). It should be noted that most of our knowledge on biological functions of the SMC5/6 complex, especially at the molecular level, comes from studies in budding yeast (Aragon 2018). To what extent these functions are conserved in higher eukaryotes, especially in plants remains an open question.

1.3.2.1 SMC5/6 and replication forks stability

The replication machinery mediated progressive separation of the parental DNA strands results in the accumulation of positively supercoiled DNAahead of the replication fork and formation of sister chromatid intertwining (SCIs), both of which are structurally problematic because they induce topological stress and impede sister

chromatid separation during mitosis, respectively. Therefore, they need to be removed to keep regular cellular activities (DiNardo, et al. 1984). In budding yeast, DNA supercoils are resolved by the coordinated actions of type I TOPOISOMERASE 1 (TOP1) and type II TOPOISOMERASE 2 (TOP2), the latter of which is responsible for the removal of SCIs (Bermejo, et al. 2007). The SMC5/6 complex was recently found to be involved in removal of DNA supercoils and formation of SCIs in *S. cerevisiae*. The SMC5/6 complex is thought to promote fork rotation by secluding nascent SCIs that emerge behind the replication machinery, which could reduce the degree of replication-induced supercoiling (Jeppsson, et al. 2014a; Kegel, et al. 2011). It was demonstrated that TOP2 and the SMC5/6 complex act as ATP-dependent DNA linkers, promoting intermolecular interaction of DNA molecules through their topological entrapment(Kanno, et al. 2015).Moreover, TOP2 causes the dissociation of the SMC5/6 complex from chromosome arms under non-stress conditions (Jeppsson, et al. 2014a; Kegel, et al. 2011).In the absence of TOP2 activity, the SMC5/6 complex may resist the SCI stabilizing activity of the cohesin complex, which promote passive resolution of sister chromatid at the end of chromosomes (Jeppsson, et al. 2014a). These findings suggest that the SMC5/6 complex controls the TOP2-independent SCI resolution pathway.

The replication-derived toxic HR intermediates occur during bypass synthesis, when DNA polymerase encounters a block during DNA synthesis and returns to the original template after the damage. In yeast it was found that RECQ type helicase SGS1, a member of the STR (SGS1, TOP3 and RMI1 proteins) complex, functions together with the SMC5/6 complex to inhibit the accumulation of these abnormal intermediates (Bermudez-Lopez, et al. 2016). The resolution of intermediates is likely depended on SUMOylation ability of NSE2/MMS21, as the *sgs1* mutants showed impaired recognition of SUMOylated SMC5/6 complex. In addition, it was proposed that SMC5/6 complex acts antagonistically to MPH1, an ortholog of human FANCM, which prevents accumulation of toxic recombination intermediates (Bermudez-Lopez, et al. 2010; Bermudez-Lopez, et al. 2016).

1.3.2.2 Homologous chromosome synapsis

In mice, SMC6 is located at synapsed chromosomes and co-localize with the synaptonemal complex (SC) central region proteins synaptonemal complex protein 1 (SYCP1). In *Sycp1* knockout spermatocytes, the presence of SMC6 were not able to detect, while SMC6 still appeared in *rec8* and *smc1β* knockout spermatocytes, suggesting that loading of SMC6 to the mouse SC is dependent on SYCP1 while is independent of meiosis-specific cohesin subunits REC8 and SMC1β (Gomez, et al. 2013). These results demonstrate that the SMC5/6 complex facilitates SC assembly or supports the SC machinery.

1.3.2.3 Meiotic recombination

During meiosis, aberrant joint molecules (JMs) can potentially block chromosome segregation. Such aberrant JMs emerge when meiotic recombination intermediates are not properly resolved to form either crossover or non-crossover (Copsey, et al. 2013). In budding yeast, the *smc6-56* mutant exhibited the accumulation of unresolved recombination intermediates to the number, which is more than twice higher than wild type. In addition, COs and NCOs assay revealed that the levels of both these recombination products are not significantly altered in *smc6-56* mutant. These results suggest that the SMC5/6 complex is required to prevent the accumulation of improper recombination intermediates (Xaver, et al. 2013). In budding yeast, they are three resolvases with overlapping function responsible for eliminating aberrant joint intermediates: MUS81-MMS4, SLX1-SLX4, and YEN1 (Jessop and Lichten 2008; Oh, et al. 2008). Genetic analysis of resolvases showed that .YEN1 and SLXl–SLX4 have only minor role in JMs resolution (Copsey, et al. 2013). The genetic interaction between MMS21 (a subunit of SMC5/6 complex) and MUS81-MMS4 revealed that JMs accumulate in *mms21 mms4* double mutants while JMs were successfully resolved in both single mutants (Copsey, et al. 2013), suggesting that the unresolved recombination intermediates in *mms21* is depend on MUS81-MMS4 for resolution.

1.3.3 SMC5/6 complex in plants

Current research on plant SMC5/6 complex is limited to *Arabidopsis*. Plant SMC5/6 complex consists of two large subunits SMC5 and SMC6 (encoded by two paralogs *SMC6A* and *SMC6B*) and four evolutionarily conserved non-SMC elements (NSEs): NSE1–NSE4 as well as two plant specific SMC5/6 subunits known as SNI1 and ASAP1 (Yan, et al. 2013). Homozygous mutants in multiple complex subunits are lethal in *Arabidopsis*, specifically, *SMC5* (alias EMBRYO DEFECTIVE 2782), *NSE1* (alias EMBRYO DEFECTIVE 1379), *NSE3, ASAP1* and *SMC6A SMC6B* double mutant do not produce viable seeds (Li, et al. 2017b; Watanabe, et al. 2009; Yan, et al. 2013). This significantly hampers investigation of SMC5/6 roles in meiosis.

1.3.3.1 DNA damage repair

Subunits of the SMC5/6 complex have long been implicated as important for DNA damage repair. For instance, mutants of *SMC6B* gene demonstrated hypersensitivity after DNA-damaging treatments and the mutation results in moderate hypersensitivity to UV, x-rays and MMC and strong hypersensitivity to methyl methane sulfonate (MMS) and zebularine (Mengiste, et al. 1999; Raschle, et al. 2015). Interestingly, over-expression of SMC6 resulted in elevated levels of

intrachromosomal recombination (Hanin, et al. 2000). NSE2 was subsequently proved to have similar hypersensitivity effects with SMC6B, which exhibited an increased number of DSB after treatment with the toxic agents (Xu, et al. 2013). SNI1 was also identified to take part in DNA DSB response (Yan, et al. 2013).

DSBs can be repaired by homologous recombination (HR) or by nonhomologous end-joining (NHEJ) (Chapman, et al. 2012). A study that analyzed HR and sister chromatid alignment in somatic cells with and without induced DNA damage in *Arabidopsis smc5/6* mutants showed HR frequencies was reduced, suggesting the SMC5/6 complex is required for homologous recombination (HR) between sister chromatids (Watanabe, et al. 2009) .

1.3.3.2 Development

Several studies on *Arabidopsis* show that the SMC5/6 complex is involved in many development processes other than genome stability. NSE2, mutation of which produces viable seeds, is the most described subunit involved in developmental regulation. *nse2* mutants were identified as having a short root and partial sterility phenotype, which displayed an increased frequency of cell death and disorganization in root apical meristems (Huang, et al. 2009). A recent study demonstrated that NSE2/MMS21 regulates the protein stability of BRAHMA chromatin remodeling factor in root development (Zhang, et al. 2017).

NSE2 was recently found to affect flowering time (Kwak, et al. 2016). The *mms21* mutant showed an early flowering phenotype under short-day and long-day condition, in which the level of transcript and protein of FLOWERING LOCUS C (FLC) was down-regulated while floral inducers SUPPRESSOR OF CONSTANS (SOC1) and FLOWERING LOCUS T (FT) was up-regulated, indicating the SMC5/6 complex boosts FLC transcription.

In addition to NSE2 involved in plant development, knock-out mutants of NSE5A were embryolethal and loss function of NSE1 and NSE3 led to disordered cell mitosis in early embryo, suggesting that SMC5A、NSE1 and NSE1 were involved in embryo development in *Arabidopsis* (Li, et al. 2017b; Watanabe, et al. 2009).

Although how the SMC5/6 complex regulates seed development remains elusive, there is, however, plenty of evidence that the SMC5/6 complex is required for this process. For example, *NSE1* and *NSE3* homozygous mutants did not produce viable seeds while *NSE2* could partially complement *NSE1* and *NSE3* homozygous mutant, resulting in half proportion of wild-type seed set with reduced viability (Li, et al. 2017b; Liu, et al. 2014). The similar seed phenotype observed in cohesin and condensin mutants (Liu, et al. 2002) prompts to speculate that the underlying mechanism of seed development functions via coordination of cohesin and SMC5/6 complex action.

1.3.3.3 Stress response

Plants have evolved various adaptation strategies in response to stresses. Drought

stress exerts a huge impact on plant development and yields. Abscisic acid (ABA) plays an important role in the stress response and it accumulates upon drought stress (Cutler and Krochko 1999). Study showed that *NSE2/MMS21* mutants could improve resistance to drought and over-expression of *NSE2/MMS21* could reduce resistance to drought. In addition, the expression level of *NSE2/MMS21* was reduced with ABA treatment. These results suggest that *MMS21* is involved in the drought stress response (Zhang, et al. 2013).

1.3.3.4 Plant immunity

Systemic acquired resistance (SAR) is a general plant defense response and triggers up-regulation of *PR1* that used as a molecular marker for SAR (Uknes, et al. 1992). *NONEXPRESSER OF PR GENES 1* (*NPR1*) is a key gene involved in regulation of plant disease resistance, mutation of which could abolish the accumulation of *PR1* or onset of SAR in the presence of SA (Cao, et al. 1997). A gene named *SUPPRESSOR OF NPR1-1, INDUCIBLE* (*SNI1*) was identified via suppressor screening of *npr1* and discovered structurally highly similar to yeast NSE6 (Li, et al. 1999; Yan, et al. 2013). These results indicate SNI1 may function as a negative regulator of SAR (Yan, et al. 2013).

1.3.3.5 Meiosis

It was reported that NSE2/MMS21 mutants exhibit a reduction in seeds number and pollen viability. Furthermore, cytology of *NSE2*/*MMS21* mutants in *Arabidopsis* displayed chromosome fragments and bridges between bivalents at anaphase I and disturbed segregation of the sister chromatins at anaphase II, suggesting abnormal meiotic chromosome behavior was caused by the loss function of *AtMMS21* (Liu, et al. 2014).

2. Aims of the Project

We previously used a substitution line LLCLL (where chromosome 1, 2, 4, and 5 are Col/Ler segregating) to cross with Col-*420*, aiming to investigate the impact of other four chromosomes on *420* interval CO rate in chromosome 3(Figure 5A). We discovered two major QTL between Col and Ler accession in *A. thaliana.* The first one was located on chromosome 1 and was identified as *HEI10* (Figure 5B) (Ziolkowski, et al. 2017). The main goal of the project was to identify the second *trans*-modifier in Col/Ler cross, located on chromosome 4.

Trans-modifiers can be proteins with very different biological functions and only some of them, like the previously described HEI10 and in human RNF212, are proteins directly involved in the recombination process (Dluzewska, et al. 2018). Therefore, the second goal of the study was the broad characterization of the identified QTL4, including the recognition of the influence of the corresponding gene on crossover formation, as well as an extensive analysis of genetic interactions with other factors involved in meiotic recombination. Together, these findings should improve our understanding of the mechanisms controlling crossover frequency and distribution in plants providing new perspective for crop breeding.

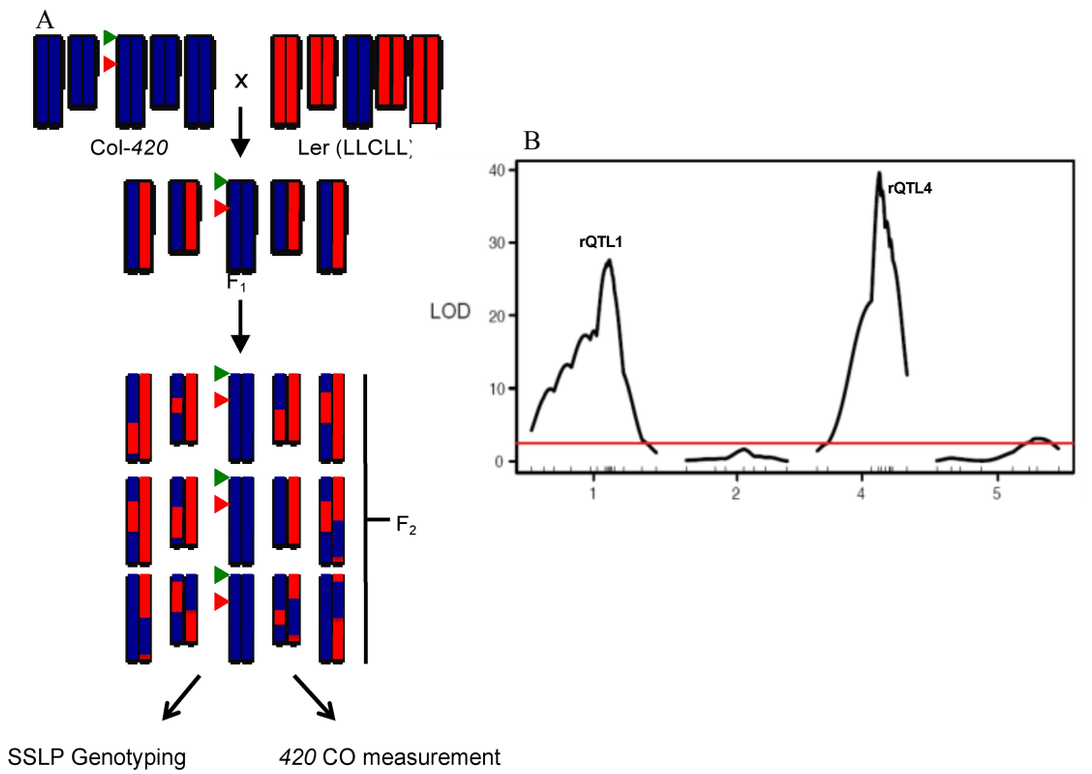

Figure 5 (A) Diagram illustrating generation of F_2 population for *QTL* mapping. Blue color corresponds to Col, while red corresponds to L*er*. (B) Col-*420* × LLCLL F_2 multiple (two-dimensional) QTL scan indicating the location of two *QTL*. X axis shows the position on A. thaliana chromosomes and Y axis shows LOD scores. Chromosome 3 was excluded from the analysis as it carried *420* reporters used for crossover measurements (Ziolkowski et al. 2017).

3. Materials and Methods

3.1 Plant methods

3.1.1 Plant materials and growth conditions

Arabidopsis thaliana Col-0 and L*er*-0 accessions were originally obtained from the Nottingham *Arabidopsis* Stock Centre (NASC). The CCCLC chromosome substitution line used to construct the Col-*420*×CCCLC F2 population was kindly provided by Erik Wijnker, Jose van der Belt and Joost Keurentjes (University of Wageningen). Col-*420* FTL was provided by Avi Levy (The Weizmann Institute), *I3bc* and *I5a* FTLs were provided by Greg Copenhaver (University of North Carolina), and *CTL1.12*, *CTL1.18*, *CTL1.23*, *CTL3.4*, *CTL3.9* and *LTL5.5* were provided by Scott Poethig (University of Pennsylvania). A full list of mutants used in this study is detailed in Table 1. Plants were grown in growth chambers at 20°C with long-day light period (16 hours photoperiod, 60% humidity and 150 μmol light intensity). Prior to germination, seeds were planted into the soil and kept for two days in the dark at 4°C to stimulate germination.

Table 1 Plant materials used in the study

Gene	Mutant name	Mutant type	Provider
SNI1	*sni1-1*	EMS	Xinnian Dong (Duke University)
	sni1-2	CRISPR-Cas9	This study
FANCM	*fancm-1*	EMS	Raphael Mercier (Max Planck Institute for Plant Breeding Research),
AT4G18450	SALK_205943	T-DNA	Nottingham Arabidopsis Stock Centre (NASC)
AT4G18460	SALK_060156	T-DNA	NASC
AT4G18465	SALK_007841	T-DNA	NASC
AT4G18480	SAIL_230_D11	T-DNA	NASC
AT4G18490	SALK_121019	T-DNA	NASC
SMC6A	*smc6a-1*, SALK_009818	T-DNA	NASC
SMC6B	*smc6b-2*, SALK_135638	T-DNA	NASC
ASAP1	GABI_218F01	T-DNA	NASC
NSE2	*nse2-2*, SAIL_77_G06	T-DNA	NASC
MUS81	*mus81-2*, GABI_113F11	T-DNA	NASC
RECQ4A	*recq4a-4*, GABI_203C07	T-DNA	NASC

RECQ4B	*recq4b-2*, SALK_011357	T-DNA	NASC
ZIP4	*zip4-2*, SALK_068052	T-DNA	NASC
NSE4A	*nse4a-2*, GK-768H08	T-DNA	Ales Pecinka (Institute of Experimental Botany)
EDS1	Col-*eds1-2*	T-DNA	Jane Parker (Max Planck Institute for Plant Breeding Research)
BRCA2A	GABI_290C04	T-DNA	NASC
BRCA2B	SALK_037617	T-DNA	NASC
RAD51	GK_134A01	T-DNA	NASC
ATR	*atr-2*, SALK_032841	T-DNA	NASC
SPO11-1	*spo11-1-3,* SALK_146172	T-DNA	Chris Franklin (University of Birmingham)

3.1.2 Sterilization of *Arabidopsis* seeds

Seeds were sterilized by incubation in a solution of 70% ethanol a 5 minutes period with occasional rotation. Then removed ethanol and added 95% ethanol solution for further 5 minutes incubation. Seeds were allowed to dry well on filter paper in a sterile dish plate before being sown on pellets.

3.1.3 Fertility assay

Pollen viability was assessed from 1,500 pollen grains collected from open flowers of 3 plants per genotype, using Alexander staining (Alexander 1969). Stage 12 buds were collected and fixed with Carnoy's fixative solution (Table 2) at room teperature (RT) for 3 days. The fixed buds were placed on a microscope slide and the six anthers were separated. A few drops of (2-3) staining solution (Table 2) was immediately added after carefully removed the fixative solution. A heating block was used to rapidly heat the slide to 60°C for 1.5 minutes and then fix the anthers with a cover glass. The prepared slides were used for analysis of pollen viability and density (number of pollen grain per anther). Pictures were taken using a Leica DM4 B light microscope equipped with a camera.

Seed set and silique length were assessed from 5 fruits, located at positions 6-10 of the main stem, in 10 plants per genotype.

Table 2 Composition of the solution s used in fertility assays

Carnoy`s fixative solution		Alexander staining solution	
Ethanol	300 ml	Ethanol (95%)	10 ml
Chloroform	150 ml	Malachite green	1 ml
Acetic acid	50 ml	Glycerol	25 ml

Total	500 ml	Acid fuchsin (1%)	5 ml
		Orange G (1%)	0.5 ml
		Glacial acid	4 ml
		Ddwater	Up to 100 ml

3.1.3 Agrobacterium-mediated transformation of *Arabidopsis*

Agrobacterium transformation was performed using the floral dip method as described (Clough and Bent 1998). In summary, a GV3101 *Agrobacterium tumefaciens* strain carrying a binary vector containing the desired expression cassette or CRISPR-Cas9 construct was used to inoculate liquid Lysogeny Broth (LB) with kanamycin (50µg/ml). This culture was grown at 28°C until cells reached the stationary growth phase (OD600 ~1.5–2.0). These cells were then pelleted and resuspended in sucrose solution medium (5% [wt/vol]) to a final OD600 of ~0.8. Approximately 6 weeks old plants were cut back 6 days prior to dipping in this solution to stimulate flowering. Immediately after dipping, plants were maintained at high humidity in the dark for 24 hours, before being returned to standard long day growth chamber conditions. A second dipping was performed one week later to improve transformation efficiency.

T1 seed were harvested, sterilized and placed on soil pellets. Pellets were kept at 4°C in the dark for 2 days and then transferred to long day growth chambers. Seedlings were treated with BASTA once they had two true leaves on the soil pellets.

3.1.4 Measurement of crossovers using seed-based systems

Crossover frequencies were measured using seed-based fluorescent reporters as previously described (Ziolkowski, et al. 2015). If F_2 or further self-fertilized generations of plants were to be scored, pre-selection of those seeds containing the fluorescent reporters in hemizygous state was conducted to obtain scorable individuals (Figure 6A). Seeds from plants containing red and green reporter can be distinguished under a UV microscope based on their fluorescence under green fluorescent protein (GFP) and red fluorescent protein (RFP) filters (Figure 6B). The majority of these individuals will contain the single copy fluorescence reporter on the same chromosome, in *cis* orientation (*RG*/++). A small number will, however, contain the fluorescence reporter on different chromosomes, in *trans* orientation (*R*+/*G*+), which are rare as they require a recombination event in the interval to have previously occurred on each chromosome in both parental gametes. The plants with reporters in *trans* were not used for measurements as they usually result in imprecise measurements.

Seeds harvested from preselected plants (RG/--) were photographed using epifluorescent stereomicroscope Lumar.V12 (Zeiss) equipped with a CCD camera in bright field, UV through a dsRed filter and UV through a GFP filter. These images

were then analyzed using CellProfiler image analysis software v2.1.1 and an adapted pipeline which identifies seed objects and assigns a dsRed and eGFP fluorescence intensity value to each seed object (Ziolkowski, et al. 2015). Diploid seed can contain zero, one or two copies of each fluorescent reporter (Figure 6C), however, single and double copy fluorescence categories tend to overlap in intensity, therefore, only the distinction between non-fluorescent and fluorescent seed is used for recombination measurements. Histograms of seed fluorescence in CellProfiler program were used to classify fluorescent and non-fluorescent seed for each color (Figure 6D). The genetic distance is calculated as cM=100×(1–(1−2(*NG*+*NR*)/*NT*)1/2), where *NG* is the number of green alone seeds, *NR* is the number of red alone seeds and *NT* is the total number of seeds analyzed. The ratio of fluorescent to non-fluorescent seeds for both fluorescent reporters should be ~3:1 and only measurements with ratios between 2.7 and 3.3 were included for analyses with the purpose of quality control.

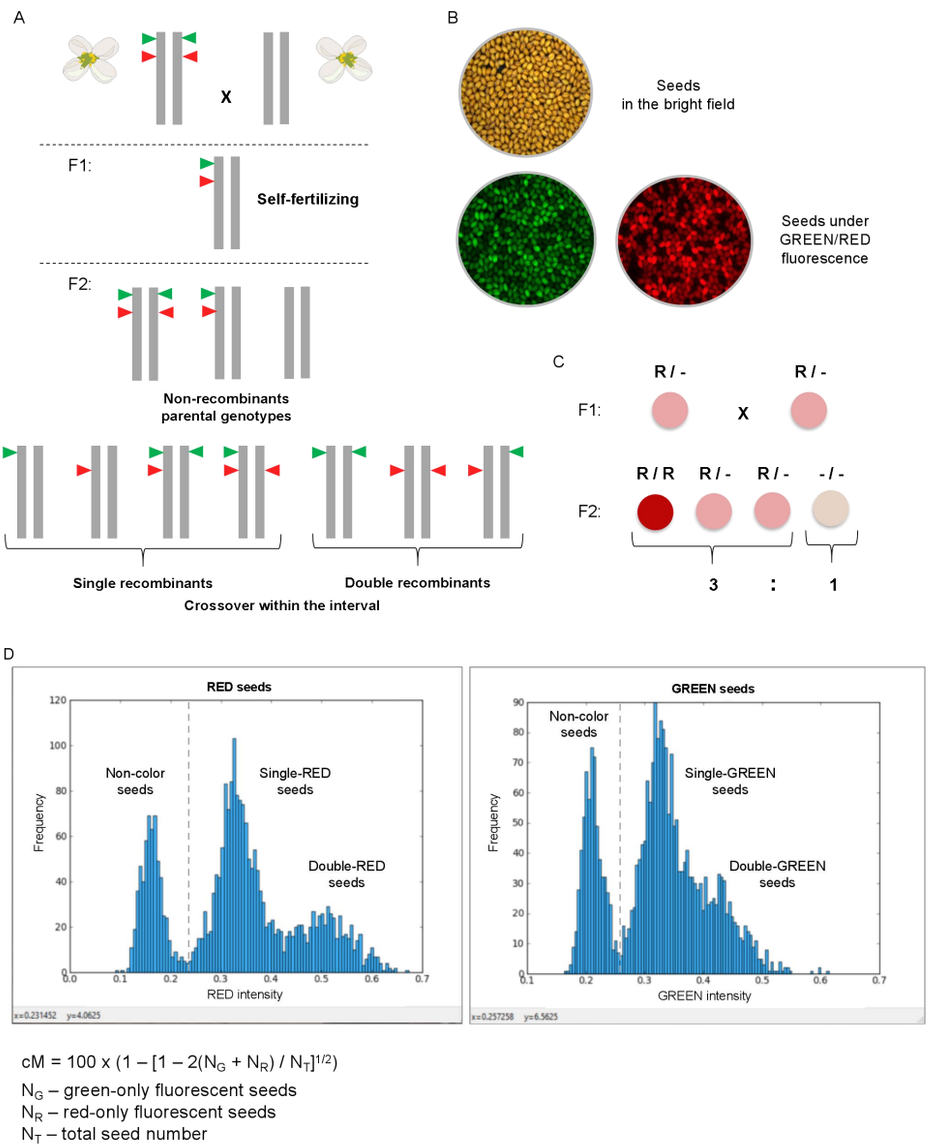

$cM = 100 \times (1 - [1 - 2(N_G + N_R) / N_T]^{1/2})$

N_G – green-only fluorescent seeds
N_R – red-only fluorescent seeds
N_T – total seed number

Figure 6. Measurement of crossover frequency using CellProfiler image analysis of FTL fluorescent seed. (A) Genetic chart exhibiting the experimental approach with a single chromosome shown for simplicity. (B) Fluorescent micrographs of seed from a self-fertilized Col-420 (RG/--) plant under red, green and bright field. (C) Segregation of red fluorescent reporter in F2 diploid seeds obtained from self-fertilized plants. (D) Histogram displaying red and green fluorescence intensity of identified seed objects. The dashed line denotes a manually set threshold between fluorescent and non-fluorescent seed. 3.2 Molecular biology methods

3.2.1 DNA extraction

Genomic DNA for genotyping was extracted from leaf tissue using the 96-well plate format. In briefly, plant tissue was ground in 1.2 ml 8-Strip reaction tubes with 200 µl of extraction buffer (200 mM Tris-HCl pH 7.5, 250 mM NaCl, 25 mM EDTA) using 3 mm glass beads and a TissueLyser II (QIAGEN). A further 200 µl of extraction buffer with 1% SDS was added, then centrifuged and the supernatant was transferred to an equal volume of isopropanol for DNA precipitation. The pellet was washed with ethanol (70%), then air dried and re-suspended in 100 µl of water.

Genomic DNA for cloning genes and making genotyping-by sequencing libraries was extracted from rosette stage leaf tissue using the modified cetyltrimethylammonium bromide (CTAB) method. To this end, approximately 200 mg of rosette leave samples were collected to Eppendorf tubes, frozen in liquid nitrogen and mechanically ground with 3 mm glass beads (for 90 seconds, at 30 Hz). Grinded samples were incubated in 700 µl of CTAB buffer (140 mM sorbitol, 220 mM Tris pH 8, 22 mM EDTA, 800 mM NaCl, 0.1% [v/v] N-Lauryl sarcosine, 0.8% [w/v] CTAB) at 65°C for 30 minutes with agitation.

An equal volume of chloroform was added to each tube after incubation and then vortexed and centrifuged at 12,000 rpm at room temperature. The upper phase was transferred to a new tube and an equal volume of isopropanol was added to precipitate DNA. The solution was centrifuged at 12,000 rpm for 20 minutes at 4°C. The supernatant was removed and the pellet washed with 70% ethanol and left to air dry. The pellet was re-suspended in a TE solution containing 100 mg/ml RNaseA at 37°C for 30 minutes. A second precipitation was performed by adding 1/10 volume of sodium acetate (3M) and 2.5 volumes of ethanol before freezing at -20°C for one hour. A final centrifugation at 4°C for 15 min produced DNA pellet which was washed with 70% ethanol and left to air dry. Finally, the pellet was resuspended in TE buffer.

3.2.2 RNA extraction

Extraction of RNA from *A. thaliana* buds and leaves was performed using RNeasy mini Kits (Qiagen) according to the manufacturer's instructions. Briefly, approximately 30-50 mg leaves or floral buds at state 9 were collected to Eppendorf tubes, frozen in liquid nitrogen and mechanically ground with 3 mm glass beads (for 90 seconds, at 30 Hz).An total of 350 µl of Buffer RLT (lysis) was added to each tube

and then mixed by pipetting. Add 350 µl of 70% ethanol to the sample and mix well by pipetting and the solution was transferred to an RNeasy Mini spin column placed in a 2 ml collection tube. The collection tube was centrifuged for 15 s at 10000 rpm and then the flow-through was discarded. The tube was then washed with Buffer RW1 and Buffer RPE. After washing, 30–50 µl RNase-free water was directly added to the spin column membrane. Transfer the column to the new tube and centrifuge to elute the RNA.

3.2.3 Plasmid DNA extraction

Extraction of plasmid was performed using GeneJET Plasmid Miniprep Kit (ThermoFisher) according to the manufacturer's instructions. In summary, 3-4 ml bacterial cultures were put in 10 ml falcon tube and centrifuged at 10000 rpm for 1 min. Discard the supernatant and re-suspend the cells with 250 µl of Resuspension Solution. 250 µl of Lysis Solution was added and then invert the tube 4-6 times. Add 350 µl of Neutralization Solution and invert the tube 4-6 times. Centrifuge 5 minutes and transfer the supernatant to the Thermo Scientific GeneJET Spin Column. Centrifuge 1 minute and then wash the spin column twice with 500 µl of Wash Solution at 10000 rpm for 1 min. After washing, 20–50 µl RNase-free water was directly added to the spin column membrane. Transfer the column to the new tube and centrifuge to elute the plasmid.

3.2.4 Chemical transformation of bacteria

Transformation of plasmid DNA into E. coli was performed using the heat shock method (Froger and Hall 2007). The Eppendorf tube containing a mixture of competent *E.coli* cells (100 µl) and plasmid DNA (50 ng) was incubated on ice for 30 minutes. After the incubation, the tube was placed at 42°C for 1 minute (heat shock) and then placed back in ice for 2 minutes. Approximately 600-700 µl of LB culture was added into the tube and the mixture culture was incubated at 37°C for 60 minutes with agitation. After incubation, Pipette 100-200 µl culture cells into a LB agar dish plate containing the appropriate antibiotic and spread the cells with a spreader. Put the plate at 37°C overnight for colonies to form.

Transformation of plasmid DNA into *Agrobacterium* was performed using freeze-thaw method (Jyothishwaran, et al. 2007). The eppendorf tube containing a mixture of competent *Agrobacterium* cells (100 µl) and plasmid DNA (100-200 ng) was incubated on ice for 5 minutes. After the incubation, the tube was transferred to liquid nitrogen for 5 minutes and then incubated at 37°C for 5mins and placed back in ice for 2 minutes. 500 µl of LB culture was added into the tube and then shake at 28°C for 2-3 hours. The cells were collected by spinning 2 minutes at 5000 rpm, and re-suspend in 100-200 µl LB. Spread them on a LB agar plate containing the appropriate antibiotic and incubated the cells for 2 days at 28°C for colonies to form.

3.2.5 Plant genotyping

For QTL mapping, simple sequence length polymorphism (SSLP) and derived cleaved amplified polymorphic sequence (dCAPS) markers for genotyping were designed using the Salk 1,001 Genomes Browser (http://signal.salk.edu /atg/3.0/gebrowser.php). To design SSLP marker, genomic sequences from Col-0 and L*er*-0 accessions were compared in the region of interest to identify deletions of size 30-250bp in Col-0 or L*er*-0. dCAPS markers were designed using the online tool dCAPS Finder 2.0 (Neff, et al. 2002). A full list of makers used in this study is detailed in Table 3.

Table 3 SSLP and dCAPS oligonucleotides used for *QTL* mapping.

Primer	Col product size (bp)	L*er* product size (bp)	Chr	TAIR10 Coordinate	Nearest gene	Sequence
4-230-F	267	209	4	230388	At4g00520	GCGTTCACCTTTAGCATTCCA
4-230-R	267	209	4	230388	At4g00520	GCAGCTACACTCATGCCCTCT
4-2450-F	242	184	4	2450565	At4g04840	GCGATGATGTGCTTAGGTTGG
4-2450-R	242	184	4	2450565	At4g04840	GGATTCAATCACATTTCTTTTCAA
4-4852-F	146	108	4	4852373	At4g08028	TGGGCCAACGACTCTGTTTA
4-4852-R	146	108	4	4852373	At4g08028	TCGTTGTCGAACAACACACC
4-8358-F	166	132	4	8358967	AT4g14560	GGATTGTGTCCCCATTCCTA
4-8358-R	166	132	4	8358967	AT4g14560	GAGAGTTTCGTGTGGCATGTT
4-9652-F	234	172	4	9652287	At4g17200	GTTGCCCACTTGTGTGGTCT
4-9652-R	234	172	4	9652287	At4g17200	TCTTGTTTGGATGTGAAATTGGA
4-10019-F	240	206	4	10019159	AT4G18050	GCCGTCAAACCAAGAATCTCG
4-10019-R	240	206	4	10019159	AT4G18050	ATCACACGCACTGAGAAGTT
4-10051-F	142	108	4	10051270	AT4G18150	CATCAGAGGCTCAAGAGAGCAGC AGTAAAGCCCCG
4-10051-R	142	108	4	10051270	AT4G18150	TCACTAAATTGGTCGGAAGAAA
4-10131-F	131	96	4	10131270	AT4G18340	GCAAAGGCACTAAGGATTTGAGGG TTAGTGTCGTC
4-10131-R	131	96	4	10131270	AT4G18340	CTTGGCATCAATTACGGACA
4-10176-F	131	96	4	10176270	AT4G18422	CGGCTGATATGATCGCCGGAACAA GAAGAAACAATCG
4-10176-R	131	96	4	10176270	AT4G18422	ATGTCTCCGACACTTGAGACC
4-10229-F	130	100	4	10229380	AT4G18570	GTTTCAATTTCATATGCTAAATGTA GGATGATT
4-10229-R	130	100	4	10229380	AT4G18570	TTGAGAGAGTAATAAAAATATGAAA AGTTTG
4-10245-F	142	104	4	10245200	AT4G18600	GGAGACTATGTGTTCATAAAAGCTT TCATCCAT
4-10245-R	142	104	4	10245200	AT4G18600	CACTGCAGGTATGGCTTTACTC

4-10256-F	142	110	4	10256200	AT4G18630	CTTTACGATGACTTAAACATTGATG ATGATACTTA
4-10256-R	142	110	4	10256200	AT4G18630	CACAAAGCCTTGGCAAGAA
4-10477-F	186	140	4	10476582	At4g19160	TTGGCTGATCGACAAAGTGA
4-10477-R	186	140	4	10476582	At4g19160	GTAGTGCATGTTGCGTTTCG
4-10847-F	254	196	4	10846502	At4g20030	TTCCCTTCTTTTGTGGCTTC
4-10847-R	254	196	4	10846502	At4g20030	CCGTCACAATCCTGACTCAA
4-11840-F	147	110	4	11840149	At4g22470	ATTTACGGCGGTTCTTGATG
4-11840-R	147	110	4	11840149	At4g22470	TTTTTGGGTTCCAACAATGTAA
4-12848-F	138	100	4	12848948	At4g24980	CTCCAAGCTCCTTGTTTTGG
4-12848-R	138	100	4	12848948	At4g24980	AATCGTCCGGTCAATCTGAG
4-12981-F	180	128	4	12981959	At4g25400	GCTGAGGTACAATATCTCGAGCTTAC
4-12981-R	180	128	4	12981959	At4g25400	GACAAGATCGAAAACATTAACAAAGT
4-14558-F	168	136	4	14558575	At4g29730	AAATCAAAACCCCATGAAAGG
4-14558-R	168	136	4	14558575	At4g29730	TTGTGGGGTGAGGGAGTTAG
4-18526-F	478	319	4	18526361	At4g39950	GACGAACAAGGCAACCCATT
4-18526-R	478	319	4	18526361	At4g39950	CCGGTTTGTTCACCATCTCC
4-10186-F	130	96	4	10186225	At4g18440	TTGACCACAACTTATAGCTCAAGAC TTAGATAGAA
4-10186-R	130	96	4	10186225	At4g18440	CAATTTATAGGTCGGTGACTTGC
4-10190-F	100	137	4	10189947	At4g18450	ACCGTCTGCATTAGTTTTCTGAC
4-10190-R	100	137	4	10189947	At4g18450	ATATGTGGTAATTGGGAAACATGTT GGGTCG
4-10193-F	115	87	4	10193856	At4g18470	GGACGTTTGTCTTCTCTTTTTGA
4-10193-R	115	87	4	10193856	At4g18470	TCTTTTGTTCATGTTCTGAATCAG CTGTCG
4-10197-F	110	148	4	10197505	At4g18465	AATTTTGATAGGAGTCAAAGGTT GCGACTTT
4-10197-R	110	148	4	10197505	At4g18465	CCCCAACAGCTATTGAGCTA
4-10203-F	120	150	4	10203354	At4g18480	GGAGAAGCCCAGATTGCAGAAGA AGATGTTCG
4-10203-R	120	150	4	10203354	At4g18480	ACCACAGAAACAAACATAAGCCA
4-10206-F	100	131	4	10206483	At4g18490	ACCACCATGGAATCAAGTTATGT
4-10206-R	100	131	4	10206483	At4g18490	TTATCCTGTATTTCTGCCTGAGT GTCGGTAC
4-10208-F	101	136	4	10208262	At4g18500	CTATCTATATATTTCTATTAAATT TGCATACT
4-10208-R	101	136	4	10208262	At4g18500	GTTTGAGTGTTCATCATGTGTCC
4-10229-F	130	100	4	10176270	AT4g18422	GTTTCAATTTCATATGCTAAATGTAGGATGATT
4-10229-R	130	100	4	10229380	AT4g18422	TTGAGAGAGTAATAAAAATATGAAAAGTTTG

For T-DNA insertion line genotyping, three primer types have been used: LP, RP (gene-defined primers) and LB (left border of T-DNA insertion). LP and RP primers produce the wild type product while LB and RP primers provide the product of T-DNA insert (Figure 7). The primers used for genotyping are listed in Table 4.

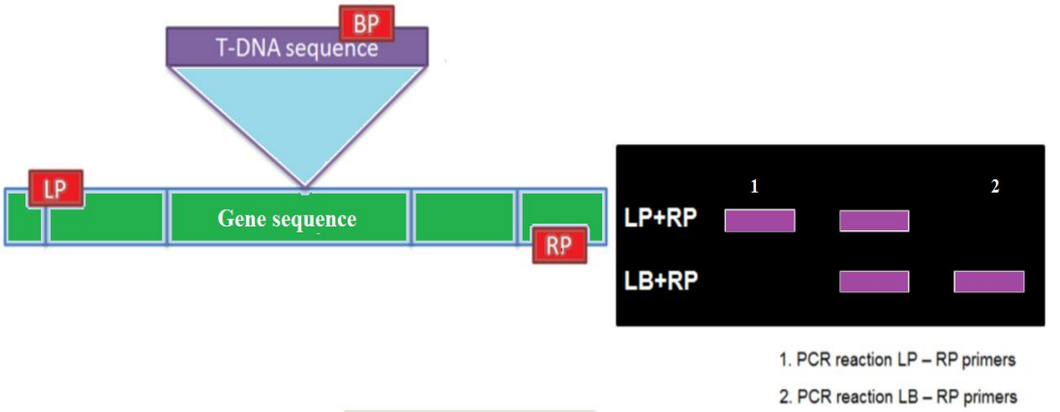

Figure 7. Scheme of the T-DNA genotyping experiment - localization of LP, RP and LB primers with PCR reaction products; Adapted from http://signal.salk.edu/tdnaprimers.2.html

Table 4 Oligonucleotides used for mutant genotyping

Primer name	Gene ID	Primer sequence	Comments
450LP	AT4G18450	AATTCTAACCGCGGCTTTATC	
450RP		CCCCTGATTTTATGTGGAACC	
460LP	AT4G18460	AATCGTATCGGAGATTGGTCC	
460RP		ACCTGCATCATAGCTCCAAAC	
SNI1-dCAPS-F	AT4G18470	TGGTTTTGTTTTGCAGGCTTGGTCACCAT	dCAPS – digestion with *Tsp509I*
SNI1-dCAPS-R		GTGAAATCTAGCTTAAGAACATGAGCAAGA	
480LP	AT4G18480	CTTCTTCCGGATTTCCTGAAC	
480RP		TTCAAAGAAGAGTGCGAGACC	
490LP	AT4G18490	TGGGTCAAGTTTGAACCCTAC	
490RP		ATTATCGCGAGATCCCATACC	
smc6a-LP	AT5G07660	ATTGATGCAGGTCGAACAATC	
smc6a-RP		GGTGATGTCTCTCAATCGCGT	
smc6b-2-LP	AT5G61460	CCATGGATGACAAAGCTCTTC	
smc6b-2-RP		CTTCACGAGATGACAGAAGCC	
asap1-LP	AT2G28130	ATCTGCTTGTGACTTTTGGTG	
asap1-RP		ATTTTCGTCGCTGTCCTGT	
nse2-2-LP	AT3G15150	AGTTCGCAGGTACAATGGATG	
nse2-2-RP		GGCTTCAACTTGTTTCATTGC	
nse4a-LP	AT1G51130	GCTCAACAGGCGGTCATTTG	
nse4a-RP		ACAAAAGCCACTTAACTGCTACA	
nse4a-BP		ATAATAACGCTGCGGACATCTAC	
mus81-LP	AT4G30870	AGTGAATCTGATAGTGAGTG	

mus81-RP		GCAGCATCAATAAGCTCTTG	
mus81-BP		GACCATCATACTCATTGCTG	
zip4-LP	AT1G56590	TTGCTACCTTGGGCTCTCTC	
zip4-RP		ATTCTGTTCTCGCTTTCCAG	
fancm-dCAPS-F	AT1G35530	ACAATATATGTTTCGTGCAGGTAAGACATTGGAAG	dCAPS – digestion with *MboII*
fancm-dCAPS-R		CACCAATAGATGTTGCGACAAT	
recq4a-F	AT1G10930	ATCAGAGCCACTCATTGTTG	
recq4a-wt-R		GTCCTGATCGTGTTGGACAG	
recq4a-mut-R		ATATTGACCATCATACTCATTGC	
recq4b-wt-F	AT1G60930	TCAGAAAGTTGCTCTGCGTC	
recq4b-wt-R		ACCAAGACCCTGCATATTGC	
recq4b-mut-F		ACTAGAGATACTTCAGGAGCTGAGC	
recq4b-mut-R		GCTTTCTTCCCTTCCTTTCTC	
spo11-1-3_F	AT3G13170	TTTCAGTGTAGTCGGTACAACTTGAATGTG	
spo11-1-3_R		CCACAACCAGTATGTACTCAGCTAAGCTAAC	
Lbb1		GCGTGGACCGCTTGCTGCAACT	
brca2awtF	AT4G00020	TGTATTGTCACTCTATTAGATAGACAGTGAGTA	For wild type
brca2awtR		TCGGTCCGCCCAGTGAGC	
brca2aTF		GTGATTGTCACTCTATTAGATAGACAGTGAGTA	For the mutant
brca2aTR		TTGGACGTGAATGTAGACAC	
brca2bwtF	AT5G01630	GCTCTGAATATCAGTAAACCTGC	For wild type
brca2bwtR		AGGAAACCTCAAGTGGTGAT	
brca2bTF		GATTTAACCATGTGAACCAGTC	For the mutant
brca2bTR		TCGGAACCACCATCAAACAG	
rad51-LP	AT5G20850	CTCCCCTTCCAGAGAAATCTG	
rad51-RP		ATGCCAAGGTTGACAAGATTG	
atr2LP	AT5G40820	GAGCAAATGCAAGAACTCTGG	
atr2RP		ACTTCAAGGGTTCCGATGTTC	
LB1.3		ATTTTGCCGATTTCGGAAC	For SALK mutants
LB3		TAGCATCTGAATTTCATAACCAATCTCGATACAC	For SAIL mutants

GK-BP		ATATTGACCATCATACTCATTGC	For GABI-Kat mutants

3.2.6 Quantitative PCR

Reverse transcription was performed with SuperScript II reverse kit (Vazyme) following with the manufacturer's instructions. *SNI1* and *PR1* expression was measured by qPCR using primers described in Table 5. The meiosis-specific gene *DMC1* was used as a control for ΔCt calculations for *SNI1* and *UBC* was used as a control for *PR1*. Three biological samples and four technical replicates per sample were used for each experiment. The 2−ΔΔCt method was used to quantify relative transcript levels in comparison with Col plants.

Table 5 Oligonucleotides used for RT-qPCR

Primer name	Gene ID	Primer sequence
qSNI1-F	AT4G18470	TCATTCTCGACGAGCTGACTT
qSNI1-R		TTCGGGTACGTACAACAGGC
qDMC1-F	AT3G22880	TGAAGAAACGAGCCAGATGC
qDMC1-R		GCGTTTATACCTTGTGCGATCA
qUBC-F	AT5G25760	CTGCGACTCAGGGAATCTTCTAA
qUBC-R		TTGTGCCATTGAATTGAACCC
qRT-PR1F	AT2G14610	CATGGGACCTACGCCTACC
qRT-PR1R		TTCTTCCCTCGAAAGCTCAA

3.2.7 Complementation of SNI1 and construction of CRISPR-Cas9 mutant in Ct background

A DNA fragment containing *SNI1* was amplified from *pGreen* vectors containing Col or L*er* genomic DNA using primers described in Table 6. The PCR products were cloned into the *pFGC* binary vector using one step cloning kit (Vazyme). These vectors were transformed into *E.coli* and plasmids were extracted. These vectors were further sent for sequencing to check the validity. After verification, these vectors were transformed into *Agrobacterium* strain *GV3101* and then transformed into Col-*420* and *sni1-1-420* hemizygous plants by floral dipping. After plant transformation, seeds were collected, sown on the soil pellets and screened with Basta. Progenies were collected from surviving plants and taken pictures to measure recombination frequency in *420* interval.

gRNA primers were designed using the online CRISPOR program (http://www.crispr.tefor.net/) (Concordet and Haeussler 2018). For *SNI1*, the genomic DNA sequence containing the first 3 exons was pasted into the program to obtain the appropriate gRNA primers. Select *Arabidopsis thaliana* as a targeting genome and

NGG as PAM to run the program. Appropriate gRNA primers should meet the following criteria based on the parameters given on the website: high specificity score, high predicted efficiency and low off-targets. Finally, a single gRNA targeted within the first exon of the gene was designed to obtain a *sni1* mutant in Ct background (*sni1-2*). The gRNA expression cassette was created by a PCR reaction using a previously constructed *pJET1.2-U6* vector containing AtU6-26 promoter and gRNA scaffold sequence as a template and primers in Table 6. PCR products were purified, phosphorylated and self-ligated before being transformed into *E.coli* to produce an entry vector containing the desired gRNA scaffold and AtU6-26 promoter sequence.

The desired plasmids were extracted and sent for sequencing to check the validity. After verification, the gRNA expression cassette was further cloned into the modified *pFGC-I2Cas9* binary vector with DsRed fluorescent reporter using one step cloning kit (Vazyme) and primers in Table 6. Then the binary vector was transformed into *Agrobacterium* strain *GV3101* and then transformed into Ct plants by floral dipping. Seeds were collected, sown on the soil pellets and screened with Basta. Transformants were genotyped in PCR reaction with primers flanking the *SNI1* gRNA target site (Table 6). PCR products with deletion bands were purified and clone into *pJET* vectors before being transformed into *E.coli*. Sanger sequencing was performed to detect deletions. Mutants with heritable deletions causing a frame shift in *SNI1* were identified and selfed. M2 plants were screened for non-DsRed fluorescent individuals without carrying the CRISPR-Cas9 construct.

Table 6 Oligonucleotides used for *SNI1* cloning in L*er* and Col accessions and SNI1 targeting in Ct (gRNA).

Primer name	Primer sequence (5'-3')
SNI1-GenomeF	ACGACGGCCAGTGCCAAGCTTTCATCAAGGGTAGGCAACG
SNI1-Genome R	TCTATCGATCAATCAGGATCCTGTAAACGATGGTCCGGTCA
PJET-F	GTTTTAGAGCTAGAAATAGCAAG
U6-SNI1-gRNA	CCGGAGCTAAAGACAGTCGCAATCACTACTTCGACTCTAGCTGT
VRF1	ATGTTACTAGATCGGGGATCCGGATGGCTCGAGTTTTCAGC
R1VF	AGAATTCCCATGGAAGGATCCTCGAGGCTGCAGGAATTCGATATCAAGC
SNI1-CheckF	CAGAGTGATGAGTGGCTATGG
SNI1-CheckR	AATTGAGTCAAAAGCTGGAAACT

3.2.6 Library preparation for Genotyping-by-Sequencing

Genomic DNA was extracted from leaves of F2 plants using CTAB method as described (see method 3.2.1). The quality of isolated DNA was verified in 1% agarose gel followed by analysis on Qubit 2.0 fluorometer with the high-sensitivity DNA quantification reagents (Invitrogen) and the quantity of DNA was normalized to 1.25ng/ul. Prior to start Tagmentaion, it is necessary to prepare the Tn5. Tn5ME-A or Tn5ME-B (Table 7) were mixed with an equal volume of Tn5MErev (Table 7)

(working stock, 50 μm, 10-20 μl aliquots for storage) and annealed with following the PCR program: 95°C 5 min， slowly cool down to 65°C (0.1°C /sec); 65°C 5 min， slowly cool down to 4°C (0.1°C /sec). Mixed the same volume of annealed linker oligonucleotides (Tn5ME-A/Tn5MErev and Tn5ME-B/Tn5MErev) and then diluted 5-fold in nuclease-free water with the addition of one volume of glycerol. Ez-Tn5 transposase (1 U/μl) was mixed with diluted oligonucleotides at 4:1 (oligo:transposase) ratio and then the mixture was shaken continuously for 30-40 min at 23 °C. After preparation of Tn5, 1 μl of each DNA sample was mixed with equal volume of Tagmentation Buffer (40mM Tris-HCl pH=7.5, 40 mM MgCl2), 0.5 μl of DMF (Sigma), 2.35 μl of Nuclease-free water (Thermo Fisher) and 0.15 μl of Tn5 (EZ-Tn5 Transposase, Lucigen).

Table 7 Oligonucleotides used for GBS library preparation.

Name	Oligonucleotide sequence
Tn5ME-A	TCGTCGGCAGCGTCAGATGTGTATAAGAGACAG
Tn5ME-B	GTCTCGTGGGCTCGGAGATGTGTATAAGAGACAG
Tn5MErev	[phos]CTGTCTCTTATACACATCT
N701	CAAGCAGAAGACGGCATACGAGATTCGCCTTAGTCTCGTGGGCTCGG
N702	CAAGCAGAAGACGGCATACGAGATCTAGTACGGTCTCGTGGGCTCGG
N703	CAAGCAGAAGACGGCATACGAGATTTCTGCCTGTCTCGTGGGCTCGG
N704	CAAGCAGAAGACGGCATACGAGATGCTCAGGAGTCTCGTGGGCTCGG
N705	CAAGCAGAAGACGGCATACGAGATAGGAGTCCGTCTCGTGGGCTCGG
N706	CAAGCAGAAGACGGCATACGAGATCATGCCTAGTCTCGTGGGCTCGG
N707	CAAGCAGAAGACGGCATACGAGATGTAGAGAGGTCTCGTGGGCTCGG
N708	CAAGCAGAAGACGGCATACGAGATCCTCTCTGGTCTCGTGGGCTCGG
N709	CAAGCAGAAGACGGCATACGAGATAGCGTAGCGTCTCGTGGGCTCGG
N710	CAAGCAGAAGACGGCATACGAGATCAGCCTCGGTCTCGTGGGCTCGG
N711	CAAGCAGAAGACGGCATACGAGATTGCCTCTTGTCTCGTGGGCTCGG
N712	CAAGCAGAAGACGGCATACGAGATTCCTCTACGTCTCGTGGGCTCGG
N714	CAAGCAGAAGACGGCATACGAGATTCATGAGCGTCTCGTGGGCTCGG
N715	CAAGCAGAAGACGGCATACGAGATCCTGAGATGTCTCGTGGGCTCGG
N716	CAAGCAGAAGACGGCATACGAGATTAGCGAGTGTCTCGTGGGCTCGG

N718	CAAGCAGAAGACGGCATACGAGATGTAGCTCCGTCTCGTGGGCTCGG
N719	CAAGCAGAAGACGGCATACGAGATTACTACGCGTCTCGTGGGCTCGG
N720	CAAGCAGAAGACGGCATACGAGATAGGCTCCGGTCTCGTGGGCTCGG
N721	CAAGCAGAAGACGGCATACGAGATGCAGCGTAGTCTCGTGGGCTCGG
N722	CAAGCAGAAGACGGCATACGAGATCTGCGCATGTCTCGTGGGCTCGG
N723	CAAGCAGAAGACGGCATACGAGATGAGCGCTAGTCTCGTGGGCTCGG
N724	CAAGCAGAAGACGGCATACGAGATCGCTCAGTGTCTCGTGGGCTCGG
N726	CAAGCAGAAGACGGCATACGAGATGTCTTAGGGTCTCGTGGGCTCGG
N727	CAAGCAGAAGACGGCATACGAGATACTGATCGGTCTCGTGGGCTCGG
S501	AATGATACGGCGACCACCGAGATCTACACTAGATCGCTCGTCGGCAGCGTC
S502	AATGATACGGCGACCACCGAGATCTACACCTCTCTATTCGTCGGCAGCGTC
S503	AATGATACGGCGACCACCGAGATCTACACTATCCTCTTCGTCGGCAGCGTC
S504	AATGATACGGCGACCACCGAGATCTACACAGAGTAGATCGTCGGCAGCGTC
S505	AATGATACGGCGACCACCGAGATCTACACGTAAGGAGTCGTCGGCAGCGTC
S506	AATGATACGGCGACCACCGAGATCTACACACTGCATATCGTCGGCAGCGTC
S507	AATGATACGGCGACCACCGAGATCTACACAAGGAGTATCGTCGGCAGCGTC
S508	AATGATACGGCGACCACCGAGATCTACACCTAAGCCT TCGTCGGCAGCGTC
S509	AATGATACGGCGACCACCGAGATCTACACGGCTACTCTCGTCGGCAGCGTC
S510	AATGATACGGCGACCACCGAGATCTACACCCTCAGACTCGTCGGCAGCGTC
S511	AATGATACGGCGACCACCGAGATCTACACTCCTTACGTCGTCGGCAGCGTC
S512	AATGATACGGCGACCACCGAGATCTACACACGCGTGGTCGTCGGCAGCGTC
S513	AATGATACGGCGACCACCGAGATCTACACGGAACTCCTCGTCGGCAGCGTC
S514	AATGATACGGCGACCACCGAGATCTACACTGGCCATGTCGTCGGCAGCGTC
S515	AATGATACGGCGACCACCGAGATCTACACGAGAGATTTCGTCGGCAGCGTC
S516	AATGATACGGCGACCACCGAGATCTACACCGCGGTTATCGTCGGCAGCGTC
S517B	AATGATACGGCGACCACCGAGATCTACACGACCGCCATCGTCGGCAGCGTC

S518	AATGATACGGCGACCACCGAGATCTACACTAAGATGGTCGTCGGCAGCGTC
S519	AATGATACGGCGACCACCGAGATCTACACATTGACATTCGTCGGCAGCGTC
S520	AATGATACGGCGACCACCGAGATCTACACAGCCAACTTCGTCGGCAGCGTC
S521	AATGATACGGCGACCACCGAGATCTACACTACTAGGTTCGTCGGCAGCGTC
S522	AATGATACGGCGACCACCGAGATCTACACTCACGGTTTCGTCGGCAGCGTC
S523	AATGATACGGCGACCACCGAGATCTACACTGTAATGATCGTCGGCAGCGTC
S524	AATGATACGGCGACCACCGAGATCTACACCACGTCAGTCGTCGGCAGCGTC

The tagmentation reaction was performed for 2 min at 55°C, then samples were put on ice with the addition of 1 µl 0.1% SDS and incubated for 10 min at 65°C. The tagmented DNA was cooled on ice and amplified using the KAPA2G Robust PCR kit (Sigma) and custom P5 and P7 indexing primers as described (Table 7). A total of 5 µl of each library was analysed in a 2% agarose gel to check the library success rate and size distribution. Samples were grouped based on the intensity of the bands and 5 µl of each library was used for pooling. The pooled samples were run on 2% agarose and the fragments of 450-700 bp were cut out and purified using GeneJET Gel Extraction Kit (Thermo Fisher). The quality of the libraries was verified with the Bioanalyzer High Sensitivity DNA Analysis (Agilent) and Qubit 2.0 fluorometer, and sequenced on HiSeq X-10 instrument (Illumina).

3.2.7 Genotyping-by-Sequencing analysis

Raw sequencing data have been demultiplexed and the quality was checked using FastQC Screen. To identify polymorphic sites for crossover identification, 100 samples from F_2 Col×Ct population were aligned to the TAIR10 reference assembly using Bowtie 2(Langmead and Salzberg 2012) and were used to call single-nucleotide polymorphisms (SNPs) by SAMtools and BCFtools that compress, sort and index data and identify variant sites, respectively. SNPs were further filtered to remove those variants located in the organelle genomes (mitochondria and chloroplast), and indels. Those SNPs with high coverage and quality were used to generate the file with variant positions.

Demultiplexed sequencing data from 305 samples from F2 Col×Ct population, and 229 samples from $Col^{sni1\text{-}1}$×$Ct^{sni1\text{-}2}$ population were aligned to Col reference genome. SAMtools and BCFtools were used to obtain read count data for previously defined variant positions in each sample, which was further written into files suitable as input for the Trained Individual GenomE Reconstruction (TIGER) CO analysis pipeline to identify the CO breakpoints (Rowan, et al. 2015). The coordinates of crossover intervals identified by TIGER were subsequently used for analysis using custom scripts in the R language (Yelina, et al. 2015). Crossovers were tallied in 500

kb windows along the five chromosomes and normalized by the number of F2 individuals analyzed.

3.2.8 Pollen-based measurements of genetic distance and crossover interference

Preparation of samples for flow cytometry was performed as described previously (Yelina, et al. 2013). Wild-type inflorescences were pooled from 4-6 individuals while the mutant pool is a collection of at least 8 individual plants due to the relatively low pollen density. The flow cytometry was performed on Guava easyCyte 8HT Cytometer (Millipore) and the events in all gates were calculated using GuavaSoft 3.3 programme (Millipore). *I3bc* line was used to cross with the mutant for measuring crossover interference (Berchowitz and Copenhaver 2008). The genetic distances in *I3b* and *I3c* intervals were calculated by dividing the sum of recombinant gametes in particular interval by total number of pollen grains. Crossover interference was calculated by counting the coefficient of coincidence, which is the ratio between the expected and the observed DCO number.

4. Results

4.1 Fine mapping of the quantitative trait locus *QTL4*

As it was already mentioned, variation in crossover rate observed in Col/L*er* populations is caused by two major recombination *quantitative trait loci* (*QTL*), one of which has been identified as *HEI10*. To exclude the effect of *HEI10* on *420* interval CO frequency, another substitution line, CCCLC (where only chromosome 4 is L*er* while the others are Col) was used and crossed with Col-*420*. This resulted in generation of an F_2 population (n=102), which all individuals were genotyped using simple sequence length polymorphism (SSLP) PCR markers (n=11) distributed throughout the previously identified *QTL4* region (Ziolkowski, et al. 2017). *QTL* mapping was performed using the R/qtl package in the R programming with the genotyping data combined with the *420* CO measurements in the F_2 population. The results revealed a strong *QTL* association between markers 4-9652 and 4-10366 with an LOD score of 31.72 (Figure 8A) and the *QTL* was semi-dominant with the Col allele (Figure 8B).

One F_2 individual, region of which is heterozygous over *QTL4*, was selected and used to construct an F_3 population (n=2280). Markers 4-8358, 4-10847, and 4-11840 were used to genotype all the individuals in the F_3 population. This allowed identification of 325 recombinant individuals with a crossover event between these markers. These recombinant individuals were further measured for *420* crossover frequency and genotyped using 16 markers in the region between markers 4-8358 and 4-11840. This narrowed the credible interval to a 53 kb region containing 26 genes (Figure 8C and D).

The progeny of F_3 population was used as a starting point for the below described PhD project. We selected one individual from F_3 and constructed an F_4 population (n=152), which was genotyped using five markers within the credible interval (makers 4-10019, 4-10131, 4-10176, 4-10229 and 4-10256). This allowed us to identify one individual fixed for L*er* upstream of the interval, which showed *420* crossover frequency equivalent to the Col/L*er* heterozygous *QTL4* level (mean=21.31 cM). An F_5 population (n=1056) was established based on the progeny of this individual and genotyped using makers 4-10193 and 4-10229. In this F_5 population, we looked for recombinants that would enable us to further narrow the credible interval. We identified a few such individuals using makers 4-10186, 4-10190, 4-10193 and 4-10203; and one of them was fixed on the other side of the credible interval. This individual, H-27, includes only a 19.5 kb Col/L*er* heterozygous region containing 6 genes, and the remainder of the genome is fixed for Col or L*er* (Figure 8E).

To confirm that the 19.5-kb interval in H-27 line contains the *QTL4*, we genotyped the progeny of this plant (n=48) using maker 4-10193 and measured *420* crossover frequency. The results showed variation in recombination frequency similar to that observed in the original Col-*420*×CCCLC F_2 population (Figure 8F).

Genotyping within the 19.5 kb interval showed that plants fixed for Col allele present an average *420* crossover frequency of 21.52 cM, whereas heterozygotes showed 23.35 cM and L*er*/L*er* homozygotes showed 25.23 cM. Therefore, we concluded that *QTL4* corresponds to one of the 6 identified genes in the 19.5 kb interval.

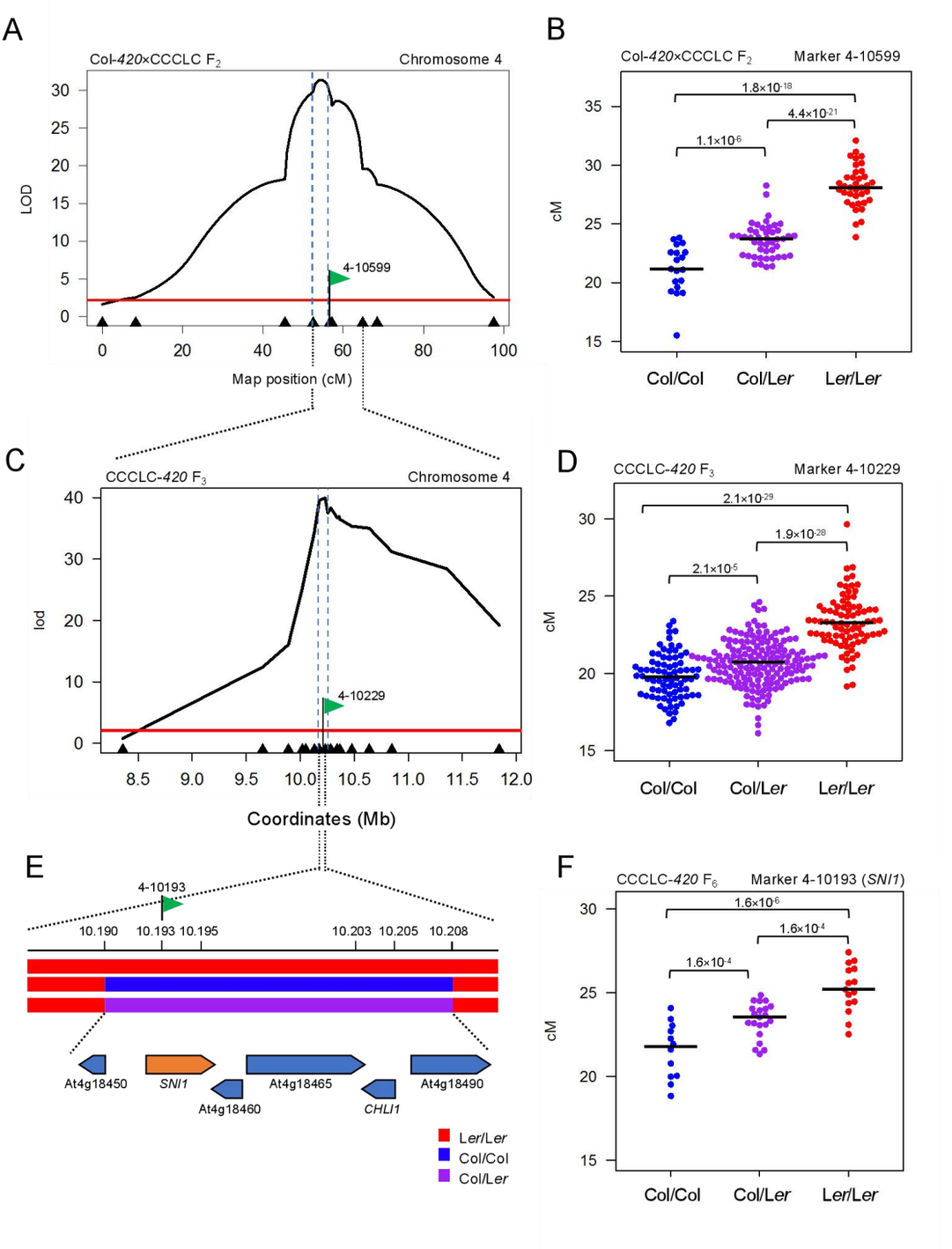

Figure 8. Fine-mapping of the *QTL4* recombination modifier locus (A) LOD scores for markers associated with *420* crossover frequency from *Col-420*×CCCLC F_2 population. X-axis corresponds to chromosome 4 genetic map with markers used for mapping indicated by

arrowheads. The red line indicates the 95% significance threshold and blue dashed lines mark the credible interval. The marker 4-10599 is labelled by a green flag. (B) Effect plots showing *420* crossover frequency for Col/Col, Col/L*er* and L*er*/L*er* individuals in the F_2 population. Each dot represents one individual. *P*-values were estimated by Welch t-test. (C) As in A, but showing the *Col-420*×CCCLC F_3 population. X-axis corresponds to chromosome 4 physical positions (Mb). The marker 4-10229 is labelled by a green flag. (D) As in *B*, but for the marker 4-10229 in the F_3 population. (E) the genotypes of progeny of the recombinant plant, which has only a 19.5-kb region segregating for Col/L*er* and the reminder of the genome being fixed. Gene models are shown beneath the genotypes. The marker 4-10193 is labelled by a green flag. (F) As in *B*, but for the marker 4-10193 in the progeny of the F_5 recombinant.

4.2 Determination of the quantitative trait locus (*QTL4*)

Since we observed a significant difference in recombination frequency between Col and L*er* allele, we hypothesized that mutation of the *QTL4* causal gene should result in a significant difference in recombination frequency of plants obtained from crosses with F_6 $^{Col/Col}$ and F_6 $^{Ler/Ler}$ plants. To test this, we performed an allelism test by crossing T-DNA mutants in all 6 genes with F_6 individuals fixed for Col/Col and L*er*/L*er* over the *QTL4* interval, aiming to determine which candidate gene is corresponding to *QTL4*.

We found that only *sni1-1* (At4g18470) showed a significant difference in *420* crossover frequency between the two crosses, strongly implying that this gene corresponds to *QTL4* (Figure 9A and B). In addition, when we compared Col and L*er* accessions, *SNI1* was the only candidate gene that showed non-synonymous substitutions in the coding sequence (Figure 9B).

Next, we measured *420* crossover frequency of homozygous mutants for the genes present in the fine mapping interval (Figure 9C). This assay was, however, not possible for *chli1* (At4g18480), which showed a very strong dwarf phenotype (Koncz, et al. 1990), and for At4g18490 due to the FTL reporter silencing. From the remaining four gene mutants, a *sni1-1* carrying an 11 bp-deletion in the *SNI1* coding sequence (Li, et al. 1999) showed a significant increase in crossovers (29.41 cM, n=12) in comparison with the wild type (21.58 cM, n=8) (Figure 9C). To confirm that the effect observed in *sni1-1* is caused by the mutation in this gene,we conducted complementation experiments on the complementation of Col and L*er SNI1* allels in *sni1-1* mutant background. To this end, genomic fragments encoding Col and L*er* alleles of *SNI1* were first cloned into a binary vector and transformed into *Agrobacterium*; then transformed into *sni1-1* homozygous mutants carrying segregating *420* reporters by floral dip mathod. In parallel, *420* segregating wild-type plants were used as a control. Both Col and L*er* alleles could fully suppressed the effect of *sni1-1* on a *420* crossover rate, which shows that it is due to the missense mutation in *SNI1*, rather than a secondary mutation (Figure 9D). We also observed a slightly while not statistically significant difference in *420* crossover frequency between $SNI1^{Ler}$ transformants and $SNI1^{Col}$ transformants.

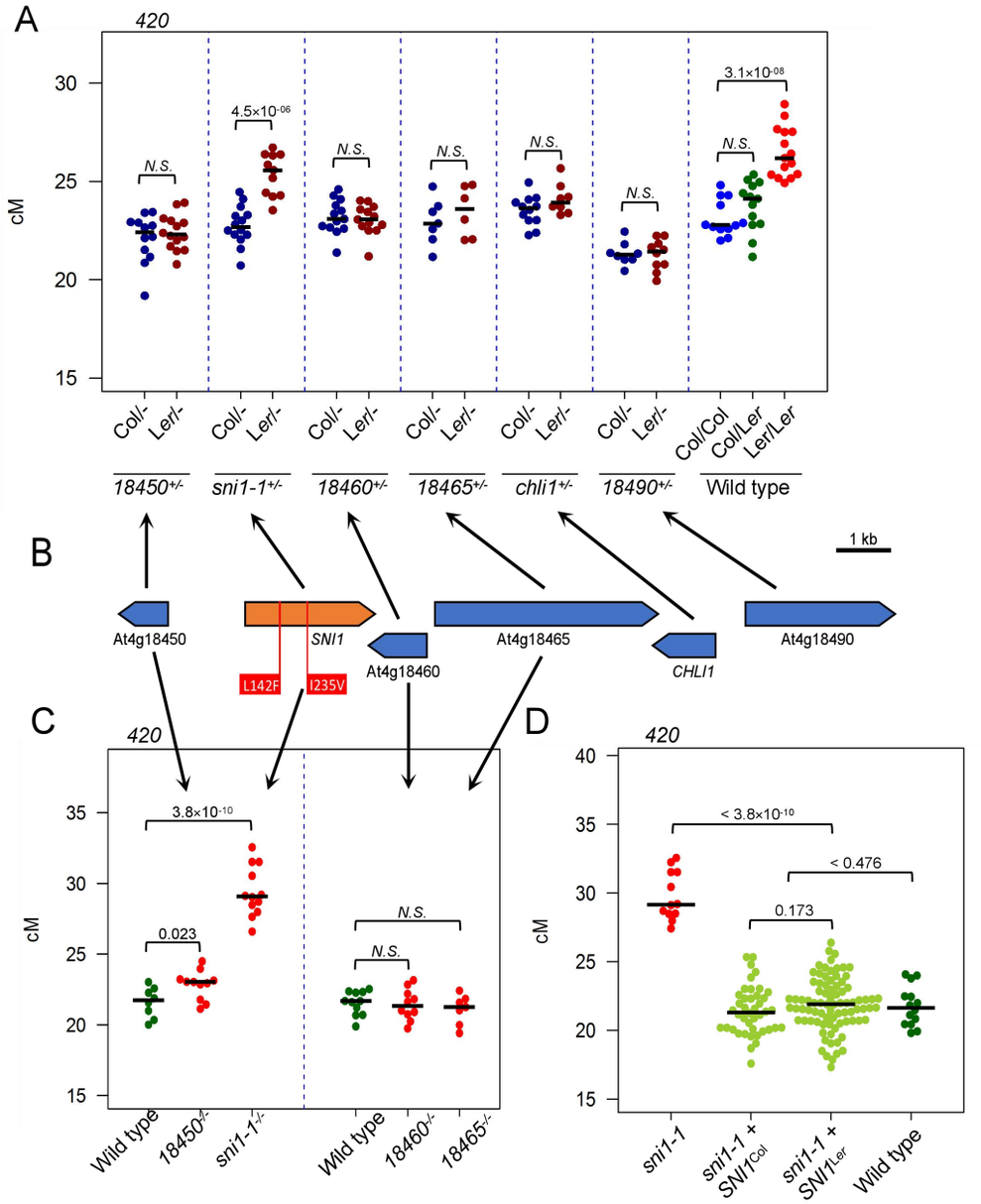

Figure 9. *SNI1* corresponds to *QTL4*. (A) *420* crossover frequency for F_1 plants obtained from the cross between mutant lines for the six genes and F6 individuals fixed for Col/Col andL*er*/L*er* over the *QTL4* interval. Wild-type F_6 individuals for Col/Col, Col/L*er* and L*er*/L*er* were measured and used as a control. Each dot represents one individual in A, C, D and E. Significance in a, c and d was assessed by Welch t-test. (B) The *QTL4* 19.5-kb Col/L*er* segregating interval containing genes with non-synonymous substitutions indicated. (C) *420* crossover frequency was measured for the mutants of genes located within *QTL4* locus. (D) Complementation of the *sni1* mutation with *SNI1* Col and *SNI1* L*er* alleles restores wild-type *420* crossover frequency in T1 generation.

4.3 *QTL*4 is determined by genetic variation in *SNI1*

To test whether the difference in crossover frequency between the Col and L*er*

allele is caused by *SNI1* expression, we performed RT-qPCR from closed flower buds, comparing *QTL4* F_6 individuals (the progeny of individual H-27). We did not observe a significant difference in expression between the Col and L*er SNI1* alleles (Figure 10A). In addition, transformation of additional *SNI1* copies to wild type Col-*420* plants did not change *420* crossover frequency (Figure 10B). These results indicated that the observed variation observed most likely does not act via mRNA expression level.

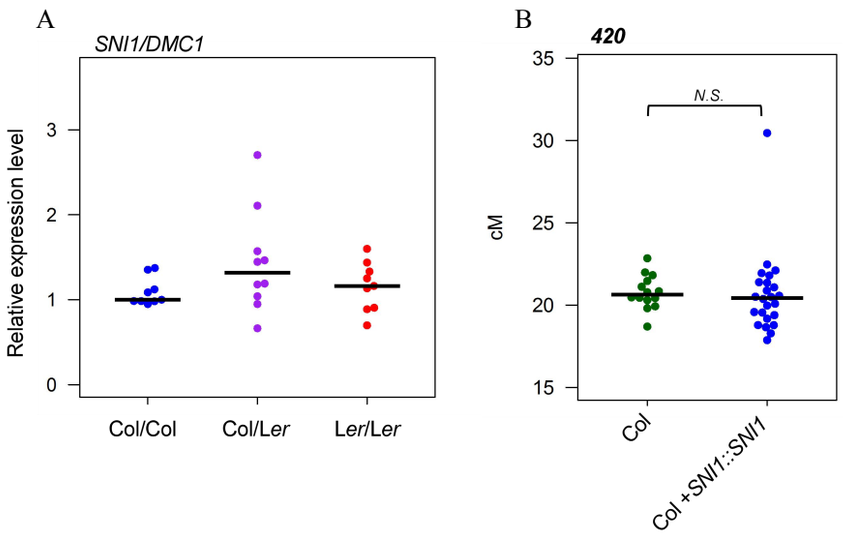

Figure 10 (A) *SNI1* transcript levels in flower buds of F_6 individuals (H-27 progeny) carrying Col/Col, Col/L*er* and L*er*/L*er* SNI1 alleles measured by qRT-PCR. Meiosis-specific gene *DMC1* was used as a reference. Each data point corresponds to one biological replicate (single plant). (B) Crossover frequency in *SNI1::SNI1*^{Col} transformants compared with untransformed Col-*420*×Col controls. Each data point represents one individual. Significance was estimated by Welch t-test.

Next, we conducted an additional experiment to explore how the two alleles might modify recombination rate under different environmental conditions. We chose temperature stress because it is the only stress described so far with a pronounced effect in terms of meiotic recombination (Modliszewski, et al. 2018). We took advantage of the fact that F_6^{Col} and F_6^{Ler} differ only in the 19.5 kb interval containing *SNI1*. We observed that the progeny of F_6 line carrying the *SNI1*^{Ler} allele was less responsive to temperature stress than the line with *SNI1*^{Col} (Figure 11). This may indicate that the natural variation in *SNI1* might evolve to modify response to growth conditions at the level of crossover recombination.

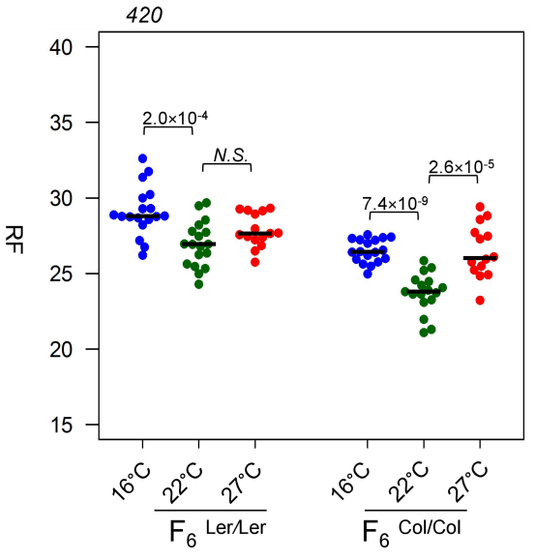

Figure 11. F_6 lines carrying *SNI1*^{Ler} is less responsive to temperature stress than the *SNI1*^{Col} as measured in the *420* interval.

As already mentioned, two non-synonymous substitutions were discovered by the comparison between the *SNI1* alleles of Col and L*er*: L142F and I235V. Therefore, we undertook an attempt to explore which of them is responsible for the meiotic recombination phenotype of *SNI1*. The first substitution is also present in Ct-1 and Mt-0 accessions, which were previously used in crosses with Col-*420* to map *QTL* (Figure 12) (Ziolkowski, et al. 2015). Because none of those mapping populations revealed *QTL* located on chromosome 4, we inferred that the second substitution, I235V, is most likely responsible for the *SNI1* recombination phenotype.

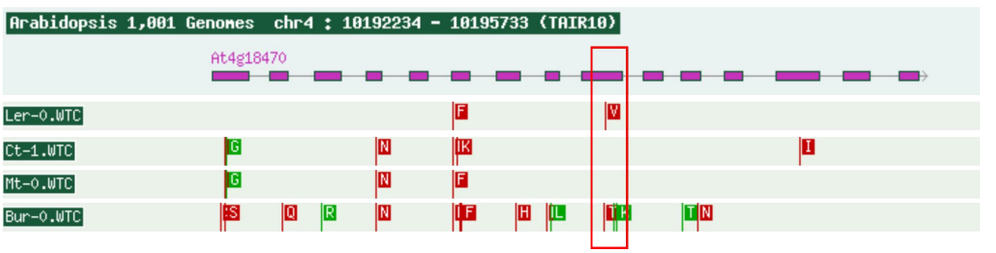

Figure 12. Polymorphisms in the *SNI1* gene. Comparison of synonymous (green) and non-synonymous (red) substitutions in the *SNI1* gene between the reference (Col) and four different *A. thaliana* accessions previously used in *QTL* mapping. Mutation at the position 235 (red rectangle) in L*er* is not present in other accessions (Ct-1, Mt-0, Bur-0), which do not show *QTL4*.

4.4 The landscape of meiotic crossovers in *sni1-1*

Next, we decided to analyze how the mutation in *SNI1* affects changes in crossover frequency and distribution in a broader scale. We crossed *sni1-1* with five different FTL reporter lines located in different chromosomes (*Col Traffic Lines*, *CTLs*)(Wu, et al. 2015). Significant changes in *sni1-1* crossover rates were observed. Specifically, we observed crossover increases in distal chromosomal regions, ranging from 23.81cM versus 19.42cM wild type (mean value, interval *CTL1.18*) to 11.8cM versus 7.8cM wild type (mean value, interval *CTL3.4*) and a reduction in the pericentromeric interval *CTL3.9* (Figure 13A). These observations suggested that there is a global redistribution of crossover frequency in *sni1-1*.

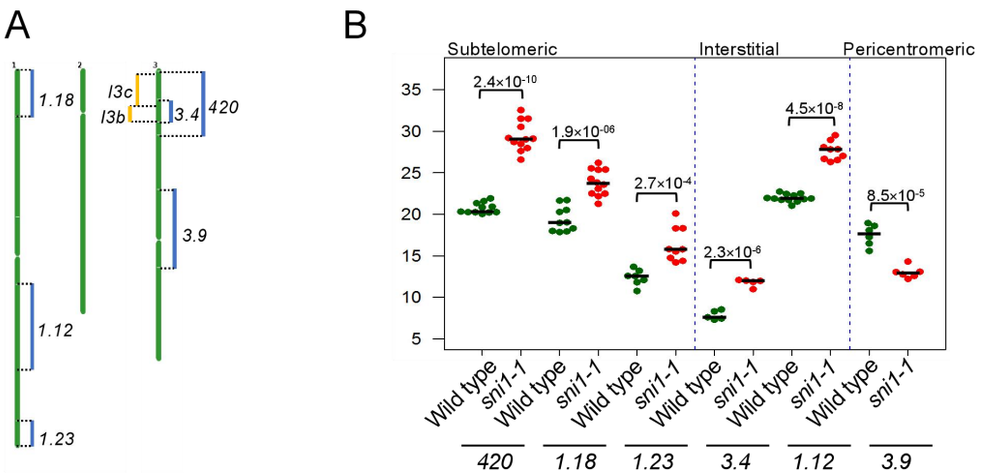

Figure 13. The *sni1* mutants exhibit a global redistribution of crossover frequency (A) Ideograms of *Arabidopsis* chromosomes 1, 2 and 3 showing the positions of fluorescent reporter intervals for seed- (blue) and pollen-based (yellow) systems. (B) Crossover frequency in the seed-based intervals as measured in wild-type (green) and *sni1-1* (red) F_2 siblings. Each dot represents single individual, Welch t-test was used to assess significance.

Next, we applied genotyping-by-sequencing (GBS) to investigate crossover pattern in the *sni1-1* mutant. This approach is based on construction of large number (usually >200) of sequencing libraries from F_2 individuals, which are further pooled and sequence at low coverage (~2×) using an Illumina platform. In GBS, identification of crossover sites is based on detection of DNA polymorphism between both parents and reflects crossover pattern in the F_1 plant. Thus, to observe the crossover landscape in the mutant background, the investigated mutation needs to be present in both parents. As *sni1* mutants in other *A. thaliana* accessions were unavailable, we used CRISPR-Cas9 strategy to create the desire mutant in the Ct-1 background. To this end, gRNAs targeting first exon of *SNI1* were designed using Geneious software. To simplify selection of mutants, one single gRNA was used, which was expected to cause a frame shift in the coding sequence. The gRNAs was ligated with *pFGC-I2Cas9* vector that contains Basta resistant gene and DsRed gene

driven by the napin promoter. This construct was transformed into Ct-1 plants by floral dip method and the T1 seeds were selected by Basta on pellets. After Basta selection, plants containing deletion products were detected by genotyping and these products were sent for sequencing to check whether the mutations could be classified as loss-of-function. A few of plants were selected to go to the next generation. One of the T_2 mutants obtained was identified as carrying a frame-shift mutation which resulted in the appearance of premature stop codon.We considered it to be a null mutant as the mutation occurred in the first exon (Figure 14), Seeds from null mutant lines were collected and further selected for non-DsRed under fluorescence microscope to eliminate the construct. This stable mutant line in Ct-1 background, which we called *sni1-2*, was crossed to *sni1-1* (Col background) to produced $Col^{sni1\text{-}1}\times Ct^{sni1\text{-}2}$ F_1 hybrids. A large number of F_2 individuals derived from *sni1* F_1 hybrids were used to explore the impact of *sni1-1* on crossovers genome-wide via genotyping -by-sequencing (GBS).

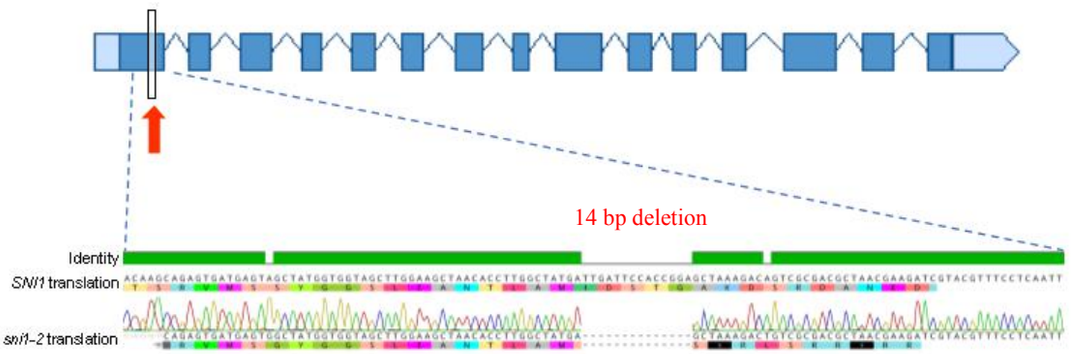

Figure 14. Representative sequencing result of a PCR-amplified genomic clone from a single homozygous plant obtained via CRISPR-Cas9 based mutagenesis. Alignment with a fragment of the reference genomic sequence of *SNI1* from Ct is shown for comparison. The deletion of 14 bp occurred in the exon 1 causing a frame shift mutation, as shown on the *SNI1* gene scheme.

A total of 229 F2 individuals were collected from the $Col^{sni1\text{-}1}\times Ct^{sni1\text{-}2}$ population and for each of them the Illumina-compatible library was constructed using Tn5 tagmentase (with the help of my colleague Maja Szymanska-Lejman). The libraries were further pooled and sent for sequencing on HiSeq X-10 machine. Following demultiplexing, the DNA sequences were aligned to the *A. thaliana* reference genome and a 2,260 crossovers per $Col^{sni1\text{-}1}\times Ct^{sni1\text{-}2}$ population were identified respectively, using the TIGER pipeline (Rowan, et al. 2015)(analyzed by my colleague Maja Szymanska-Lejman). Wild type F_2 population crossovers from Col×Ct F_1 hybrids, which were generated previously, were used as a control (Blackwell, et al. 2020). We observed a slightly higher total crossover numbers per individual in *sni1-1* than in wide type (Figure 15A), with elevated crossovers in the chromosome arms and less in the pericentromeres (Figure 15B and C).

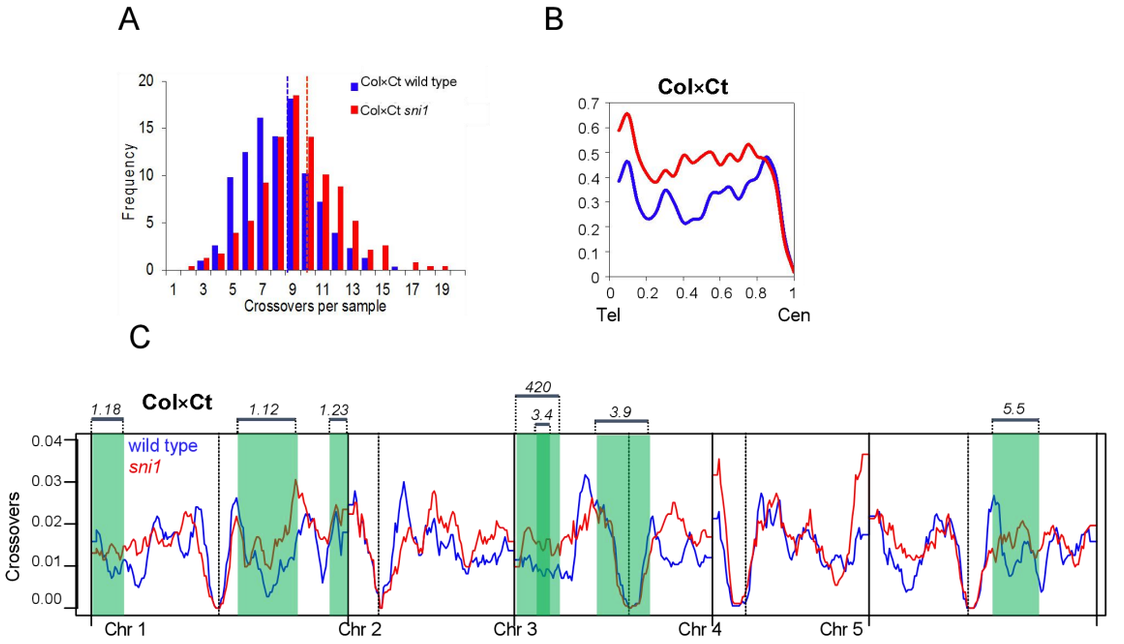

Figure 15. The *sni1* mutant exhibits elevated crossover levels in chromosome arms and subtelomeric regions but reductions in pericentromeres. (A) Histograms presenting the number of crossovers perindividual in Col×Ct (blue) and Col$^{sni1\text{-}1}$×Ct$^{sni1\text{-}2}$ (red) (bottom panel) F_2 as analyzed by GBS. Mean crossover number of eachpopulation is denoted by a vertical dashed line. (B) Crossover frequency along the proportional (scaled) length of the chromosomes from telomeres (TEL) to centromeres (CEN) in Col×Ct (blue) and Col$^{sni1\text{-}1}$×Ct$^{sni1\text{-}2}$ (red) (right panel). (C) Crossover frequency over five *Arabidopsis* chromosomes in Col×Ct (blue) and Col$^{sni1\text{-}1}$×Ct$^{sni1\text{-}2}$ (red) (bottom panel) as deduced from the F_2 populations. Interval regions used for CO measurement in this study (see Fig. 13) are denoted by green shaded rectangles, telomere regions and centromere regions are indicated by solid line and dashed line, respectively.

4.5 Crossover interference analysis in *sni1-1*

In most eukaryotes, one crossover event will inhibit crossover event in the adjacent region, which is a phenomenon known crossover interference. Fluorescent-tagged lines where two linked intervals contain three different markers (red, cyan or yellow fluorescent protein) enable to relatively easy measure crossover interference (Berchowitz and Copenhaver 2008).We crossed *sni1-1* with the three maker FTL *I3bc* line that overlaps the 420 seed interval on chromosome 3 and used it to measure male-specific crossover frequency at two adjacent intervals, *I3b* and *I3c* and calculate interference (Berchowitz and Copenhaver 2008) (analyzed by my colleague Maja Szymanska-Lejman). We observed a significant reduction in crossover interference in *sni1-1* when compared to wild type (Welch t-test *P*=1.6×10-9; Figure 16A-C).

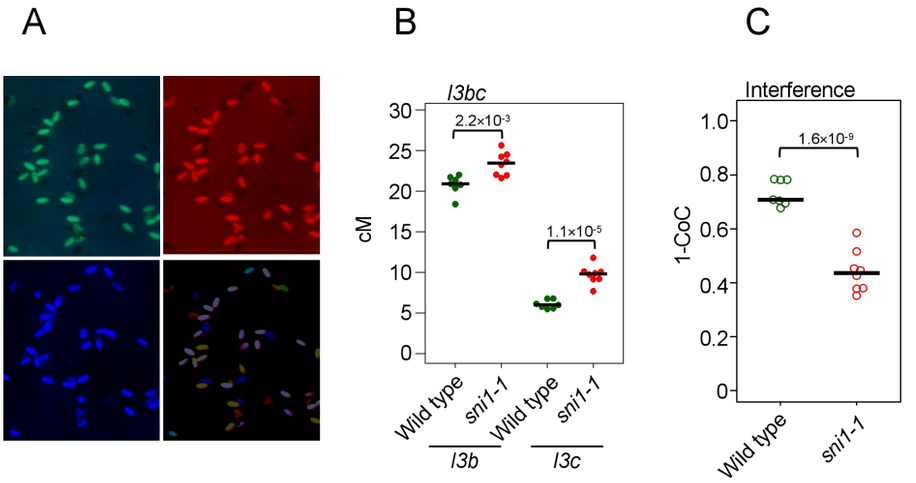

Figure 16. The *sni1-1* mutant shows a reduction of crossover interference. (A) Microphotographs of segregating I3bc pollen grains as seen in three fluorescent channels. Composite image was also shown. (B) I3b and I3c genetic distances in wild type and *sni1-1*. Each dot represents measurements from 4-10 pooled individuals. Significance was assessed by Welch t-tests. (C) Crossover interference in wild type and *sni1-1*. Significance was assessed by Welch t-tests in (B) and (C).

4.6 The meiotic recombination phenotype of *sni1* is likely not related to systemic acquired resistance (SAR)

SNI1 was initially identified in a genetic screen of *npr1* and NPR1is a regulator of the salicylic acid (SA)-mediated defense response (Li, et al. 1999). Mutation of SNI1 can *s*uppress systemic acquired resistance (SAR) (Durrant, et al. 2007).To test whether the effect of *sni1* on meiotic recombination is connected to its role in SAR, we investigated how SA, the main trigger in SAR, influences crossover frequency. Flowering Col$^{sni1\text{-}1}$-*420* and wild type Col-*420* individuals were treated with SA by spraying flowering buds (1 mM SA solution on a weekly basis). Then, we collected the closed flower buds and extracted RNA that was used for RT-qPCR assays. We observed a significant induction of *PR1* gene expression, one of the stress response markers, which indicated that SA successfully triggered SAR (Figure 17A). Next, we measured *420* crossover rate in these plants. Neither *sni1-1* nor wide type showed any change in any change in *420* crossover frequency, suggesting that the effect on meiotic recombination observed in the *sni1-1* mutant is not linked with the *SNI1* role in SAR (Figure 17B).

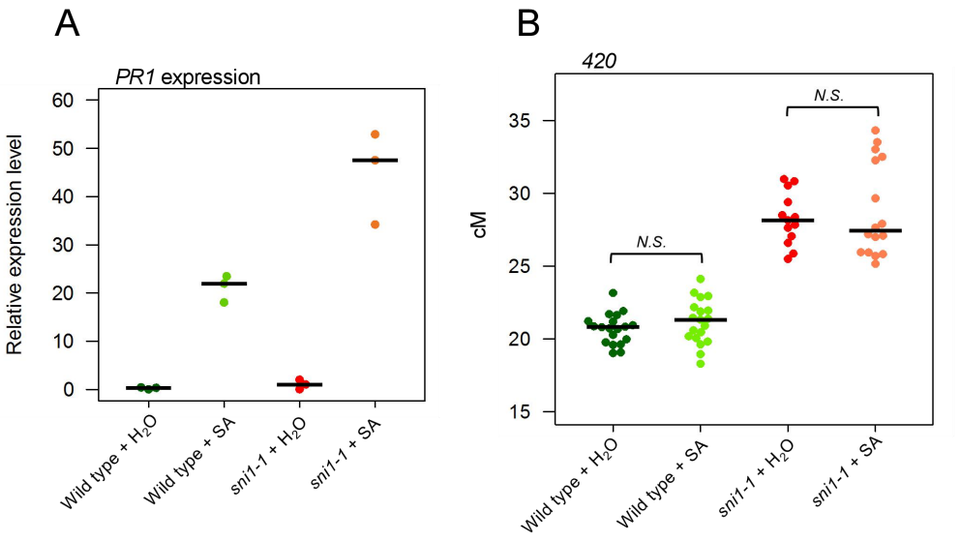

Figure17. Recombination phenotype of the *sni1-1* mutant is unrelated to the *SNI1* role in SAR pathway. (A) *PR1* transcript levels in flower buds of wild-type (Col) and the *sni1-1* mutant plants treated with 1 mM SA measured by qRT-PCR. Each dot represents one biological replicate. Meiosis-specific *DMC1* gene was used as reference. (B),*420* crossover frequency (cM) in wild-type (Col-0) and *sni1-1* plants treated with 1 mM SA. Water-sprayed plants were used as control. Welch t-test was used to verify significance in (B).

Recent studies have shown that mutation in some DNA repair genes such as *BRCA2* and *RAD51* as well as *ATR*, could partially suppress the retarded growth of *sni1-1* (Durrant, et al. 2007; Wang, et al. 2010). In the background of the reporter *420,* double mutants *sni1-1 rad51*, *sni1-1 brca2a*, *sni1-1 brca2b* and *sni1-1 atr* were generated to investigate whether they have an effect on the meiotic phenotype of *sni1-1*. We observed that the *sni1-1* mutation was not able to suppress the sterility phenotype of *rad51* (Figure 18A) and no suppression of recombination was observed in the remaining double mutants (Figure 18B). Interestingly, we observed a further increase of *420 recombination* frequencies in the *sni1-1 atr* mutant and no improvement in the fertility of the double mutant compared to *sni1-1,* measured by seed set, suggesting that the meiotic recombination phenotype of *sni1-1* is independent of *ATR* (Figure 18C and D).

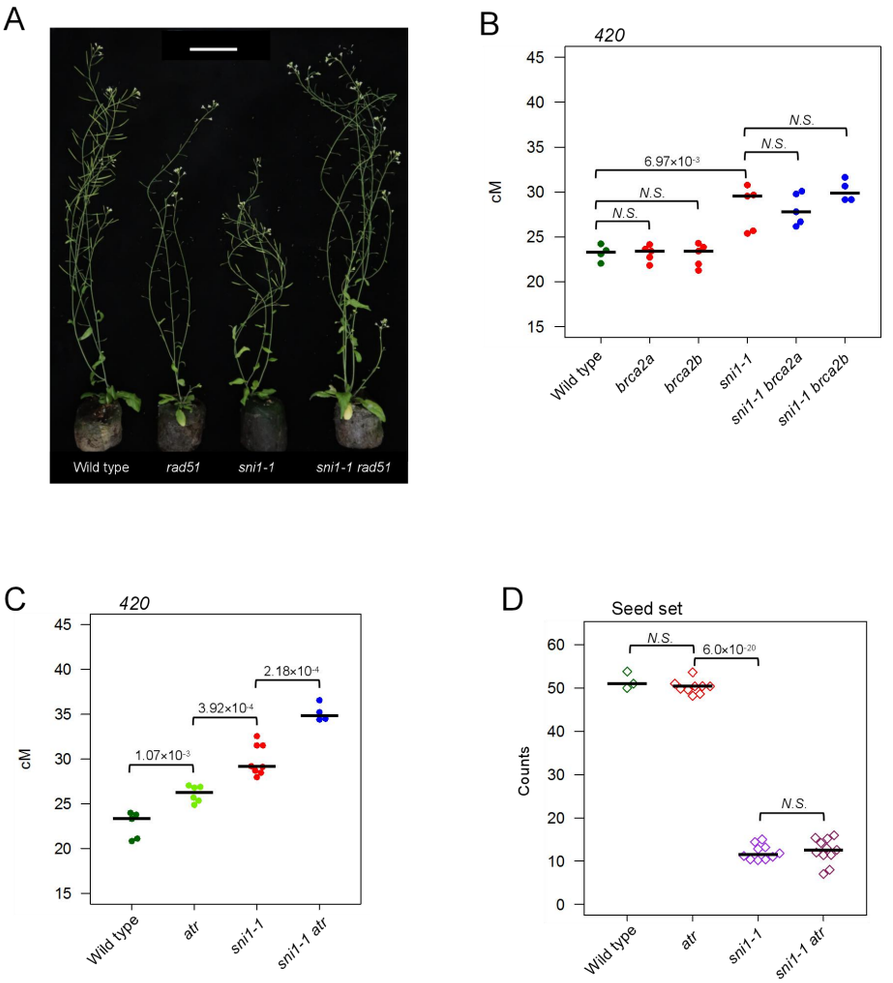

Figure 18. Mutations that suppress *sni1-1* vegetative phenotype fail to suppress its meiotic phenotype. (A) *sni1-1 rad51* double mutant plants remain sterile. Bar, 5cm. (B) *sni1-1 brca2a* and *sni1-1 brca2b* double mutants show *420* crossover frequency not different from the *sni1-1* single mutant. (C) *sni1-1 atr* double mutant shows elevated *420* crossover frequency when compared to the *sni1-1* single mutant. (D) *sni1-1 atr* show similar seed set as *sni1-1*. Significance was assessed by Welch t-tests.

Plants have evolved different cell types that can recognize and respond to pathogens. The plant innate immune system is the first line of inducible defense against invading pathogens. Surface localized pattern recognition receptors (PRRs) and intracellular nucleotide binding leucine rich repeat (NLR) receptors are examples of plant innate immune receptors (Dodds and Rathjen 2010).Mutation in *EDS1*, the NLR signaling component, could partially suppress immunity-related phenotypes of *sni1*. In the double homozygous mutant *sni1 eds1-2,* plant growth is partially restored and transcript accumulation of *PR1*, is abolished (Rodriguez, et al. 2018). Therefore, we crossed *sni1-1-420* line with *eds1-2* to test whether the meiotic phenotypes of *sni1* are dependent on *EDS1* (with help of my colleague Julia Dłużewska). We did not observe a significant difference in crossover frequency between *sni1* and *sni1 eds1-2*

double mutant (Figure 19), indicating a probable independence of the meiotic recombination phenotype of *sni1* from *EDS1*. This result again supports our hypothesis that the meiotic phenotype of the *sni1* mutant is not related to the role of *SNI1* in SAR.

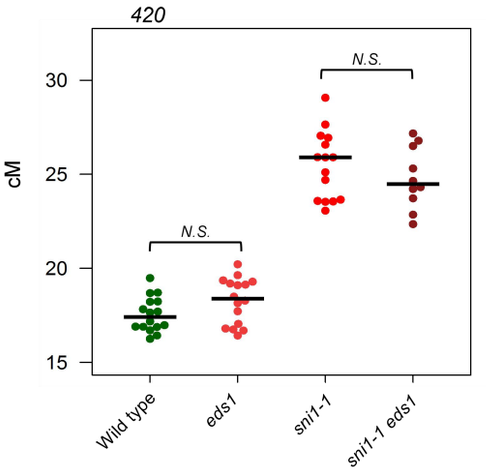

Figue.19. The *420* crossover frequency in wild-type (Col-0), *eds1*, *sni1-1* and *sni1-1 eds1* plants. Each dot represents one individual. Statistical significance was tested with Welch t-test.

4.7 Mutation of *SNI1* is not capable of restoring fertility of *spo11*

Previous work reported elevated numbers of somatic DSBs in the *sni1* mutant, which were due to inefficient DNA damage repair (Yan, et al. 2013).Therefore, the cause of the increase in the crossover rate in the *sni1* mutants might result from the formation of additional DNA double-strand breaks, which are independent on the meiosis-specific DSBs generated by the SPO11 endonuclease. To test this hypothesis, we created a double *sni1-1 spo11-1* mutant. The double mutant was sterile showing that *sni1-1* mutation is not able to restore fertility in *spo11-1* (Figure 20), indicating that DSB formation occurs normally in *sni1-1* and the mutant does not produce SPO11-independent DSBs that could be repaired as crossovers.

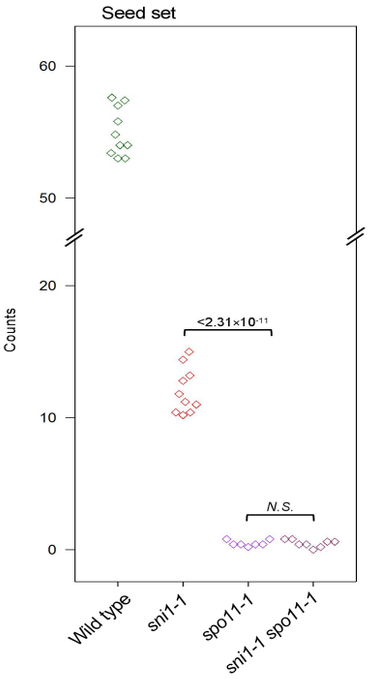

Figure 20. Seed set of the *sni1-1 spo11 double* mutant compared to wild type and both single mutants. There is no difference in seed set between *sni1-1 spo11-1* and *spo11-1*, indicating that fertility of *sni1* depends on SPO11-dependent DSBs.

4.8 Meiotic recombination of other components of the SMC5/6 complex

SNI1 was previously identified as a component of SMC5/6 complex and a homolog of NSE6 (Yan, et al. 2013). If the meiotic phenotype of the *sni1* mutant is related to the role of this protein in the functioning of the SMC5/6 complex, then mutants of the other SMC5/6 complex components should show similar phenotypes. In *A. thaliana*, all homologues of the SMC5/6 complex subunit homologues have been identified that are either embryonic lethal or show strongly disruptive development, resulting in partial or complete sterility (Figure 21A). Many proteins of the SMC5/6 complex are encoded by two functionally redundant genes in *A. thaliana*. For instance, *SMC6* is encoded by two functionally redundant copies, namely, *SMC6A* and *SMC6B* and mutations in either of these genes do not induce any visible phenotype, while the simultaneous shutdown of both genes is embryolethal (Watanabe, et al. 2009). In turn, *NSE4* is encoded by two functionally non-redundant copies, *NSE4A* and *NSE4B*, where *NSE4A* is significantly more highly expressed than *NSE4B* and mutation of *NSE4A* shows a fertility defect.

We backcrossed mutants of *NSE4A*, *ASAP*1 (homolog of *NSE5*), and a combination of mutants for *SMC6A* and *SMC6B* subunits to the Col-420 reporter line in order to asses crossover frequency. Crossovers were dramatically elevated in the *nse4a* mutant (30.71 cM; Figure 21A). Since *asap1* is sterile and *smc6a smc6b* double

mutants are lethal in the homozygous state, which prevents measurement of recombination frequency, we thus tested the effect of mutation in the heterozygous state. We detected a significant crossover increase from 21.06 to 23.22 cM in the *ASAP1/asap1* heterozygotes (Figure 21B). Of the *smc6* mutants tested, *smc6a* did not showed any effect on crossover frequency, whereas *smc6b* showed a though slight significant increase (24.13 cM). We also constructed *smc6a smc6b* sesquimutants (one mutation being homozygous and the other heterozygous) and observed a similar increase in 420 crossover frequencies as the single *smc6b* mutant (22.16 cM and 23.35 cM, respectively). These results showed consistent changes in crossover frequencies with those observed in the *sni1-1* mutant. The smaller effects in these mutants can be explained by the fact that in these cases, unlike in *SNI1*, there is not a complete lack of the protein in question.

In addition to *SNI1*, mutants of *NSE2* are also viable in *A. thaliana* and produce enough seeds, which allow us to assess crossover frequency using FTL reporters. NSE2 is located on chromosome 3, within the interval 420; therefore it was not possible to use this FTL to test for potential changes in recombination frequency. Instead, we crossed *nse2-2* with CTL1.23 and CTL3.9, which represent a subtelomeric and pericentromeric interval, respectively (interval locations showed in Figure 13A). The *nse2* mutant showed significant changes in both intervals compared to the wild type (Figure 21C) (CTL1.23: wild type 12.0 cM, *nse2* 15.1 cM; CTL3.9: wild type 16.9 cM, *nse2* 13.4 cM), which is consistent with those observed in *sni1-1* (CTL1.23: *sni1-1* 15.9 cM ; CTL3.9: *sni1-1* 13.0 cM).

We also generated double *sni1-1 nse2* and *sni1-1 nse4a* mutants, both of which showed severe developmental abnormalities and did not flower (Figure 21D). This indicates that the lack of several components of the SMC5/6 complex leads to a complete loss of its function, which is lethal. Altogether, out data strongly support a hypothesis that the meiotic recombination phenotype of the *sni1* mutant is a consequence of loss of the SMC5/6 complex functionality.

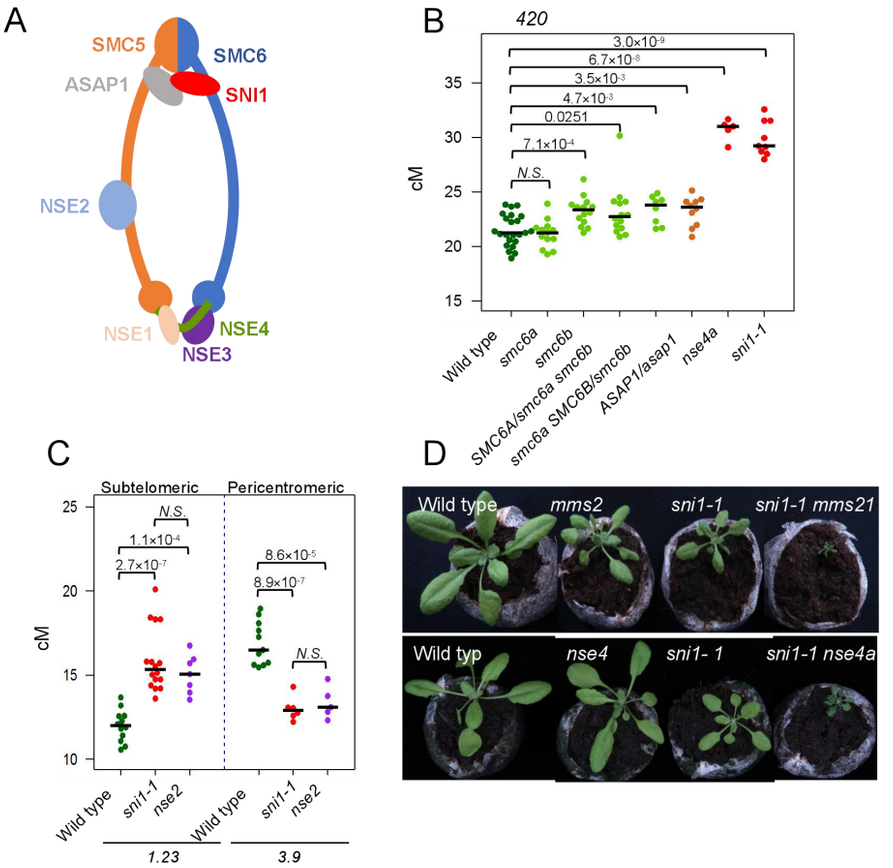

Figure 21. The meiotic phenotype of the SMC5/6 complex mutants. (A) Schematic representation of the SMC5/6 complex. (B) *420* crossover frequency in SMC5/6 complex mutants. (C) CTL1.23 and CTL3.9 genetic distances (cM) in wild type, *sni1* and *nse2-2*. Significance in B-C was assessed by Welch t-test, each dot represents one individual.(D) Three weeks old representative plants of *mms21*, *sni1-1*, *sni1-1 mms21, nse4a*, *sni1-1* and *sni1-1 nse4a* mutants compared to wild type plants.

4.9 Genetic interaction between crossover factors and *SNI1*

In budding yeast, SMC5/6 complex affects the activity of two helicases, which apart from their somatic functions act as anti-crossover factors by inhibiting D-loop formation (Xaver et al. 2013, Copsay et al. 2013). Therefore, we wanted to check whether the elevated crossover number observed in *sni1* is also connected with DNA helicase activity. For this purpose, we crossed *sni1-1* with mutants of *RECQ4* (this gene has two functionally redundant copies in *A. thaliana*, *RECQ4A* and *RECQ4B*) and *FANCM*. The triple mutant plants *sni1-1 recq4a recq4b* died early after germination (Figure 22A) and the same was observed for *sni1 RECQ4A*/*recq4a recq4b* mutant. The lethality of triple mutants resemble the synthetic lethality of triple mutants, in which *recq4a recq4b* mutations were combined with the mutation of Class II crossover endonuclease MUS81 (Hartung, et al. 2006). Therefore, we crossed *sni1-1* with *mus81* and observed that the double mutants are also lethal (Figure 22B).

Synthetic lethality of these two types of triple mutants indicates somatic roles *SNI1* and its requirement for survival in condition when both RECQ4 and MUS81enzymes are not available. However, it does not allow verifying interdependence of SNI1 and RECQ4 or MUS81.

Next, we crossed *sni1-1* with *fancm* to test the genetic interaction. In *Arabidopsis,* the *FANCM* mutation causes a dramatic increase in the frequency of recombination via the Class II crossover pathway (Crismani, et al. 2012a). The resulting *sni1-1 fancm* double mutant did not suppress the developmental phenotypes of *sni1-1* (Figure 22C), We compared *420* crossover recombination in both single mutants to the double *sni1-1 fancm* mutants and observed an additive effect of the two mutations (29.41 cM in *sni1-1* and 34.78 cM in *fancm* and 40.93 cM in *sni1-1 fancm*) (Figure 22D). These results indicated that increase in crossovers observed in *sni1-1* mutants is likely independent from *FANCM*.

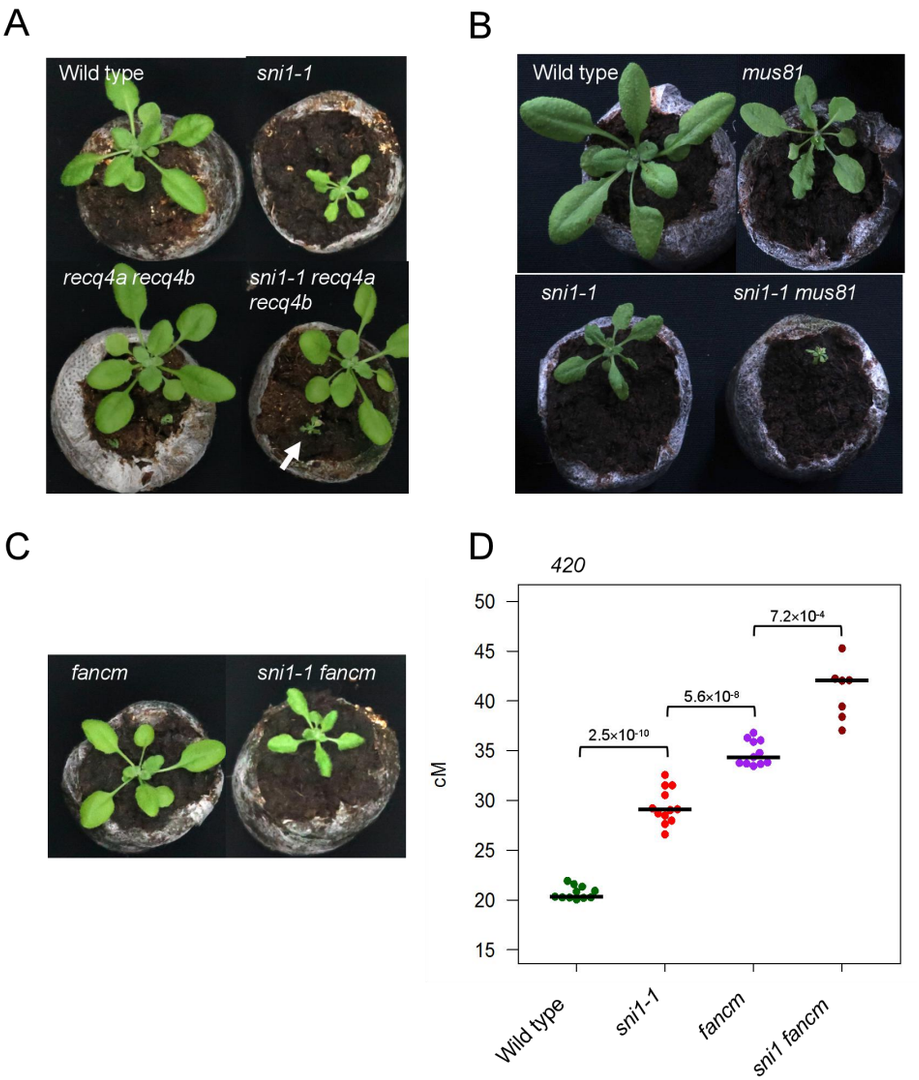

Figure 22. The genetic interaction between *sni1-1* and crossover factors. (A) Synthetic lethality of *sni1-1 recq4a recq4b* (marked by an arrow). (B) Synthetic lethality of *sni1-1 mus81*. (C) Three weeks old representative plants of *sni1-1*, *fancm*, *sni1-1 fancm* compared to wild type. (D) *420*

crossover frequency in wild-type, *sni1*, *fancm* and *sni1 fancm* plants. Significance was assessed by Welch t-test, each dot represents one individual.

4.10 The *sni1-1* mutant can partially restore fertility to Class I pathway mutants

Since a significant reduction in crossover interference was observed in *sni1-1*, we hypothesized that the increase in *420* crossover frequency in *sni1-1* is caused by a higher number of Class II crossovers. If this is so, we would expect *sni1-1* to partially restore fertility to Class I pathway mutants where Class I crossovers are switched off (Mercier, et al. 2015). To test this, we crossed *sni1-1* with *fancm zip4* and with my colleague dr Alexandre Pelé we analyzed pollen viability, silique length and seed set in the double and triple mutants (Figure 23A-C). For all the traits analyzed, *sni1-1* exhibits reduced values compared to wild type, indicating that the fertility is decreased in this mutant (Figure 23A-D). However, we observed significantly higher fertility in the *sni1-1 zip4* double mutant than in the *zip4* single mutant, supporting the hypothesis that crossover elevation observed in the *sni1-1* mutant results from additional Class II events (Figure 23A-C). Interestingly, we found that the *fancm* mutation is not able to completely restore fertility in the *zip4* mutant when *sni1-1* mutation is present (Figure 23A-C). This is likely due to other meiotic abnormalities observed in the absence of SNI1, including anaphase I bridges and chromosome fragments, which were reported by Nadia Fernández-Jiménez and Mónica Pradillo (Zhu, et al. 2021).

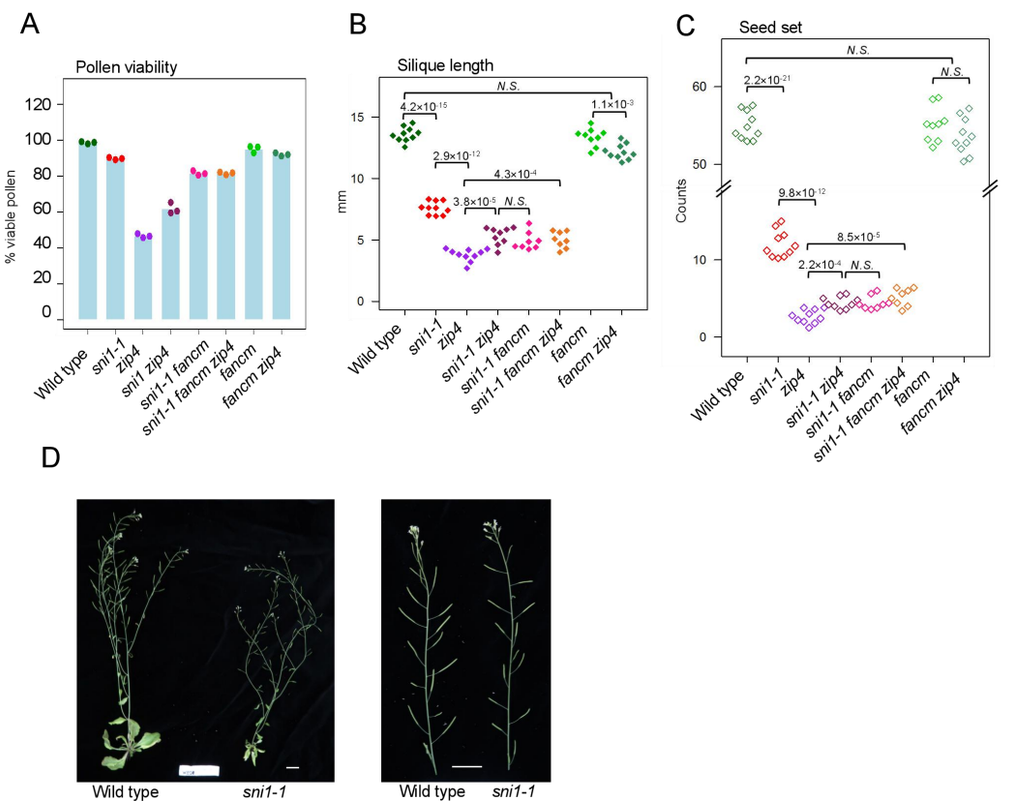

Figure 23. SNI1 affects Class II crossover repair.(A-C) Fertility assays in *sni1-1, zip4, fancm* mutants and their combinations as assessed via pollen viability (A) silique length (B) andseed set (C) Significance was assessed by Welch t-test. (D) Reduced size and fertility of *sni1-1* mutant plant in comparison with wild type. Primary inflorescences (right panel) are shown. Bar 2 cm.

5. Discussion

5.1 Identification of SNI1 as a novel modifier of recombination

We identified SNI1, a protein that was previously found as a component of the SMC5/6 complex (Yan et al. 2013), as a modifier of crossover frequency in the model plant *A. thaliana*. This finding indicates that SMC5/6 complex, which plays multiple roles in somatic cells during DNA damage repair, replication fork restarting, and telomere maintenance (Diaz and Pecinka 2018), is also involved in meiotic recombination. Most subunits of SMC5/6 complex are highly conserved and the complex is essential across eukaryotes. However, NSE6 (functional homolog of SNI1), together with NSE5 (functional homolog of ASAP1), forms a module in yeast, which is not permanently bound to the SMC5/6 complex (Bustard, et al. 2012).Therefore, the absence of NSE6 could be tolerated in many organisms including fission and budding yeast, vertebrate cells, and plants (Bustard, et al. 2012; Pebernard, et al. 2006; Raschle, et al. 2015). Furthermore, although SNI1 protein shows structural similarities among different organisms, which includes several armadillo repeat domains, the amino acid sequence of SNI1 is poorly conserved (Mosher, et al. 2006). These data suggest that SNI1/NSE6 is more susceptible to variation, which is likely a reason why this gene can act as a modifier of recombination.

HEI10, a conserved ubiquitin E3 ligase, was previously identified as a natural crossover recombination modifier in Col×L*er* population (Ziolkowski, et al. 2017). The introduction of additional copies of *HEI10* could boost crossover in wild-type, suggesting that HEI10 is a dosage-sensitive modifier, which may underlie the association with crossover variation. However, the transformation of additional *SNI1* copies is not sufficient to boost crossover frequency (Figure 8B), opposite to HEI10, indicating that *SNI1* is not dosage-sensitive, which is different from HEI10. In an attempt to understand the molecular basis of phenotypic differences between Col and L*er* alleles of SNI1, we modeled both alleles using I-TASSER server and observed a structural difference between both isoforms close to the substitution site (Figure 24), suggesting that the SNI1 protein structure may underlie the association with crossover variation. However, this analysis is based on a structure simulation and should be treated with caution. It is interesting to note that the $SNI1^{Ler}$ allele resembles the *sni1-1* mutant in that it exhibits an increased frequency of 420 crossover rate, which may suggest that it has reduced functionality.

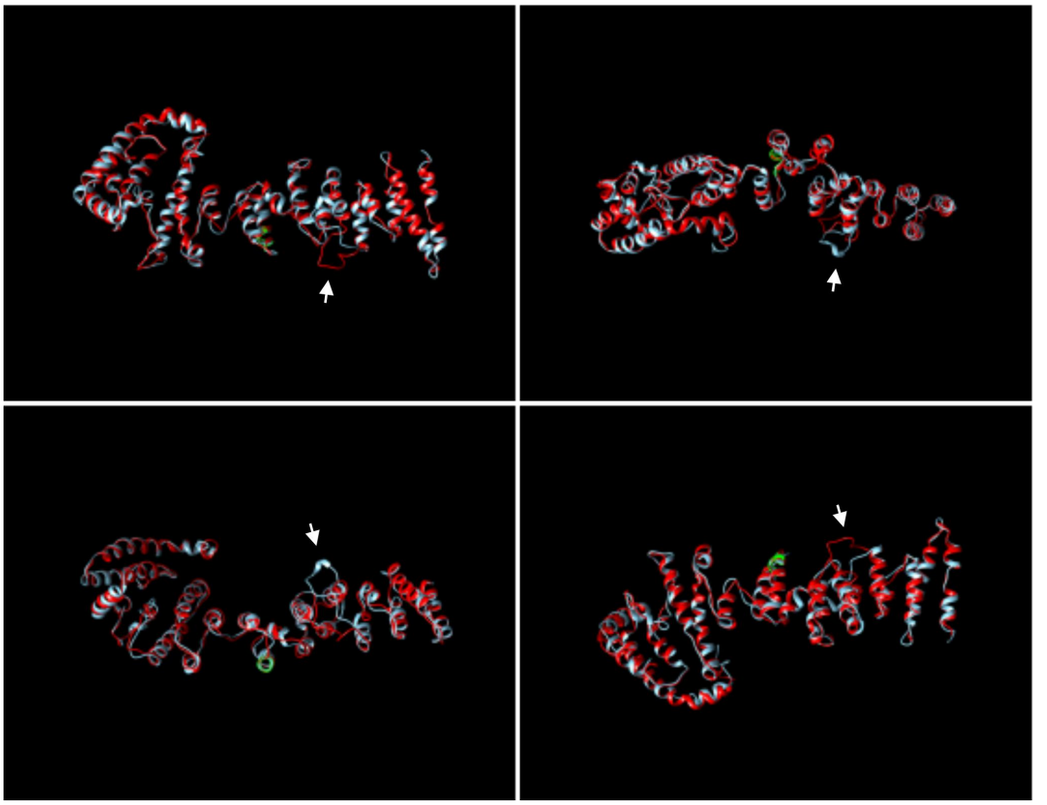

Figure 24. The 3D structure of Col (red) and L*er* (light blue) isoforms of *SNI1* as predicted by the I-TASSER server and aligned in Chimera. The position of I235V mutation was labelled in green while structural difference was indicated by arrows.

5.2 Meiotic chromosome formation in *sni1-1*

The structural maintenance of chromosome (SMC) complexes are crucial for chromosome organization, and thestructure and function of cohesin, condensin, and the SMC5/6 have been characterized in diverse systems (Haering, et al. 2002; Losada and Hirano 2005; Yuen and Gerton 2018). In yeast, the cohesion complex includes three core, essential subunits, namely, SMC1 and SMC3, and one non-SMC protein, Scc1 (Figure 25). These subunits form a ring structure by interacting with each other (Haering, et al. 2008). In addition, there are several proteins that associate with the cohesin ring, including two essential HEAT proteins, Scc3, Pds5 and Wpl1 (Haering, et al. 2002; Kulemzina, et al. 2012; Muir, et al. 2016). Cohesin is a component of the chromosome axis that binds sister chromatids and organizes them into multiple chromatin loops, depletion of which results in the premature separation of sister chromatids due to sister chromatid cohesion defects (Nasmyth 2011). Recently, the variation in REC8, a meiosis-specific component of cohesin, has been reported as causative for genome-wide recombination rates variation in even-toed ungulates and plants (Johnston, et al. 2016; Sandor, et al. 2012; Wright, et al. 2015). Anchoring chromatin loops to the axis with REC8-cohesin leads to local exclusion of the

recombination machinery and promotes intersister repair of DSBs (Lambing, et al. 2020).

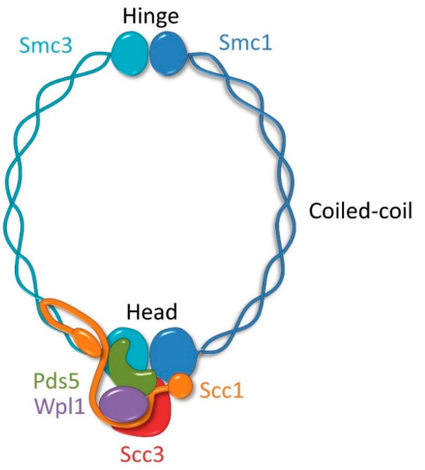

Figure 25. The structure of cohesin in yeast. Cohesin is composed of Smc1 and Smc3 proteins that contain two globular domains, called the hinge and the head, separated by a long coiled-coil domain. Pds5 and Scc3 are stably bound cohesin subunits that interact with cohesin through Scc1. Wpl1 binds to cohesin only temporarily through Scc3, Pds5, Scc1, and Smc3, (Robert Wysocki et,al, 2018)

The proposed overall structure of cohesin, which is reminiscent to the SMC5/6 complex, and genome-wide recombination rates variation caused by REC8, prompted us to hypothesize that like cohesin, the SMC5/6 complex could also affect recombination by influencing the chromosome structure at meiosis, especially at the level of synaptonemal complex (SC) formation. To test this possibility, we established a collaboration with Mónica Pradillo group (Universidad Complutense de Madrid, Spain), who examined ZYP1 (ZIP1 homolog) and SYN1 (REC8 homolog) synaptonemal complex (SC) components in the wild type and *sni1-1* (Figure 26). They found that synapses in the *sni1-1* mutant are normal without apparent cohesion failures, indicating that SNI1, the subunit of SMC5/6 complex, is not necessary for the proper formation of the meiotic chromosome axis and sister chromatid cohesion. On the other hand, in yeast the SMC5/6 complex, similarly to cohesin, can hold two sister chromatids inside its ring, aligning them and promoting homologous recombination (Kegel and Sjogren 2010) Therefore, further studies are required to test if there is an interaction between the cohesin and SMC5/6 complex during meiotic recombination.

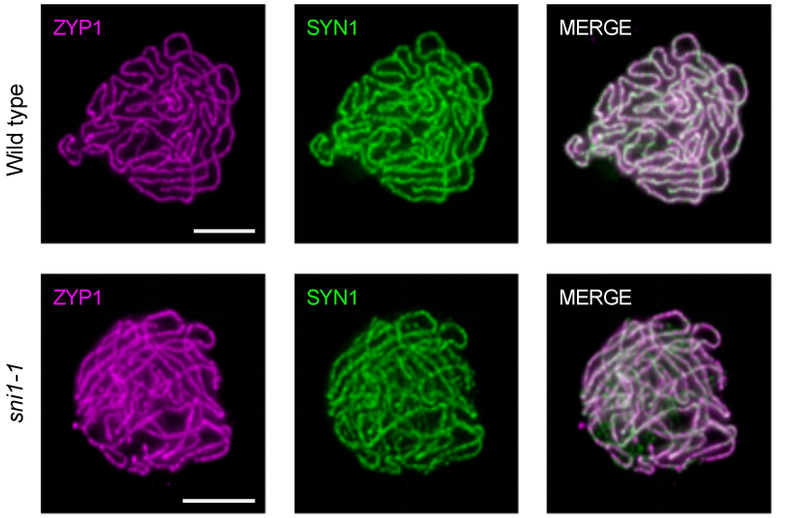

Figure 26. Representative images of ZYP1 (magenta) and SYN1 (green) coimmunostaining on wild type (Col-420) and *sni1-1* male meiocytes at pachynema. (scale bar, 5 μm.) The results were obtained by Mónica Pradillo's group.

5.3 The DSBs formation in *sni1-1*

The role of SMC5/6 in the formation of meiotic crossovers has not been fully characterized; nevertheless, the involvement of SMC5/6 complex in proper resolving of meiotic recombination intermediates has been described in budding yeast (Copsey, et al. 2013; Lilienthal, et al. 2013; Xaver, et al. 2013). In collaboration with Mónica Pradillo's group, chromosome spread at different stages of meiosis in wild-type and *sni1-1* anthers as well as RAD51 foci (a RecA homolog that mediates strand invasion, which is a marker for DSBs) and ASY1 (a HORMA domain protein which forms part of the meiotic chromosome axis) were examined (Figure 27).We observed chromosome fragments at anaphase I in *sni1-1*(Figure 26A), which is consistent with those found in *Arabidopsis nse2* mutants (Liu, et al. 2014).Quantification of axis-associated RAD51 foci at leptotene stage showed no significant differences between *sni1-1* and wild type (Figure 27B), which is consistent with our fertility assay in *sni1-1/spo11-1*(Figure 20), suggesting that recombination changes in *sni1-1* are not caused by additional DSBs.

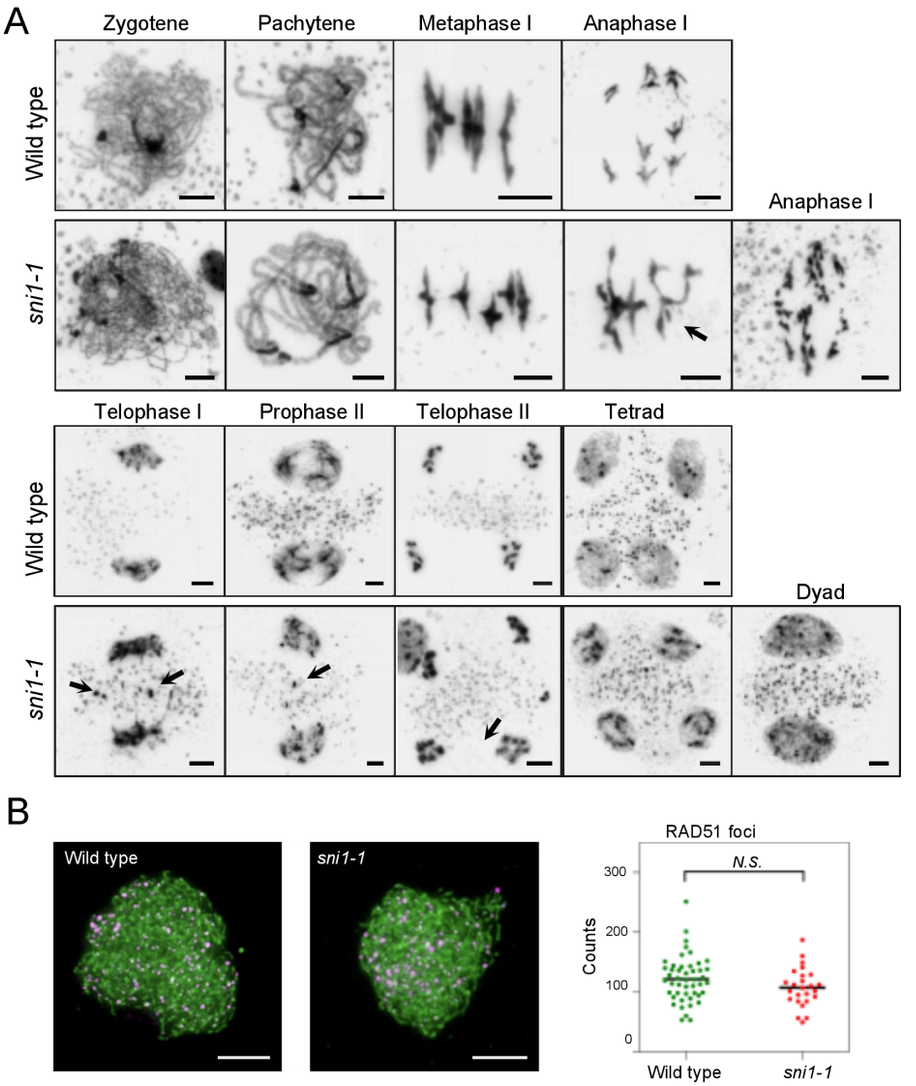

Figure 27. The meiotic cytological phenotype of the *sni1* mutant. (A),Cytological characterization of the *sni1* mutant in comparison to wild type (Col). The stages of meiotic progression were labelled. Chromosome fragments and micronuclei observed in the *sni1* mutant are indicated by arrows. Bar 5 µm. (B),Representative images of ASY1 (green) and RAD51 (magenta) co-immunostaining on wild-type (Col-*420*) and *sni1-1* male meiocytes at zygonema. The results were obtained by Mónica Pradillo's group.

To confirm that *sni1-1* does not yield SPO11-independent DSBs that can be repaired by crossovers, cytology was performed on *sni1-1 spo11* double mutants (by my colleague dr Alexandre Pelé). Cells were not observed at pachytene stage both in *spo11-1*(Figure 28A) and *sni1-1 spo11-1*(Figure 28C), indicating synapsis did not occur in these mutants. As a result, no bivalents were found at metaphase I neither in *spo11-1* (Figure 28B) or *sni1-1 spo11-1* (Figure 28 D). Interestingly, chromosome fragments were detected (n=8) in *sni1-1 spo11-1* cells (n=43) (Figure 28E and F), while this was not found in *spo11-1* (n=23). The *sni1-1* mutant may experience mechanical chromosomal breakage at the metaphase I – anaphase I transition, due to

the physical tension caused by the contraction of the spindle. This phenotype is common in mutants such as cohesin component *syn1* mutant with meiotic chromosome condensation defects (Bai, et al. 1999; Cai, et al. 2003).Incomplete condensation of chromosomes is proposed to make them more sensitive to physical tensions, which causes chromosome breakage. These chromosomal fragments observed in *sni1-1 sspo11-1* are likely rather due to chromosome condensation problems than additional DSBs, as immunostaining with RAD51 antibodies did not show an increase in the number of DSBs in the *sni1-1* (Figure 27B).

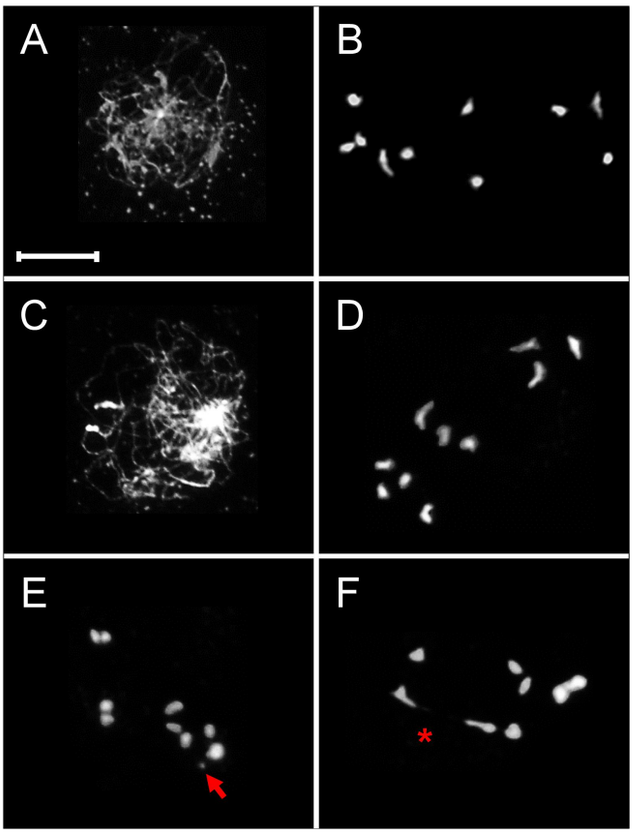

Figure 28. Representative images of spo11-1 (A, B) and *sni1-1 spo11-1* (C-F) at prophase I (A and C) and metaphase I (B, D, E and F). At prophase I, no cells were observed at pachytene stage both in *spo11-1* and *sni1-1 spo11-1*. At metaphase I, ten univalents were regularly observed in both mutants. Occasionally, chromosome fragments were observed in *sni1-1 spo11-1* (E, indicated by an arrow). In two cases, a single bivalent was observed in *sni1-1 spo11-1* (F, indicated by an asterisk). Cell numbers were shown in each case. The results were obtained by Alexandre Pelé.

5.4 The role of SNI1 and the SMC5/6 complex in meiotic recombination

In budding yeast, SGS1 helicase can cooperate with MUS81/MMS4 endonuclease to assure proper recombination intermediate metabolism during meiosis. SGS1 is a central regulator of meiotic recombination intermediate metabolism, role of which is to prevent joint molecules (JMs) accumulation, while MUS81/MMS4

promotes JMs resolution (Oh, et al. 2008). Unresolved JMs are accumulated in *sgs1 mus81/mms4* double mutant (Jessop and Lichten 2008). In budding yeast, meiotic aberrant JMs are observed in the absence of SMC5/6 complex and require MUS81-MMS4 to be repaired (Lilienthal, et al. 2013; Xaver, et al. 2013). The elevation of recombination frequency in chromosome distal region (Figure 15C and D) and partial restoration of the Class I *zip4* mutant fertility (Figure 23), demonstrating that some of these abnormal JMs are repaired as Class II crossovers. Moreover, our genetic assays show that these crossovers are independent of *FANCM* (Figure 22D). Although the multiple mutants are lethal, based on the data and previous studies, we propose that additional Class II crossovers observed in the *sni1-1* mutant are likely due to MUS81- MMS4 repair in conditions where RECQ4 helicases, not properly controlled by SMC5/6 complex, are not efficient in dissolving aberrant intermediates (Figure 29).

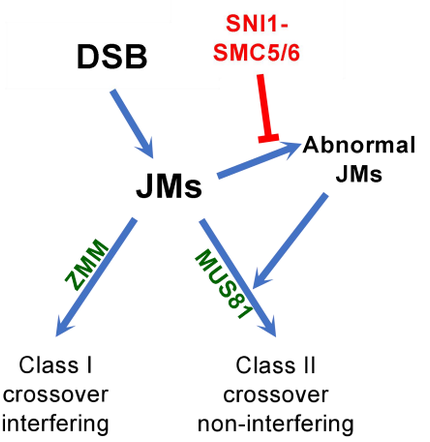

Figure 29. Model of SNI1 role in meiotic crossover formation.

5.5 The role of SNI1 in somatic cells

When DNA damage occurs, the DNA damage response (DDR) is triggered for repair in order to maintain genome integrity. Homologous recombination (HR) and nonhomologous end joining (NHEJ) pathway are the major pathways to repair somatic DSBs (Chapman, et al. 2012). It has been previously reported that loss function of *SNI1* resulted in the elevated expression of DDR related genes such as *BRCA1* and *RAD51*,which are components of the HR pathway, suggesting that *SNI1* is involved in DNA repair (Yan, et al. 2013). The lethality at early stage (no entry into meiosis) in *sni1-1 mus81* and *sni1-1 recq4* double mutants indicates that SNI1 and two other proteins are likely involved in parallel repair pathways of DNA repair. MUS81 has been speculated to be involved in the cleavage of the leading strand during DNA replication, thus able to effectively rescue broken replication forks in yeast (Constantinou, et al. 2002; Whitby, et al. 2003). Several RecQ helicases are

also reported to be involved in the repair of stalled replication forks (Bennett and Keck 2004). Interestingly, a synthetic lethal phenotype is obtained when loss of MUS81 is combined with deletion of the RecQ helicase SGS1 or RQH1 in *S.pombe* and *S.cerevisiae* (Boddy, et al. 2000; Mullen, et al. 2001).A similar situation is also observed in *Arabidopsis*, where mutation in MUS81 and RECQ4A is synthetically lethal, indicating that both MUS81 and RECQ4A proteins are involved in dissolving stalled replication forks in parallel pathways (Hartung, et al. 2006). In plants, at least two HR pathways exist to repair a genomic DSB, namely, single-strand annealing (SSA) (Siebert and Puchta 2002) and synthesis-dependent strand annealing (SDSA) pathway(Puchta 1998),thus, further studies are required to investigate which HR pathway SNI1 is involved in.

5.6 The *sni1-1* is likely a hypomorphic allele

Initially, two different SNI1 alleles, namely, *sni1*-SAIL mutant allele (SAIL_298_H07) and *sni1-1* allele were used to investigate the meiotic crossover. Of the two alleles tested, the SAIL allele shows severe growth defects with very low-yield seeds, preventing analysis of meiotic crossover, which is the main topic of this study. Moreover, *sni1-1* mutant is very well characterized and used by many groups as a reference mutant to study SNI1 roles in different biological processes (Durrant, et al. 2007; Kim, et al. 2012; Maldonado, et al. 2014; Pape, et al. 2010a; Pape, et al. 2010b).We therefore chose to work with *sni1-1* due to the mild growth defects. The difference in phenotype between these two alleles makes us suspect that *sni1-1* is a hypomorphic allele. Recently, the *sni1*-SAIL allele has been characterized and displayed a stronger phenotype (Chen, et al. 2021). Strikingly, the *sni1-SAIL* allele could suppress *rad51* phenotype while *sni1-1 rad51* double mutant is sterile in our study (Figure 18A).This supports the idea that *sni1-1* allele is hypomorphic. However, comparison of our cytological results for *sni1-1* with those for *sni1*-SAIL published by Chen et.al (2021) did not reveal obvious differences in meiosis progression: both *sni1-1* and *sni1*-SAIL show full synapsis and normal pachytene chromosomes, form five bivalents at diakinesis, and show chromosome fragmentation starting with metaphase I which are significantly enhanced in anaphase I (Figure 27A). It should be noted that chromosome fragmentation was significantly more severe in *sni1*-SAIL than in *sni1-1*, however this is observed in meiotic stages following zygotene-pachytene, where meiotic recombination takes place (Figure 27A). Therefore, even though these two alleles show difference in phenotypes, but this would not affect interpretation of the role of *SNI1* in meiotic recombination.

SUMMARY

In conclusion, I have identified SNI1, the component of SMC5/6 complex, as a natural modifier of crossover frequency in *Arabidopsis*. The *sni1-1* mutant exhibits a modified pattern of recombination across the genome with crossovers elevated in chromosome distal regions, but reduced in pericentromeres. Mutations in *SNI1* result in reduced crossover interference and can partially restore the fertility of a Class I crossover pathway mutant, which suggests that the protein is involved in affects non-interfering crossover repair. Genetic analysis of other SMC5/6 mutants confirms the observations of crossover redistribution made for *sni1-1*. How SNI1 and SMC5/6 complex mechanistically function in meiotic recombination remains to be addressed in future studies.

REFERENCES

Alexander, M. P.

1969 Differential staining of aborted and nonaborted pollen. Stain Technol 44(3):117-22.

Anderson, L. K., K. D. Hooker, and S. M. Stack

2001 The distribution of early recombination nodules on zygotene bivalents from plants. Genetics 159(3):1259-69.

Aragon, L.

2018 The Smc5/6 Complex: New and Old Functions of the Enigmatic Long-Distance Relative. Annual Review Of Genetics, Vol 52 52:89-107.

Bai, X., et al.

1999 Isolation and characterization of SYN1, a RAD21-like gene essential for meiosis in Arabidopsis. Plant Cell 11(3):417-30.

Baudat, F.

2010 PRDM9 is a major determinant of meiotic recombination hotspots in humans and mice (vol 327, pg 836, 2010). Science 328(5979):690-690.

Bennett, R. J., and J. L. Keck

2004 Structure and function of RecQ DNA helicases. Critical Reviews In Biochemistry And Molecular Biology 39(2):79-97.

Berchowitz, L. E., and G. P. Copenhaver

2008 Fluorescent Arabidopsis tetrads: a visual assay for quickly developing large crossover and crossover interference data sets. Nat Protoc 3(1):41-50.

Berchowitz, L. E., et al.

2007 The role of AtMUS81 in interference-insensitive crossovers in A. thaliana. PLoS Genet 3(8):e132.

Bergerat, A., et al.

1997 An atypical topoisomerase II from Archaea with implications for meiotic recombination. Nature 386(6623):414-7.

Bermejo, R., et al.

2007 Top1- and Top2-mediated topological transitions at replication forks ensure fork progression and stability and prevent DNA damage checkpoint activation. Genes & Development 21(15):1921-1936.

Bermudez-Lopez, M., et al.

2010 The Smc5/6 complex is required for dissolution of DNA-mediated sister chromatid linkages. Nucleic Acids Research 38(19):6502-6512.

Bermudez-Lopez, M., et al.

2016 Sgs1's roles in DNA end resection, HJ dissolution, and crossover suppression require a two-step SUMO regulation dependent on Smc5/6. Genes & Development 30(11):1339-1356.

Blackwell, A. R., et al.

2020 MSH2 shapes the meiotic crossover landscape in relation to interhomolog polymorphism in Arabidopsis. EMBO J 39(21):e104858.

Boddy, M. N., et al.

2000 Damage tolerance protein Mus81 associates with the FHA1 domain of checkpoint

kinase Cds1. Molecular And Cellular Biology 20(23):8758-8766.

Bomblies, K., J. D. Higgins, and L. Yant

2015 Meiosis evolves: adaptation to external and internal environments. New Phytol 208(2):306-23.

Borner, G. V., N. Kleckner, and N. Hunter

2004 Crossover/noncrossover differentiation, synaptonemal complex formation, and regulatory surveillance at the leptotene/zygotene transition of meiosis. Cell 117(1):29-45.

Brown, M. S., and D. K. Bishop

2014 DNA strand exchange and RecA homologs in meiosis. Cold Spring Harb Perspect Biol 7(1):a016659.

Bundock, P., and P. Hooykaas

2002 Severe developmental defects, hypersensitivity to DNA-damaging agents, and lengthened telomeres in Arabidopsis MRE11 mutants. Plant Cell 14(10):2451-62.

Bustard, D. E., et al.

2012 During Replication Stress, Non-Smc Element 5 (Nse5) Is Required for Smc5/6 Protein Complex Functionality at Stalled Forks. Journal Of Biological Chemistry 287(14):11374-11383.

Cai, X., et al.

2003 The Arabidopsis SYN1 cohesin protein is required for sister chromatid arm cohesion and homologous chromosome pairing. Journal Of Cell Science 116(14):2999-3007.

Campbell, C. L., et al.

2015 Escape from crossover interference increases with maternal age. Nat Commun 6:6260.

Cao, H., et al.

1997 The Arabidopsis NPR1 gene that controls systemic acquired resistance encodes a novel protein containing ankyrin repeats. Cell 88(1):57-63.

Chapman, J. R., M. R. G. Taylor, and S. J. Boulton

2012 Playing the End Game: DNA Double-Strand Break Repair Pathway Choice. Molecular Cell 47(4):497-510.

Charlesworth, D.

2002 Plant sex determination and sex chromosomes. Heredity 88:94-101.

Chelysheva, L., et al.

2007 Zip4/Spo22 is required for class I CO formation but not for synapsis completion in Arabidopsis thaliana. PLoS Genet 3(5):e83.

Chelysheva, L., et al.

2012 The Arabidopsis HEI10 Is a New ZMM Protein Related to Zip3. Plos Genetics 8(7).

Chen, H., et al.

2021 RAD51 supports DMC1 by inhibiting the SMC5/6 complex during meiosis. Plant Cell 33(8):2869-2882.

Choi, K. H., et al.

2013 Arabidopsis meiotic crossover hot spots overlap with H2A. Z nucleosomes at gene promoters. Nature Genetics 45(11):1327-+.

Choulet, F., et al.

2014 Structural and functional partitioning of bread wheat chromosome 3B. Science 345(6194):1249721.

Chowdhury, R., et al.
2009 Genetic Analysis of Variation in Human Meiotic Recombination. Plos Genetics 5(9).
Clough, S. J., and A. F. Bent
1998 Floral dip: a simplified method for Agrobacterium-mediated transformation of Arabidopsis thaliana. Plant J 16(6):735-43.
Cole, F., S. Keeney, and M. Jasin
2010 Comprehensive, Fine-Scale Dissection of Homologous Recombination Outcomes at a Hot Spot in Mouse Meiosis. Molecular Cell 39(5):700-710.
Concordet, J. P., and M. Haeussler
2018 CRISPOR: intuitive guide selection for CRISPR/Cas9 genome editing experiments and screens. Nucleic Acids Research 46(W1):W242-W245.
Constantinou, A., et al.
2002 Holliday junction resolution in human cells: two junction endonucleases with distinct substrate specificities. Embo Journal 21(20):5577-5585.
Copsey, A., et al.
2013 Smc5/6 Coordinates Formation and Resolution of Joint Molecules with Chromosome Morphology to Ensure Meiotic Divisions. Plos Genetics 9(12).
Couteau, F., et al.
1999 Random chromosome segregation without meiotic arrest in both male and female meiocytes of a dmc1 mutant of Arabidopsis. Plant Cell 11(9):1623-1634.
Crismani, W., et al.
2012a FANCM Limits Meiotic Crossovers. Science 336(6088):1588-1590.
—
2012b FANCM limits meiotic crossovers. Science 336(6088):1588-90.
Cutler, A. J., and J. E. Krochko
1999 Formation and breakdown of ABA. Trends In Plant Science 4(12):472-478.
Da Ines, O., et al.
2013 Meiotic Recombination in Arabidopsis Is Catalysed by DMC1, with RAD51 Playing a Supporting Role. Plos Genetics 9(9).
de Massy, B.
2013 Initiation of Meiotic Recombination: How and Where? Conservation and Specificities Among Eukaryotes. Annual Review Of Genetics, Vol 47 47:563-599.
De Muyt, A., et al.
2009 A high throughput genetic screen identifies new early meiotic recombination functions in Arabidopsis thaliana. PLoS Genet 5(9):e1000654.
De Muyt, A., et al.
2007 AtPRD1 is required for meiotic double strand break formation in Arabidopsis thaliana. Embo Journal 26(18):4126-4137.
Diaz, M., and A. Pecinka
2018 Scaffolding for Repair: Understanding Molecular Functions of the SMC5/6 Complex. Genes (Basel) 9(1).
DiNardo, S., K. Voelkel, and R. Sternglanz
1984 DNA topoisomerase II mutant of Saccharomyces cerevisiae: topoisomerase II is required for segregation of daughter molecules at the termination of DNA replication. Proc

Natl Acad Sci U S A 81(9):2616-20.

Dion, E., et al.

2007 An Arabidopsis MLH1 mutant exhibits reproductive defects and reveals a dual role for this gene in mitotic recombination. Plant Journal 51(3):431-440.

Dluzewska, J., M. Szymanska, and P. A. Ziolkowski

2018 Where to Cross Over? Defining Crossover Sites in Plants. Frontiers In Genetics 9.

Dodds, P. N., and J. P. Rathjen

2010 Plant immunity: towards an integrated view of plant-pathogen interactions. Nat Rev Genet 11(8):539-48.

Drouaud, J., et al.

2013 Contrasted patterns of crossover and non-crossover at Arabidopsis thaliana meiotic recombination hotspots. PLoS Genet 9(11):e1003922.

Durrant, W. E., S. Wang, and X. Dong

2007 Arabidopsis SNI1 and RAD51D regulate both gene transcription and DNA recombination during the defense response. Proc Natl Acad Sci U S A 104(10):4223-7.

Ederveen, A., et al.

2015 Modulating crossover positioning by introducing large structural changes in chromosomes. Bmc Genomics 16.

Fang, Z., et al.

2012 Megabase-Scale Inversion Polymorphism in the Wild Ancestor of Maize. Genetics 191(3):883-U426.

Fayos, I., et al.

2019 Engineering meiotic recombination pathways in rice. Plant Biotechnol J 17(11):2062-2077.

Fernandes, J. B., et al.

2018 FIGL1 and its novel partner FLIP form a conserved complex that regulates homologous recombination. Plos Genetics 14(4).

Fransz, P. F., et al.

2000 Integrated cytogenetic map of chromosome arm 4S of A-thaliana: Structural organization of heterochromatic knob and centromere region. Cell 100(3):367-376.

Fransz, P., et al.

2016 Molecular, genetic and evolutionary analysis of a paracentric inversion in Arabidopsis thaliana. Plant Journal 88(2):159-178.

Froger, Alexandrine, and James E Hall

2007 Transformation of plasmid DNA into E. coli using the heat shock method. Journal of visualized experiments: JoVE (6).

Gallego, M. E., et al.

2001 Disruption of the Arabidopsis RAD50 gene leads to plant sterility and MMS sensitivity. Plant J 25(1):31-41.

Girard, C., et al.

2015 AAA-ATPase FIDGETIN-LIKE 1 and Helicase FANCM Antagonize Meiotic Crossovers by Distinct Mechanisms. Plos Genetics 11(7).

Girard, C., et al.

2014 FANCM-associated proteins MHF1 and MHF2, but not the other Fanconi anemia

factors, limit meiotic crossovers. Nucleic Acids Research 42(14):9087-9095.

Gomez, R., et al.

2013 Dynamic localization of SMC5/6 complex proteins during mammalian meiosis and mitosis suggests functions in distinct chromosome processes. Journal Of Cell Science 126(18):4239-4252.

Gray, S., and P. E. Cohen

2016 Control of Meiotic Crossovers: From Double-Strand Break Formation to Designation. Annu Rev Genet 50:175-210.

Grey, C., et al.

2011 Mouse PRDM9 DNA-Binding Specificity Determines Sites of Histone H3 Lysine 4 Trimethylation for Initiation of Meiotic Recombination. Plos Biology 9(10).

Grey, C., F. Baudat, and B. de Massy

2009 Genome-Wide Control of the Distribution of Meiotic Recombination. Plos Biology 7(2):327-339.

Haering, C. H., et al.

2008 The cohesin ring concatenates sister DNA molecules. Nature 454(7202):297-301.

Haering, C. H., et al.

2002 Molecular architecture of SMC proteins and the yeast cohesin complex. Mol Cell 9(4):773-88.

Hanin, M., et al.

2000 Elevated levels of intrachromosomal homologous recombination in Arabidopsis overexpressing the MIM gene. Plant Journal 24(2):183-189.

Hartung, F., et al.

2006 The role of AtMUS81 in DNA repair and its genetic interaction with the helicase AtRecQ4A. Nucleic Acids Res 34(16):4438-48.

Hartung, F., et al.

2008 Topoisomerase 3 alpha and RMI1 Suppress Somatic Crossovers and Are Essential for Resolution of Meiotic Recombination Intermediates in Arabidopsis thaliana. Plos Genetics 4(12).

Hartung, F., et al.

2007 The catalytically active tyrosine residues of both SPO11-1 and SPO11-2 are required for meiotic double-strand break induction in Arabidopsis. Plant Cell 19(10):3090-9.

Higgins, J. D., et al.

2004 The Arabidopsis MutS homolog AtMSH4 functions at an early step in recombination: evidence for two classes of recombination in Arabidopsis. Genes & Development 18(20):2557-2570.

Higgins, J. D., et al.

2008 AtMSH5 partners AtMSH4 in the class I meiotic crossover pathway in Arabidopsis thaliana, but is not required for synapsis. Plant Journal 55(1):28-39.

Huang, L. X., et al.

2009 The Arabidopsis SUMO E3 ligase AtMMS21, a homologue of NSE2/MMS21, regulates cell proliferation in the root. Plant Journal 60(4):666-678.

Hunter, N.

2015 Meiotic Recombination: The Essence of Heredity. Cold Spring Harb Perspect Biol

7(12).

Jackson, N., et al.

2006 Reduced meiotic crossovers and delayed prophase I progression in AtMLH3-deficient Arabidopsis. Embo Journal 25(6):1315-1323.

Jain, M., A. K. Tyagi, and J. P. Khurana

2006 Overexpression of putative topoisomerase 6 genes from rice confers stress tolerance in transgenic Arabidopsis plants. FEBS J 273(23):5245-60.

Jeppsson, K., et al.

2014 The maintenance of chromosome structure: positioning and functioning of SMC complexes. Nature Reviews Molecular Cell Biology 15(9):601-614.

Jessop, L., and M. Lichten

2008 Mus81/Mms4 endonuclease and Sgs1 helicase collaborate to ensure proper recombination intermediate metabolism during meiosis. Mol Cell 31(3):313-23.

Johnston, S. E., et al.

2016 Conserved Genetic Architecture Underlying Individual Recombination Rate Variation in a Wild Population of Soay Sheep (Ovis aries). Genetics 203(1):583-+.

Jyothishwaran, G., et al.

2007 A modified freeze-thaw method for efficient transformation of Agrobacterium tumefaciens. Current Science 93(6):770-772.

Kanno, T., D. G. Berta, and C. Sjogren

2015 The Smc5/6 Complex Is an ATP-Dependent Intermolecular DNA Linker. Cell Reports 12(9):1471-1482.

Keeney, S., C. N. Giroux, and N. Kleckner

1997 Meiosis-specific DNA double-strand breaks are catalyzed by Spo11, a member of a widely conserved protein family. Cell 88(3):375-84.

Kegel, A., and C. Sjogren

2010 The Smc5/6 Complex: More Than Repair? Nuclear Organization And Function 75:179-187.

Kim, H. S., et al.

2012 A NAC transcription factor and SNI1 cooperatively suppress basal pathogen resistance in Arabidopsis thaliana. Nucleic Acids Res 40(18):9182-92.

Koncz, C., et al.

1990 Isolation of a gene encoding a novel chloroplast protein by T-DNA tagging in Arabidopsis thaliana. EMBO J 9(5):1337-46.

Kulemzina, I., et al.

2012 Cohesin rings devoid of Scc3 and Pds5 maintain their stable association with the DNA. PLoS Genet 8(8):e1002856.

Kumar, S. V., and P. A. Wigge

2010 H2A.Z-Containing Nucleosomes Mediate the Thermosensory Response in Arabidopsis. Cell 140(1):136-147.

Kurzbauer, Marie-Therese, et al.

2012 The Recombinases DMC1 and RAD51 Are Functionally and Spatially Separated during Meiosis in Arabidopsis The Plant Cell 24(5):2058-2070.

Kwak, J. S., et al.

2016 Arabidopsis HIGH PLOIDY2 Sumoylates and Stabilizes Flowering Locus C through Its E3 Ligase Activity. Frontiers In Plant Science 7.

Lambing, C., et al.

2020 Interacting Genomic Landscapes of REC8-Cohesin, Chromatin, and Meiotic Recombination in Arabidopsis. Plant Cell 32(4):1218-1239.

Langmead, B., and S. L. Salzberg

2012 Fast gapped-read alignment with Bowtie 2. Nat Methods 9(4):357-9.

Lawrence, E. J., et al.

2019 Natural Variation in TBP-ASSOCIATED FACTOR 4b Controls Meiotic Crossover and Germline Transcription in Arabidopsis. Current Biology 29(16):2676-+.

Lawrence, E. J., C. H. Griffin, and I. R. Henderson

2017 Modification of meiotic recombination by natural variation in plants. J Exp Bot 68(20):5471-5483.

Lehmann, A. R., et al.

1995 The Rad18 Gene Of Schizosaccharomyces-Pombe Defines a New Subgroup Of the Smc Superfamily Involved In DNA-Repair. Molecular And Cellular Biology 15(12):7067-7080.

Li, F., N. De Storme, and D. Geelen

2017a Dynamics of male meiotic recombination frequency during plant development using Fluorescent Tagged Lines in Arabidopsis thaliana. Scientific Reports 7.

Li, G., et al.

2017b Non-SMC elements 1 and 3 are required for early embryo and seedling development in Arabidopsis. J Exp Bot 68(5):1039-1054.

Li, H., et al.

2018 Fast-Forwarding Genetic Gain. Trends Plant Sci 23(3):184-186.

Li, X., et al.

1999 Identification and cloning of a negative regulator of systemic acquired resistance, SNI1, through a screen for suppressors of npr1-1. Cell 98(3):329-39.

Lilienthal, I., T. Kanno, and C. Sjogren

2013 Inhibition of the Smc5/6 complex during meiosis perturbs joint molecule formation and resolution without significantly changing crossover or non-crossover levels. PLoS Genet 9(11):e1003898.

Liu, C. M., et al.

2002 Condensin and cohesin knockouts in Arabidopsis exhibit a titan seed phenotype. Plant Journal 29(4):405-415.

Liu, M., et al.

2014 SUMO E3 ligase AtMMS21 is required for normal meiosis and gametophyte development in Arabidopsis. Bmc Plant Biology 14.

Lloyd, A., et al.

2018 Plasticity of Meiotic Recombination Rates in Response to Temperature in Arabidopsis. Genetics 208(4):1409-1420.

Losada, A., and T. Hirano

2005 Dynamic molecular linkers of the genome: the first decade of SMC proteins. Genes & Development 19(11):1269-1287.

Macaisne, N., et al.

2008 SHOC1, an XPF endonuclease-related protein, is essential for the formation of class I meiotic crossovers. Current Biology 18(18):1432-1437.

Maldonado, A., et al.

2014 Modification of the expression of two NPR1 suppressors, SNC1 and SNI1, in soybean confers partial resistance to the soybean cyst nematode, Heterodera glycines. Funct Plant Biol 41(7):714-726.

McDonald, W. H., et al.

2003 Novel essential DNA repair proteins Nse1 and Nse2 are subunits of the fission yeast Smc5-Smc6 complex. J Biol Chem 278(46):45460-7.

McMahill, M. S., C. W. Sham, and D. K. Bishop

2007 Synthesis-dependent strand annealing in meiosis. PLoS Biol 5(11):e299.

Melamed-Bessudo, C., and A. A. Levy

2012 Deficiency in DNA methylation increases meiotic crossover rates in euchromatic but not in heterochromatic regions in Arabidopsis. Proceedings Of the National Academy Of Sciences Of the United States Of America 109(16):E981-E988.

Mengiste, T., et al.

1999 An SMC-like protein is required for efficient homologous recombination in Arabidopsis. Embo Journal 18(16):4505-4512.

Mercier, R., et al.

2005 Two meiotic crossover classes cohabit in Arabidopsis: One is dependent on MER3, whereas the other one is not. Current Biology 15(8):692-701.

Mercier, R., et al.

2015 The molecular biology of meiosis in plants. Annu Rev Plant Biol 66:297-327.

Miao, C. B., et al.

2013 CENTRAL REGION COMPONENT1, a Novel Synaptonemal Complex Component, Is Essential for Meiotic Recombination Initiation in Rice. Plant Cell 25(8):2998-3009.

Mieulet, D., et al.

2018 Unleashing meiotic crossovers in crops. Nature Plants 4(12):1010-1016.

Mirouze, M., et al.

2012 Loss of DNA methylation affects the recombination landscape in Arabidopsis. Proceedings Of the National Academy Of Sciences Of the United States Of America 109(15):5880-5885.

Modliszewski, J. L., and G. P. Copenhaver

2015 Meiotic recombination heats up. New Phytologist 208(2):295-297.

Modliszewski, J. L., et al.

2018 Elevated temperature increases meiotic crossover frequency via the interfering (Type I) pathway in Arabidopsis thaliana. PLoS Genet 14(5):e1007384.

Moose, S. P., and R. H. Mumm

2008 Molecular plant breeding as the foundation for 21st century crop improvement. Plant Physiology 147(3):969-977.

Mosher, R. A., et al.

2006 A comprehensive structure-function analysis of Arabidopsis SNI1 defines essential regions and transcriptional repressor activity. Plant Cell 18(7):1750-1765.

Muir, K. W., et al.
2016 Structure of the Pds5-Scc1 Complex and Implications for Cohesin Function. Cell Rep 14(9):2116-2126.
Mullen, J. R., et al.
2001 Requirement for three novel protein complexes in the absence of the sgs1 DNA helicase in Saccharomyces cerevisiae. Genetics 157(1):103-118.
Nasmyth, K.
2011 Cohesin: a catenase with separate entry and exit gates? Nat Cell Biol 13(10):1170-7.
Neale, M. J., J. Pan, and S. Keeney
2005 Endonucleolytic processing of covalent protein-linked DNA double-strand breaks. Nature 436(7053):1053-7.
Neff, M. M., E. Turk, and M. Kalishman
2002 Web-based primer design for single nucleotide polymorphism analysis. Trends In Genetics 18(12):613-615.
Niki, H., et al.
1992 Escherichia-Coli Mukb Protein Involved In Chromosome Partition Forms a Homodimer with a Rod-And-Hinge Structure Having DNA-Binding And Atp/Gtp Binding Activities. Embo Journal 11(13):5101-5109.
Nonomura, K. L., et al.
2004 The novel gene HOMOLOGOUS PAIRING ABERRATION IN RICE MEIOSIS1 of rice encodes a putative coiled-coil protein required for homologous chromosome pairing in meiosis. Plant Cell 16(4):1008-1020.
Oh, S. D., et al.
2008 RecQ helicase, Sgs1, and XPF family endonuclease, Mus81-Mms4, resolve aberrant joint molecules during meiotic recombination. Molecular Cell 31(3):324-336.
Osman, K., et al.
2011 Pathways to meiotic recombination in Arabidopsis thaliana. New Phytol 190(3):523-44.
Pape, S., C. Thurow, and C. Gatz
2010a The Arabidopsis PR-1 promoter contains multiple integration sites for the coactivator NPR1 and the repressor SNI1. Plant Physiol 154(4):1805-18.
—
2010b Exchanging the as-1-like element of the PR-1 promoter by the as-1 element of the CaMV 35S promoter abolishes salicylic acid responsiveness and regulation by NPR1 and SNI1. Plant Signal Behav 5(12):1669-71.
Parvanov, E. D., P. M. Petkov, and K. Paigen
2010 Prdm9 Controls Activation of Mammalian Recombination Hotspots. Science 327(5967):835-835.
Pebernard, S., et al.
2004 Nse1, Nse2, and a novel subunit of the Smc5-Smc6 complex, Nse3, play a crucial role in meiosis. Mol Biol Cell 15(11):4866-76.
Pebernard, S., et al.
2006 The Nse5-Nse6 dimer mediates DNA repair roles of the Smc5-Smc6 complex (vol 26, pg 1617, 2006). Molecular And Cellular Biology 26(8):3336-3336.
Phillips, D., et al.

2015 The effect of temperature on the male and female recombination landscape of barley. New Phytologist 208(2):421-429.

Potts, P. R., and H. T. Yu

2005 Human MMS21/NSE2 is a SUMO ligase required for DNA repair. Molecular And Cellular Biology 25(16):7021-7032.

Puchta, H.

1998 Repair of genomic double-strand breaks in somatic plant cells by one-sided invasion of homologous sequences. Plant Journal 13(3):331-339.

Qiao, H., et al.

2014 Antagonistic roles of ubiquitin ligase HEI10 and SUMO ligase RNF212 regulate meiotic recombination. Nature Genetics 46(2):194-+.

Rao, H. B. D. P., et al.

2017 A SUMO-ubiquitin relay recruits proteasomes to chromosome axes to regulate meiotic recombination. Science 355(6323):403-407.

Raschle, M., et al.

2015 Proteomics reveals dynamic assembly of repair complexes during bypass of DNA cross-links. Science 348(6234).

Ray, D. K., et al.

2012 Recent patterns of crop yield growth and stagnation. Nat Commun 3:1293.

Reynolds, A., et al.

2013 RNF212 is a dosage-sensitive regulator of crossing-over during mammalian meiosis. Nature Genetics 45(3):269-278.

Rodriguez, E., et al.

2018 DNA damage as a consequence of NLR activation. Plos Genetics 14(2).

Rowan, B. A., et al.

2015 Rapid and inexpensive whole-genome genotyping-by-sequencing for crossover localization and fine-scale genetic mapping. G3 (Bethesda) 5(3):385-98.

Salome, P. A., et al.

2012 The recombination landscape in Arabidopsis thaliana F2 populations. Heredity (Edinb) 108(4):447-55.

Sandor, C., et al.

2012 Genetic variants in REC8, RNF212, and PRDM9 influence male recombination in cattle. PLoS Genet 8(7):e1002854.

Seguela-Arnaud, M., et al.

2017 RMI1 and TOP3 alpha limit meiotic CO formation through their C-terminal domains. Nucleic Acids Research 45(4):1860-1871.

Seguela-Arnaud, M., et al.

2015 Multiple mechanisms limit meiotic crossovers: TOP3 alpha and two BLM homologs antagonize crossovers in parallel to FANCM. Proceedings Of the National Academy Of Sciences Of the United States Of America 112(15):4713-4718.

Serra, H., et al.

2018 Massive crossover elevation via combination of HEI10 and recq4a recq4b during Arabidopsis meiosis. Proc Natl Acad Sci U S A 115(10):2437-2442.

Siebert, R., and H. Puchta

2002 Efficient repair of genomic double-strand breaks by homologous recombination between directly repeated sequences in the plant genome. Plant Cell 14(5):1121-1131.

Snowden, T., et al.

2004 hMSH4-hMSH5 recognizes Holliday junctions and forms a meiosis-specific sliding clamp that embraces homologous chromosomes. Molecular Cell 15(3):437-451.

Stalker, H. D.

1976 Chromosome studies in wild populations of D. melanogaster. Genetics 82(2):323-47.

Tsubouchi, T., H. Zhao, and G. S. Roeder

2006 The meiosis-specific zip4 protein regulates crossover distribution by promoting synaptonemal complex formation together with zip2. Dev Cell 10(6):809-19.

Uanschou, C., et al.

2007 A novel plant gene essential for meiosis is related to the human CtIP and the yeast COM1/SAE2 gene. Embo Journal 26(24):5061-5070.

Uhlmann, F.

2016 SMC complexes: from DNA to chromosomes. Nature Reviews Molecular Cell Biology 17(7):399-412.

Uknes, S., et al.

1992 Acquired resistance in Arabidopsis. Plant Cell 4(6):645-56.

Underwood, C. J., et al.

2018 Epigenetic activation of meiotic recombination near&IT Arabidopsis thaliana&IT centromeres via loss of H3K9me2 and non-CG DNA methylation. Genome Research 28(4):519-531.

Verver, D. E., et al.

2016 Resolving complex chromosome structures during meiosis: versatile deployment of Smc5/6. Chromosoma 125(1):15-27.

Wang, S., et al.

2010 Arabidopsis BRCA2 and RAD51 proteins are specifically involved in defense gene transcription during plant immune responses. Proc Natl Acad Sci U S A 107(52):22716-21.

Wang, Z., et al.

2016 Effect of sex, age and genetics on crossover interference in cattle. Sci Rep 6:37698.

Watanabe, K., et al.

2009 The STRUCTURAL MAINTENANCE OF CHROMOSOMES 5/6 Complex Promotes Sister Chromatid Alignment and Homologous Recombination after DNA Damage in Arabidopsis thaliana. Plant Cell 21(9):2688-2699.

Waterworth, W. M., et al.

2007 NBS1 is involved in DNA repair and plays a synergistic role with ATM in mediating meiotic homologous recombination in plants. Plant Journal 52(1):41-52.

Whitby, M. C., F. Osman, and J. Dixon

2003 Cleavage of model replication forks by fission yeast Mus81-Eme1 and budding yeast Mus81-Mms4. Journal Of Biological Chemistry 278(9):6928-6935.

Wijeratne, A. J., et al.

2006 The Arabidopsis thaliana PARTING DANCERS gene encoding a novel protein is required for normal meiotic homologous recombination. Molecular Biology Of the Cell 17(3):1331-1343.

Wright, K. M., et al.
2015 Selection on meiosis genes in diploid and tetraploid Arabidopsis arenosa. Mol Biol Evol 32(4):944-55.
Wu, G., et al.
2015 Traffic lines: new tools for genetic analysis in Arabidopsis thaliana. Genetics 200(1):35-45.
Xaver, M., et al.
2013 Smc5/6-Mms21 Prevents and Eliminates Inappropriate Recombination Intermediates in Meiosis. Plos Genetics 9(12).
Xu, P. L., et al.
2013 AtMMS21, an SMC5/6 Complex Subunit, Is Involved in Stem Cell Niche Maintenance and DNA Damage Responses in Arabidopsis Roots. Plant Physiology 161(4):1755-1768.
Xue, Z., et al.
2016 OsMTOPVIB Promotes Meiotic DNA Double-Strand Break Formation in Rice. Mol Plant 9(11):1535-1538.
Yan, S., et al.
2013 Salicylic acid activates DNA damage responses to potentiate plant immunity. Mol Cell 52(4):602-10.
Yelina, N. E., et al.
2012 Epigenetic Remodeling of Meiotic Crossover Frequency in Arabidopsis thaliana DNA Methyltransferase Mutants. Plos Genetics 8(8).
Yelina, N. E., et al.
2015 DNA methylation epigenetically silences crossover hot spots and controls chromosomal domains of meiotic recombination in Arabidopsis. Genes Dev 29(20):2183-202.
Yelina, N. E., et al.
2013 High-throughput analysis of meiotic crossover frequency and interference via flow cytometry of fluorescent pollen in Arabidopsis thaliana. Nat Protoc 8(11):2119-34.
Yuen, Kobe C, and Jennifer L Gerton
2018 Taking cohesin and condensin in context. PLoS genetics 14(1):e1007118.
Zhang, C., et al.
2012 The Arabidopsis thaliana DSB formation (AtDFO) gene is required for meiotic double-strand break formation. Plant Journal 72(2):271-281.
Zhang, J. J., et al.
2017 A SUMO Ligase AtMMS21 Regulates the Stability of the Chromatin Remodeler BRAHMA in Root Development. Plant Physiology 173(3):1574-1582.
Zhang, S. C., et al.
2013 SUMO E3 Ligase AtMMS21 Regulates Drought Tolerance in Arabidopsis thaliana. Journal Of Integrative Plant Biology 55(1):83-95.
Zhu, L., et al.
2021 Natural variation identifies SNI1, the SMC5/6 component, as a modifier of meiotic crossover in Arabidopsis. Proc Natl Acad Sci U S A 118(33).
Ziolkowski, P. A., et al.
2015 Juxtaposition of heterozygous and homozygous regions causes reciprocal crossover remodelling via interference during Arabidopsis meiosis. Elife 4.

Ziolkowski, P. A., et al.

2017 Natural variation and dosage of the HEI10 meiotic E3 ligase control Arabidopsis crossover recombination. Genes Dev 31(3):306-317.